Multiscale Wendland radial basis functions and applications to solving partial differential equations

Author:
Chernih, Andrew

Publication Date:
2013

DOI:
https://doi.org/10.26190/unsworks/16332

Multiscale Wendland radial basis functions and applications to solving partial differential equations

September 12, 2013

A thesis presented to

The School of Mathematics and Statistics
The University of New South Wales

in fulfilment of the thesis requirement
for the degree of

Doctor of Philosophy

by Andrew Chernih

Abstract

Meshfree methods, which use linear combinations of radial basis functions (RBFs) to construct approximations, have become popular for the numerical solution of partial differential equations (PDEs).

The Wendland functions are a class of compactly supported, piecewise polynomial RBFs which are important as they use the minimum degree polynomial for a specified smoothness and their compact support leads to sparse linear systems.

A practical issue is the choice of scale to use for the RBFs. A small scale will lead to a sparser and better conditioned linear system, but at the price of poor approximation power. Conversely, a large scale will have better approximation power but at the price of an ill-conditioned linear system.

We firstly consider a generalisation of the Wendland functions, which allows greater freedom in the choice of parameters, and give sufficient and necessary conditions for these functions to be positive definite, as well as classifying the native spaces generated. We give closed form representations for and properties of the Wendland functions and their Fourier transforms.

By an appropriate choice of scaling, we investigate the behaviour of the Wendland functions as the smoothness parameter goes to infinity. This provides insights into the selection of the parameters of the Wendland functions.

We then consider multiscale algorithms for the numerical solution of PDEs. These construct the approximations over several levels, each level using a Wendland RBF with a different scaling factor.

We present a theoretical and practical analysis of two multiscale algorithms for Galerkin approximation of elliptic PDEs on bounded domains, including results on convergence and condition numbers. Convergence is investigated in terms of the mesh norm and the angles between subspaces. The issue of the supports of the RBFs overlapping the boundaries is also considered in our stability analysis.

Finally we consider a multiscale algorithm for collocation approximation of elliptic

PDEs and the Stokes problem on a bounded domain. We provide results on convergence and condition numbers. For the Stokes problem, we use a divergence free RBF constructed from the Wendland functions, since the Wendland functions are not divergence free.

Thesis Sheet

PLEASE TYPE

THE UNIVERSITY OF NEW SOUTH WALES
Thesis/Dissertation Sheet

Surname or Family name: Chernih

First name: Andrew

Other name/s:

Abbreviation for degree as given in the University calendar: PhD

School: Mathematics and Statistics

Faculty: Science

Title: Multiscale Wendland radial basis functions and applications to solving partial differential equations

Abstract 350 words maximum: (PLEASE TYPE)

Meshfree methods, which use linear combinations of radial basis functions (RBFs) to construct approximations, have become popular for the numerical solution of partial differential equations (PDEs).

The Wendland functions are a class of compactly supported, piecewise polynomial RBFs which are important as they use the minimum degree polynomial for a specified smoothness and their compact support leads to sparse linear systems.

A practical issue is the choice of scale to use for the RBFs. A small scale will lead to a sparser and better conditioned linear system, but at the price of poor approximation power. Conversely, a large scale will have better approximation power but at the price of an ill-conditioned linear system.

We firstly consider a generalisation of the Wendland functions, which allows greater freedom in the choice of parameters, and give sufficient and necessary conditions for these functions to be positive definite, as well as classifying the native spaces generated. We give closed form representations for and properties of the Wendland functions and their Fourier transforms.

By an appropriate choice of scaling, we investigate the behaviour of the Wendland functions as the smoothness parameter goes to infinity. This provides insights into the selection of the parameters of the Wendland functions.

We then consider multiscale algorithms for the numerical solution of PDEs. These construct the approximations over several levels, each level using a Wendland RBF with a different scaling factor.

We present a theoretical and practical analysis of two multiscale algorithms for Galerkin approximation of elliptic PDEs on bounded domains, including results on convergence and condition numbers. Convergence is investigated in terms of the mesh norm and the angles between subspaces. The issue of the supports of the RBFs overlapping the boundaries is also considered in our stability analysis.

Finally we consider a multiscale algorithm for collocation approximation of elliptic PDEs and the Stokes problem on a bounded domain. We provide results on convergence and condition numbers. For the Stokes problem, we use a divergence free RBF constructed from the Wendland functions, since the Wendland functions are not divergence free.

Originality Statement

ORIGINALITY STATEMENT

'I hereby declare that this submission is my own work and to the best of my knowledge it contains no materials previously published or written by another person, or substantial proportions of material which have been accepted for the award of any other degree or diploma at UNSW or any other educational institution, except where due acknowledgement is made in the thesis. Any contribution made to the research by others, with whom I have worked at UNSW or elsewhere, is explicitly acknowledged in the thesis. I also declare that the intellectual content of this thesis is the product of my own work, except to the extent that assistance from others in the project's design and conception or in style, presentation and linguistic expression is acknowledged.'

Signed ....

Date 28/3/2013 ....

Copyright statement

Acknowledgements

I would like to use this opportunity to thank some of the people who have helped me prepare this thesis.

Firstly I would like to thank my supervisor Ian Sloan for giving me the opportunity to write this thesis. I have benefitted greatly from our discussions, his guidance, advice and support. I am also very grateful for the chances to attend many conferences and exchange ideas with fellow researchers in the field.

I am also grateful to my co-supervisor Robert Womersley for being so generous with his time and always willing to make sure I had the fundamentals right before moving on.

I owe a special debt of gratitude to my co-supervisor Thong Le Gia for always having time for me. This thesis has improved greatly from our time working together.

Writing this thesis, I have had the privilege of working with Simon Hubbert, which was a great learning opportunity.

I used some datasets and code from [12] as well as Andrea Tagliasacchi's "kd-tree for matlab" library, available at `www.mathworks.com/matlabcentral/fileexchange/21512`.

This work was supported by the Australian Research Council.

Finally I would like to thank my parents for their love, support and encouragement.

Contents

Abstract **i**

Thesis Sheet **iii**

List of Figures **xv**

List of Tables **xvii**

List of Algorithms **xix**

Notation **xxi**

1 Introduction **1**

2 Preliminaries **7**

2.1 Radial functions 7

2.2 Point sets 8

2.3 Sobolev spaces 8

2.4 Sobolev and mesh norms on the boundary 9

2.5 Sampling Inequalities 9

2.6 Hypergeometric functions 10

2.7 Positive definite functions 10

3 The Wendland radial basis functions **13**

3.1 The generalised Wendland functions 13

3.1.1 Definition 13

3.1.2 Wendland functions in terms of hypergeometric functions 14

3.2 The original Wendland functions 14

3.2.1 Properties of the derivatives of the original Wendland functions . . 17
3.3 The missing Wendland functions 21

4 Fourier transform of the generalised Wendland functions 27
4.1 Fourier transforms 27
4.1.1 Definitions and preliminaries 27
4.2 Fourier transform of the generalised Wendland functions 29
4.3 Native Spaces 31
4.3.1 Norm equivalence for the scaled Wendland functions 32
4.4 Identities 33
4.4.1 Fourier transform dimension drop 33
4.5 Closed form representations for the Fourier transform of the original Wendland functions 35
4.5.1 Odd spatial dimensions d 35
4.5.2 Even spatial dimensions d 38
4.6 Closed form representation for the Fourier transform of the missing Wendland functions 43
4.6.1 Integrals leading to the result 43
4.7 Properties 46
4.7.1 When is the Fourier transform strictly decreasing 46

5 Limit of the generalised Wendland functions as $\alpha \to \infty$ 47
5.1 Generalised Wendland functions with a change of variable 47
5.2 Asymptotic behaviour as $\alpha \to \infty$ 51
5.2.1 Limiting case of the normalised equal area Wendland functions $\psi_{\mu,\alpha}$ as $\alpha \to \infty$ 51
5.2.2 Numerical results 55
5.3 On the selection of the parameter μ 59
5.4 Implications for selecting scaling parameters 60

6 Solving PDEs with Wendland functions 61
6.1 Galerkin approximation for elliptic PDEs 61
6.1.1 PDEs with Neumann and/or Robin boundary conditions 61
6.1.2 PDEs with Dirichlet boundary conditions 63

6.2 Collocation . . . 65
6.2.1 Symmetric collocation for elliptic PDEs . . . 66
6.2.2 Symmetric collocation for the Stokes problem . . . 68

7 Multiscale algorithms for Galerkin approximation of elliptic PDEs 73

7.1 Framework . . . 73
7.2 Multiscale Galerkin approximations . . . 73
7.2.1 Condition numbers . . . 77
7.3 Nested multiscale Galerkin approximations . . . 80
7.4 Numerical experiments . . . 82
7.4.1 Multiscale Algorithm . . . 82
7.4.2 Nested multiscale algorithm . . . 85
7.5 Analysis of convergence . . . 85
7.5.1 Multiscale Galerkin algorithm . . . 86
7.5.2 Nested multiscale Galerkin algorithm . . . 86

8 Multiscale algorithms for collocation of PDEs 91

8.1 Multiscale symmetric collocation of elliptic PDEs on bounded domains . 91
8.1.1 Numerical experiments . . . 95
8.2 Multiscale symmetric collocation approximation to the Stokes problem . . 96
8.2.1 Condition numbers . . . 100
8.2.2 Numerical experiments . . . 104

Bibliography 107

List of Figures

5.1 The (original) Wendland functions $\phi_{\ell,k}(r)$ for $\ell = k+2$ and $k = 1,\ldots,5$, normalised to have value 1 at $r = 0$. 48

5.2 The normalised equal area Wendland functions $\psi_{3,1}(y)$, $\psi_{4,2}(y)$, $\psi_{5,3}(y)$, $\psi_{6,4}(y)$, $\psi_{7,5}(y)$ with $\alpha = 1$ and $\exp(-y^2)$. 50

5.3 $E_{\ell,k}(y)$ with $\alpha = 1$ and $0 \leq y \leq \delta_{\ell,k}(1)$. Subplots (a) and (b) are for the missing Wendland functions and subplots (c) and (d) are for the original Wendland functions. 56

5.4 $\epsilon_{\ell,k}$ on a logarithmic scale with $\vartheta = 1$, $k = 1,\ldots,50$ and $d = 3,5,7,9$ for the original Wendland functions. 57

5.5 $\epsilon_{\ell,k}$ on a logarithmic scale with $\vartheta = 1$, $k = 0.5,\ldots,49.5$ and $d = 2,4,6,8$ for the missing Wendland functions. 58

List of Tables

3.1 The original Wendland functions $\phi_{\ell,k}(r)$ for $d = 3$ and $k = 1, \ldots, 5$. 17

3.2 The missing Wendland functions $\phi_{\ell,k+\frac{1}{2}}(r)$ for $d = 2$ and $k = 0, 1, 2$. 25

5.1 Results from the example in Section 5.2.2 showing L_2 and L_∞ errors, 2-norm condition numbers κ and minimum and maximum eigenvalues (λ_{min} and λ_{max}) when using the Wendland RBFs $\phi_{\ell,k}$, normalised to have value 1 at the origin, and the normalised equal area Wendland RBFs $\psi_{\ell,k}$ with $\vartheta = 2$. . . . 59

7.1 The number of equally spaced points used at each level and the associated mesh norm for the multiscale Galerkin approximation example 83

7.2 The scaling factors, approximation errors and condition numbers of the stiffness matrices for the multiscale Galerkin algorithm with Neumann boundary conditions 83

7.3 The scaling factors, approximation errors and condition numbers of the stiffness matrices for the multiscale Galerkin algorithm with Dirichlet boundary conditions 84

7.4 The number of centres, scaling factors, approximation errors and condition numbers of the stiffness matrices for the nested multiscale Galerkin algorithm 85

7.5 The estimated convergence rates $\widetilde{\alpha}_{1,n}$ using the results for the L_2 norm errors from the first example in Section 7.4.1 with the C^2 and C^6 Wendland functions. 86

7.6 The estimated convergence rates $\widetilde{\alpha}_{1,n}$ and $\widetilde{\alpha}_{2,n}$ using the results for the L_2 norm errors from the example in Section 7.4.2. 87

7.7 The estimates of $\sin \widetilde{\theta}_i$ with the approximation spaces $\{\widetilde{V}_i\}_{i=1}^{5}$. 89

8.1 The number of equally spaced points used at each level and the associated mesh norm for the numerical experiments 96

8.2 The scaling factors, approximation errors and condition numbers of the collocation matrices for the multiscale symmetric collocation algorithm example 96

8.3 The number of interior and boundary points used at each level and the maximum mesh norm at each level for the multiscale symmetric collocation Stokes problem example 105

8.4 The scaling factors, approximation errors and condition numbers of the collocation matrices for the multiscale symmetric collocation Stokes problem example 105

8.5 The observed order for the condition numbers for the multiscale symmetric collocation Stokes problem example 105

List of Algorithms

1 Multiscale Galerkin approximation 74
2 Nested multiscale Galerkin approximation 81
3 Multiscale symmetric collocation approximation 92
4 Multiscale symmetric collocation approximation to the Stokes problem . . . 97

Notation

$\lfloor x \rfloor$	The largest integer $\leq x$
$\lceil x \rceil$	The smallest integer $\geq x$
Δ	Laplacian operator
$\mathbf{n}$	Outward unit normal vector
$\mathbb{N}$	Set of natural numbers $\{1, 2, 3, \ldots\}$
$\mathbb{N}_0$	Set of natural numbers including zero $\{0, 1, 2, 3, \ldots\}$
$\mathbb{R}$	Set of real numbers $(-\infty, \infty)$
$C^{k,s}(\Omega)$	The Hölder space with exponent k
${}_pF_q(\cdot; \cdot; x)$	Generalised hypergeometric function
$H^\tau(\Omega)$	Sobolev space of order τ
$H^\tau(\Omega; \mathrm{div})$	Sobolev space of order τ consisting of divergence-free functions
$H_\nu(y)$	Struve function of order ν
$J_\nu(y)$	Bessel function of the first kind with order ν
$R_{m,v}(y)$	Lommel polynomials
$s_{\mu,\nu}(y)$	Lommel function of the first kind
$T_n(y)$	Chebyshev polynomial of the first kind of degree n
$U_n(y)$	Chebyshev polynomial of the second kind of degree n
$Y_\nu(y)$	Bessel function of the second kind with order ν
$\widehat{f}(z)$	Fourier transform of a function $f \in L_1(\mathbb{R}^d)$
$\mathcal{F}_d\phi(z)$	d-dimensional Fourier transform of a radial function $\Phi(\mathbf{x}) = \phi(\\|\mathbf{x}\\|_2)$
$G_\vartheta(y)$	Gaussian radial basis function with scale parameter ϑ
$\widehat{G}_\vartheta(z)$	Fourier transform of $G_\vartheta(y)$
$\phi_{\ell,k}(y)$	Original Wendland function
$\phi_{\ell,k+\frac{1}{2}}(y)$	Missing Wendland function
$\phi_{\mu,\alpha}(y)$	Generalised Wendland function

Chapter One

Introduction

The Wendland functions are a class of piecewise polynomial compactly supported radial basis functions with a user-specified smoothness parameter. The Wendland functions were originally derived in Wendland [47], generating integer-order Sobolev spaces in odd dimensions, and Sobolev spaces of order an integer plus a half in even dimensions. These were then extended to generate integer-order Sobolev spaces also in even dimensions in Schaback [38] (Schaback called these the "missing" Wendland functions). They are uniquely defined for a given spatial dimension d and a smoothness parameter k (up to a constant multiplier). All the Wendland functions are equal to zero outside [0,1].

The original Wendland functions are constructed with the minimal degree polynomial for a given smoothness that gives rise to a d-dimensional positive definite function. They are unique up to a multiplicative constant when $k > 0$. Another important property is that for an odd space dimension d and for k a non-negative integer the Wendland function is the reproducing kernel of a Hilbert space which is norm equivalent to the Sobolev space $H^{\frac{d+1}{2}+k}(\mathbb{R}^d)$ [51, Chapter 10].

Schaback [38] extended Wendland's original approach to cover the missing Wendland functions, which are the reproducing kernels of integer order Sobolev spaces in even dimensions d. An important distinction between the original Wendland functions and the missing Wendland functions is that the missing Wendland functions, whilst still being compactly supported, now have logarithmic and square-root multipliers of polynomial components. The support of the original and missing Wendland functions is $r \in [0, 1]$.

Generalised Wendland functions extend the original and missing Wendland functions by allowing greater freedom in the range of permissible parameter values. They were first considered in [38] and then studied further in [23]. Several conjectures regarding the properties satisfied by the generalised Wendland functions were raised in [38] and are confirmed in this thesis.

Radial basis functions have become increasingly important in recent years for solving PDEs due to the computational advantages of a meshfree approach, as well as due to the sparse linear systems that result from a compactly supported radial basis function.

A practical issue that arises is that of which scale to use for the radial basis functions. A small scale will lead to a sparse and consequently well-conditioned linear system, but at the price of poor approximation power. Conversely, a large scale will have better approximation power but at the price of an ill-conditioned linear system.

Many examples may naturally exhibit multiple scales, for example, constructing an approximation for the height of the earth's surface may suggest a "large scale" to be used over desert regions and a "fine scale" over areas of high variability, such as the Himalayas. It appears much more appropriate to allow different scales in different regions. Of course, this comes at the price of having to select which scales to use in which regions but this is not the topic of this thesis.

Hence it is of great interest to develop algorithms to allow approximation with the use of multiple scales. Such a multiscale algorithm for interpolation was first proposed in [14] and [37], but without any theoretical grounding. Theoretical convergence was proven in the case of the data points being located on a sphere [25] and then extended to interpolation and approximation on bounded domains in [53].

We can now list the contents and new contributions of this thesis.

Chapter 2 provides background material that will be required in the remainder of the thesis.

Chapter 3 defines and gives closed form representations for and properties of the generalised, original and missing Wendland functions. The new contributions in this chapter are:

- The closed form representation for the original Wendland functions in Theorem 3.2 (due to Simon Hubbert).;
- The properties of the original Wendland functions in Lemmas 3.3 - 3.6;
- The closed form representation for the missing Wendland functions in Theorem 3.7.

Chapter 4 investigates properties and gives closed form representations for the Fourier transform of the the generalised Wendland functions. The new contributions in this chapter are:

- Sufficient and necessary conditions for the generalised Wendland functions to generate a $d-$dimensional positive definite function in Theorem 4.4;

- The asymptotic decay of the generalised Wendland functions in Theorem 4.5 and their native spaces in Corollary 4.6;
- The Fourier transform "dimension drop" in Theorem 4.9;
- The closed form representations for the Fourier transform of the original Wendland functions in odd and even dimensions in Theorems 4.11 and 4.12. The proof that several of the $b_{1,j}$ coefficients are 0 in Theorem 4.12 is due to Simon Hubbert;
- The closed form representations for the Fourier transform of the missing Wendland functions in even dimensions in Theorem 4.13;
- Theorem 4.14 which states when the Fourier transform of the generalised Wendland functions is decreasing.

Chapter 5 considers the limiting behaviour of the generalised Wendland functions as the smoothness parameter α goes to infinity. It is shown that the generalised Wendland functions, with a change of variable, converge uniformly to a Gaussian on the real half-line. We recall that the Gaussian radial basis function with scale parameter $\vartheta > 0$, which we denote by $G_\vartheta(y)$, is given by

$$G_\vartheta(y) := e^{-\vartheta y^2}, \quad y \in \mathbb{R}.$$

The results in this Chapter are used to give insights into the selection of the user-specified parameters. The new contributions are:

- The value of the generalised Wendland functions at the origin and the area under the generalised Wendland functions in Lemmas 5.1 and 5.2;
- The definition of the normalised equal area Wendland functions in Theorem 5.3 (due to Robert S. Womersley);
- The limit as $\alpha \to \infty$ of the Fourier transform of the normalised equal area Wendland functions in Theorem 5.6;
- The limit as $\alpha \to \infty$ of the normalised equal area Wendland functions in Theorem 5.7. The proof of Theorem 5.7 was rewritten in a more concise style by Ian H. Sloan.

Chapter 6 provides an overview of solving PDEs (with a single scale) with the Wendland functions, using both Galerkin approximation and collocation. The new contributions in this chapter are:

- A L_2 error bound between the true solution and our approximation when using (single scale) Galerkin approximation for an elliptic PDE with Neumann and/or Robin boundary conditions in Lemma 6.2;
- A L_2 error bound between the true solution and our approximation when using (single scale) collocation approximation for an elliptic PDE in Lemma 6.3;
- A L_2 error bound between the true solution and our approximation when using (single scale) collocation approximation for the Stokes problem (on a bounded domain) in Theorem 6.6.

Chapter 7 provides a theoretical and practical analysis of two multiscale algorithms for Galerkin approximation of elliptic PDEs on bounded domains using Wendland functions. We note that these two multiscale algorithms have been investigated before, see [50]. The new contributions in this Chapter are:

- A proof that the approximation from the first multiscale Galerkin algorithm converges linearly to the true solution, Lemma 7.1, Theorem 7.2 and Corollary 7.3;
- An upper bound on the condition number of the Galerkin approximation matrix is in Theorem 7.4, due to Quoc Thong Le Gia, and an upper bound on the condition number of the Galerkin approximation matrix from the first multiscale Galerkin algorithm is in Theorem 7.5;
- A L_2 convergence analysis of the approximation from the second multiscale Galerkin algorithm to the true solution is in Theorem 7.8;
- Section 7.4 presents numerical experiments using the two multiscale Galerkin algorithms and then Section 7.5 provides an analysis of convergence of the experiments. This was designed together with Robert S. Womersley.

Chapter 8 provides a theoretical and practical analysis of multiscale algorithms for collocation of elliptic PDEs on bounded domains and the Stokes problem using Wendland functions. The new contributions in this Chapter are:

- A proof that the approximation from the multiscale symmetric collocation algorithm for an elliptic PDE converges linearly to the true solution, Theorem 8.1 and Corollaries 8.2 and 8.3;
- Numerical experiments with the multiscale symmetric collocation algorithm, Section 8.1.1;

- A proof that the approximation from the multiscale symmetric collocation algorithm for the Stokes problem converges linearly to the true solution, Theorem 8.5 and Corollary 8.6;
- We give lower bounds on the minimum eigenvalues and upper bounds on the maximum eigenvalues of the multiscale symmetric collocation algorithm matrix for the Stokes problem in Theorems 8.7 and 8.8. This immediately leads to upper bounds on the condition number of the multiscale symmetric collocation algorithm matrix for the Stokes problem in Theorem 8.9;
- Numerical experiments using the multiscale symmetric collocation approximation to the Stokes problem are presented in Section 8.2.2. These were designed together with Robert S. Womersley.

Finally, we mention that work from this thesis has been submitted or will appear in the following publications:

- A. Chernih and S. Hubbert, Closed form representations and properties of the generalised Wendland functions, submitted to the Journal of Approximation Theory. See Chapters 3 and 4.
- A. Chernih, I. H. Sloan and R. S. Womersley, Wendland functions with increasing smoothness converge to a Gaussian, published online in Advances in Computational Mathematics. See Chapter 5.
- A. Chernih and Q. T. Le Gia, Multiscale methods with compactly supported radial basis functions for Galerkin approximation of elliptic PDEs, published online in IMA Journal on Numerical Analysis. See Chapters 6 and 7.
- A. Chernih and Q. T. Le Gia, Multiscale methods with compactly supported radial basis functions for the Stokes problem on bounded domains, submitted to Math. Comp. See Chapters 6 and 8.
- A. Chernih and Q. T. Le Gia, Multiscale methods with compactly supported radial basis functions for elliptic partial differential equations on bounded domains, ANZIAM Journal, Vol. 54, pages C137-C152, 2013. See chapters 6 and 8.

Chapter Two

Preliminaries

This chapter covers background material relating to function spaces, point sets, special functions and other topics that will be required in the remainder of the thesis. This will be presented here to provide a single point of reference should it be required, and it will allow for a more direct presentation of the new results in later chapters. The experienced reader may decide to skip this chapter.

2.1 Radial functions

A function $\Phi : \mathbb{R}^d \to \mathbb{R}$ is said to be *radial* if there exists a function $\phi : [0, \infty) \to \mathbb{R}$ such that $\Phi(\mathbf{x}) = \phi(\|\mathbf{x}\|_2)$ for all $\mathbf{x} \in \mathbb{R}^d$, where $\|\cdot\|_2$ denotes the usual Euclidean norm in $\mathbb{R}^d$. Then we can define an RBF for a given centre $\mathbf{x}_i \in \mathbb{R}^d$ as

$$\Phi_i(\mathbf{x}) := \phi(\|\mathbf{x} - \mathbf{x}_i\|_2).$$

With a given scaling factor $\delta > 0$, we then define a scaled radial basis function as

$$\Phi_\delta(\mathbf{x}) = \delta^{-d}\phi\left(\frac{\|\mathbf{x}\|_2}{\delta}\right). \tag{2.1}$$

Note that we can extend these definitions for $\Phi : \mathbb{R}^d \times \mathbb{R}^d \to \mathbb{R}$ as

$$\begin{aligned} \Phi(\mathbf{x}, \mathbf{y}) &= \Phi(\mathbf{x} - \mathbf{y}) && (2.2) \\ \Phi_\delta(\mathbf{x}, \mathbf{y}) &= \Phi_\delta(\mathbf{x} - \mathbf{y}). && (2.3) \end{aligned}$$

The native space $\mathcal{N}_\Phi(\mathbb{R}^d)$ of Φ consists of all functions $g \in L_2(\mathbb{R}^d)$ with

$$\|g\|_\Phi^2 := \int_{\mathbb{R}^d} \frac{|\widehat{g}(\boldsymbol{\omega})|^2}{\widehat{\Phi}(\boldsymbol{\omega})} \mathrm{d}\boldsymbol{\omega} < \infty,$$

where $\widehat{g}(\boldsymbol{\omega})$ denotes the Fourier transform as defined by (4.1).

2.2 Point sets

With a given domain $\Omega \subseteq \mathbb{R}^d$ and a finite point set $X \subseteq \Omega$, we define the *mesh norm* (also known as the *fill distance*) as

$$h_{X,\Omega} := \sup_{\mathbf{x}\in\Omega} \min_{\mathbf{x}_j\in X} \|\mathbf{x} - \mathbf{x}_j\|_2,$$

which is a measure of the uniformity of the points in X with respect to Ω. We will often drop the subscripts and just write h when the point set and domain are known.

The *separation radius* is defined as

$$q_X := \frac{1}{2} \min_{j\neq k} \|\mathbf{x}_j - \mathbf{x}_k\|_2.$$

2.3 Sobolev spaces

For a given domain, $\Omega \subseteq \mathbb{R}^d$, $k \in \mathbb{N}_0$, and $1 \leq p < \infty$, the Sobolev spaces $W_p^k(\Omega)$ consist of all u with weak derivatives $D^\alpha u \in L_p(\Omega), |\alpha| \leq k$. The semi-norms and norms are defined as

$$|u|_{W_p^k(\Omega)} = \left(\sum_{|\alpha|=k} \|D^\alpha u\|_{L_p(\Omega)}^p\right)^{\frac{1}{p}} \quad \text{and} \quad \|u\|_{W_p^k(\Omega)} = \left(\sum_{|\alpha|\leq k} \|D^\alpha u\|_{L_p(\Omega)}^p\right)^{\frac{1}{p}}.$$

For $p = \infty$, these definitions become

$$|u|_{W_\infty^k(\Omega)} = \sup_{|\alpha|=k} \|D^\alpha u\|_{L_\infty(\Omega)} \quad \text{and} \quad \|u\|_{W_\infty^k(\Omega)} = \sup_{|\alpha|\leq k} \|D^\alpha u\|_{L_\infty(\Omega)}.$$

Let $1 \leq p < \infty$, $k \in \mathbb{N}_0$, and $0 < s < 1$. Then we can define the fractional Sobolev spaces $W_p^{k+s}(\Omega)$ as all u for which the norm defined by

$$\begin{aligned}
\|u\|_{W_p^{k+s}(\Omega)} &:= \left(\|u\|_{W_p^k(\Omega)}^p + |u|_{W_p^{k+s}(\Omega)}^p\right)^{1/p} \\
|u|_{W_p^{k+s}(\Omega)} &:= \left(\sum_{|\alpha|=k} \int_\Omega \int_\Omega \frac{|D^\alpha u(\mathbf{x}) - D^\alpha u(\mathbf{y})|^p}{\|\mathbf{x}-\mathbf{y}\|_2^{d+ps}} \mathrm{d}\mathbf{x}\, \mathrm{d}\mathbf{y}\right)^{1/p}
\end{aligned}$$

is finite. For the case $p = 2$, we write $W_2^\tau(\Omega) = H^\tau(\Omega)$.

We define vector-valued Sobolev spaces with $p = 2$ in the usual way as

$$\mathbf{H}^\tau(\Omega) := H^\tau(\Omega) \times \ldots \times H^\tau(\Omega),$$

with norm

$$\|\mathbf{f}\|_{\mathbf{H}^\tau(\Omega)} := \left(\sum_{j=1}^d \|f_j\|_{H^\tau(\Omega)}^2\right)^{1/2}. \tag{2.4}$$

The functions that we will be concerned with are defined on a bounded domain Ω with a Lipschitz boundary. As a result, there is an extension operator for functions defined in Sobolev spaces which is presented in the following lemma. For further details, we refer the reader to [40] and [10].

Lemma 2.1. *Suppose $\Omega \subseteq \mathbb{R}^d$ has a Lipschitz boundary. Then there is an extension mapping $\mathcal{E}_S : H^\tau(\Omega) \to H^\tau(\mathbb{R}^d)$, defined for all non-negative integers τ, satisfying $\mathcal{E}_S v|_\Omega = v$ for all $v \in H^\tau(\Omega)$ and*

$$\|\mathcal{E}_S v\|_{H^\tau(\mathbb{R}^d)} \leq C\|v\|_{H^\tau(\Omega)}.$$

In this thesis, C will denote a generic constant. Since we also have $\|v\|_{H^\tau(\Omega)} \leq \|\mathcal{E}_S v\|_{H^\tau(\mathbb{R}^d)}$, this means that when we need to consider $H^\tau(\Omega)$ norms, we can use the $H^\tau(\mathbb{R}^d)$-norm instead. This is advantageous, since we then have for $g \in H^\tau(\mathbb{R}^d)$

$$\|g\|^2_{H^\tau(\mathbb{R}^d)} = \int\limits_{\mathbb{R}^d} |\widehat{g}(\boldsymbol{\omega})|^2 \left(1 + \|\boldsymbol{\omega}\|_2^2\right)^\tau \mathrm{d}\boldsymbol{\omega}. \tag{2.5}$$

2.4 Sobolev and mesh norms on the boundary

We follow [18] to define Sobolev norms and the mesh norm on the boundary. We assume that $\partial\Omega \subseteq \cup_{j=1}^K V_j$, where $V_j \subseteq \mathbb{R}^d$ are open sets. The sets V_j are images of $C^{k,s}-$diffeomorphisms

$$\varphi_j : B \to V_j,$$

where $B = B(0,1)$ denotes the unit ball in $\mathbb{R}^{d-1}$. If $\{w_j\}$ is a partition of unity with respect to $\{V_j\}$, then the Sobolev norms on $\partial\Omega$ can be defined as

$$\|u\|^p_{W_p^\mu(\partial\Omega)} := \sum_{j=1}^K \|(uw_j) \circ \varphi_j\|^p_{W_p^\mu(B)}.$$

The mesh norm on the boundary can be defined as

$$h_{X,\partial\Omega} := \max_{1 \leq j \leq K} h_{T_j,B},$$

with $T_j := \varphi_j^{-1}(X \cap V_j) \subseteq B$.

2.5 Sampling Inequalities

We will need the following "sampling" inequalities, which are valid for both scalars and vectors [32, 33, 52].

Theorem 2.2. *Let $\Omega \subseteq \mathbb{R}^d$ be a bounded domain with Lipschitz boundary. Let $\tau > d/2$. Let $X \subseteq \Omega$ be a discrete set having mesh norm h sufficiently small. For each $w \in H^\tau(\Omega)$ with $w|X = 0$ we have for $0 \le \sigma \le \tau$ that*

$$\|w\|_{H^\sigma(\Omega)} \le Ch^{\tau-\sigma}\|w\|_{H^\tau(\Omega)}. \tag{2.6}$$

Theorem 2.3. *Let $\tau = k + s > d/2$. Let $\Omega \subseteq \mathbb{R}^d$ be a bounded domain having $C^{k,s}$ smooth boundary. Let $X \subseteq \partial\Omega$ be a discrete set with h sufficiently small. Then there is a positive constant C such that for all $w \in H^\tau(\Omega)$ with $w|X = 0$ we have for $0 \le \sigma \le \tau - 1/2$ that*

$$\|w\|_{H^\sigma(\partial\Omega)} \le Ch^{\tau-1/2-\sigma}\|w\|_{H^\tau(\Omega)}. \tag{2.7}$$

2.6 Hypergeometric functions

We need to define the generalised hypergeometric function. Further details on generalised hypergeometric functions can be found in [1] and [3].

Definition 2.4. *The generalised hypergeometric function ${}_pF_q(a_1, \ldots, a_p; b_1, \ldots, b_q; x)$ is*

$${}_pF_q(a_1, \ldots, a_p; b_1, \ldots, b_q; x) := \sum_{n=0}^{\infty} \frac{(a_1)_n \cdots (a_p)_n}{(b_1)_n \cdots (b_q)_n} \frac{x^n}{n!},$$

where none of $b_1, \ldots, b_q$ is a negative integer or zero and where

$$(c)_n := c(c+1)\cdots(c+n-1) = \frac{\Gamma(c+n)}{\Gamma(c)}, \quad n \ge 1 \tag{2.8}$$

denotes the Pochhammer symbol, with $(c)_0 = 1$. When $p \le q$ the series converges for all finite x and defines an entire function. When $p = q + 1$ the series converges absolutely for $|x| < 1$, and also at $x = 1$ if

$$\sum_{i=1}^{q} b_i - \sum_{i=1}^{p} a_i > 0.$$

2.7 Positive definite functions

A continuous function $f : \mathbb{R}^d \to \mathbb{R}$ is *positive definite* (some would say *strictly positive definite*) if for any n distinct points $\mathbf{x}_1, \ldots, \mathbf{x}_n \in \mathbb{R}^d$, the quadratic form

$$\sum_{i=1}^{n}\sum_{j=1}^{n} \varepsilon_i\varepsilon_j f(\mathbf{x}_i - \mathbf{x}_j)$$

is positive for all $\boldsymbol{\varepsilon} = [\varepsilon_1, \ldots, \varepsilon_n]^T \in \mathbb{R}^n\backslash\{\mathbf{0}\}$.

We also define a matrix-valued function $\boldsymbol{\Phi} : \mathbb{R}^d \to \mathbb{R}^{n\times n}$ as being *positive definite* if it is even, so $\boldsymbol{\Phi}(-\mathbf{x}) = \boldsymbol{\Phi}(\mathbf{x})$, symmetric, so $\boldsymbol{\Phi}(\mathbf{x}) = \boldsymbol{\Phi}(\mathbf{x})^T$, and satisfies

$$\sum_{j,k=1}^{n} \gamma_j^T \boldsymbol{\Phi}(\mathbf{x}_j - \mathbf{x}_k)\gamma_k > 0,$$

for all pairwise distinct $\mathbf{x}_j \in \mathbb{R}^d$ and all $\gamma_j \in \mathbb{R}^n$ such that not all γ_j are vanishing.

Chapter Three

The Wendland radial basis functions

This chapter will review the Wendland radial basis functions.

Wendland functions were originally introduced in [47] and then more cases were added in [38]. We will refer to the Wendland functions from [47] as the *original Wendland functions* and the Wendland functions from [38] as the *missing Wendland functions*. A thorough investigation of both types of Wendland functions in terms of hypergeometric functions and other special functions is the focus of Hubbert [23]. We firstly define the generalised Wendland functions in Section 3.1, and then the original and missing Wendland functions in Sections 3.2 and 3.3, which are special cases of the generalised Wendland functions, and then give properties and closed form representations of each.

3.1 The generalised Wendland functions

This section will present the generalised Wendland functions. These were first proposed in [38] and then investigated in [23].

3.1.1 Definition

The generalised Wendland function is defined as follows.

Definition 3.1. *With smoothness parameter $\alpha > 0$, and $\mu > -1$, let*

$$\phi_{\mu,\alpha}(r) := \begin{cases} \dfrac{1}{\Gamma(\alpha)\, 2^{\alpha-1}} \displaystyle\int_r^1 s\,(1-s)^{\mu}(s^2-r^2)^{\alpha-1}\mathrm{d}s & \text{for } 0 \le r \le 1, \\ 0 & \text{for } r > 1. \end{cases} \tag{3.1}$$

The generalised Wendland functions are continuous on $[0, \infty)$. For a given space dimension d, we can use (3.1) to generate a $d-$dimensional radial function as

$$\Phi_{\mu,\alpha}(\mathbf{x}) := \phi_{\mu,\alpha}(\|\mathbf{x}\|_2)\,, \quad \mathbf{x} \in \mathbb{R}^d. \tag{3.2}$$

3.1.2 Wendland functions in terms of hypergeometric functions

Hubbert [23] starts with the integral representation (3.1) to express the generalised Wendland functions in terms of Legendre functions. Equation (3.4) in [23] states that for $r \in (0,1]$

$$\phi_{\mu,\alpha}(r) = \frac{\Gamma(\mu+1)}{2^{\mu+\alpha}\Gamma(\mu+\alpha+1)} (1-r^2)^{\mu+\alpha} r^{-\mu} {}_2F_1\left(\frac{\mu}{2}, \alpha + \frac{\mu+1}{2}; \mu+\alpha+1; 1-\frac{1}{r^2}\right). \quad (3.3)$$

Now we apply the following identity [1, 15.3.4]

$$ {}_2F_1(a,b;c;z) = (1-z)^{-a} {}_2F_1\left(a, c-b; c; \frac{z}{z-1}\right) \quad (3.4)$$

to (3.3), which gives us, for $r \in [0,1]$, (since we recover the case of $r = 0$ by right continuity)

$$\phi_{\mu,\alpha}(r) = \frac{\Gamma(\mu+1)}{2^{\mu+\alpha}\Gamma(\mu+\alpha+1)} (1-r^2)^{\mu+\alpha} {}_2F_1\left(\frac{\mu}{2}, \frac{\mu+1}{2}; \mu+\alpha+1; 1-r^2\right). \quad (3.5)$$

3.2 The original Wendland functions

The original Wendland functions are defined by (3.1) when $\alpha = k$ where k is a positive integer with

$$\mu = \ell := \left\lfloor \frac{d}{2} \right\rfloor + k + 1.$$

Note that this choice of ℓ is the minimum value that ensures that the resulting functions are positive definite. Since $\ell = \lfloor \frac{d}{2} + \alpha \rfloor + 1$ it follows immediately that for fixed d

$$\ell \sim \alpha \text{ as } \alpha \to \infty, \quad (3.6)$$

where $x \sim y$ denotes asymptotic equality, that is, $\frac{x}{y} \to 1$. If we wish to use a different support, this can be easily achieved through scaling the function argument: if $\phi(r)$ has support $[0,1]$ then with the change of variable $y = \delta r$, $\psi(y) := \phi\left(\frac{y}{\delta}\right)$ has support $[0,\delta]$.

We now review the original derivation from [47] and important properties of the original Wendland functions.

For a function ϕ such that $t \mapsto \phi(t)\, t$ is in $L_1(\mathbb{R}^d)$, for $r \geq 0$ we define

$$(\mathcal{I}\phi)(r) := \int_r^\infty t\,\phi(t)\,\mathrm{d}t. \quad (3.7)$$

With the truncated power functions defined as

$$\phi^{\{\ell\}}(r) := (1-r)_+^\ell, \quad (3.8)$$

with $(x)_+ := \max(x, 0)$, the original Wendland functions were first presented in [47] as

$$\phi_{\ell,k} = \mathcal{I}^k \phi^{\{\ell\}}. \tag{3.9}$$

The original Wendland functions are constructed with the minimal degree polynomial for a given smoothness that gives rise to a d-dimensional positive definite function. They are unique up to a multiplicative constant when $k > 0$. From [20], we know that $\phi_{\ell,k}$ is $2k$ times differentiable at zero, positive, strictly decreasing on its support and has the form

$$\phi_{\ell,k}(r) = p_k(r)(1-r)_+^{\ell+k}, \tag{3.10}$$

where p_k is a polynomial of degree k. This representation also allows us to deduce that the first $\ell + k - 1$ derivatives of $\phi_{\ell,k}$ vanish at $r = 1$, i.e.,

$$\phi_{\ell,k}^{(n)}(1) = 0, \quad n = 0, 1, \dots, \ell + k - 1. \tag{3.11}$$

From [23], we also have the closed form representation

$$\phi_{\ell,k}(r) = \frac{1}{2^k\, k!}(1-r)_+^{\ell+k} \sum_{j=0}^{k} \frac{\binom{k}{j}}{\binom{\ell+k+j}{k+j}} (2r)^{k-j}(1-r)^j. \tag{3.12}$$

The following theorem gives a closed form representation for the original Wendland functions $\phi_{\ell,k}(r)$, expressed in powers of r.

Theorem 3.2. *Let d be a fixed space dimension and k be a positive integer. In addition let $\ell \geq (d + 2k + 1)/2$ be an integer. Then the function $\phi_{\ell,k}$ is given by*

$$\phi_{\ell,k}(r) = \frac{(-1)^k 2^k k! \ell!}{(2k+\ell)!} \sum_{j=0}^{2k+\ell} (-1)^j \binom{2k+\ell}{j} \binom{\frac{j-1}{2}}{k} r^j \quad \text{for } r \in [0,1]. \tag{3.13}$$

Proof. Applying the binomial theorem to (3.12) yields

$$\begin{aligned}
\phi_{\ell,k}(r) &= \frac{1}{2^k k!} \sum_{j=0}^{k} \frac{\binom{k}{j}}{\binom{\ell+k+j}{\ell}} 2^{k-j} \sum_{n=0}^{\ell+k+j} (-1)^n \binom{\ell+k+j}{n} r^{k+n-j} && (3.14)\\
&=: \sum_{i=0}^{2k+\ell} b_i r^i, && (3.15)
\end{aligned}$$

where, following some standard algebraic manipulation, the polynomial coefficients $(b_i)_{i=0}^{2k+\ell}$ are given by

$$\begin{aligned}
b_i &= \frac{1}{2^k k!} \sum_{j=0}^{i} (-2)^j \frac{\binom{k}{j}}{\binom{\ell+2k-j}{\ell}} \binom{\ell+2k-j}{i-j} \\
&= \frac{\ell! k!}{2^k (\ell+2k-i)! i!} \sum_{j=0}^{i} (-2)^j \binom{2k-j}{k} \binom{i}{j}
\end{aligned}$$

$$
\begin{aligned}
&= \frac{\ell!2k!}{2^k!k!(\ell+2k-i)!i!}\sum_{j=0}^{i}(-2)^j\frac{\binom{k}{j}}{\binom{2k}{j}}\binom{i}{j} \\
&= \frac{\ell!2^k\Gamma\left(k+\frac{1}{2}\right)}{\sqrt{\pi}(\ell+2k-i)!i!}\sum_{j=0}^{i}(-2)^j\frac{\binom{k}{j}}{\binom{2k}{j}}\binom{i}{j},
\end{aligned}
$$

where, in the final line we have employed the following formula from [21, 8.339.2], for evaluation of the Gamma function at the half-integers

$$
\Gamma\left(k+\frac{1}{2}\right)=\frac{\sqrt{\pi}}{4^k}\frac{(2k)!}{k!}, \qquad k\in\mathbb{N}_0. \tag{3.16}
$$

We can now employ the following identity [35, 4.2.10.13]

$$
\sum_{j=0}^{i}(-1)^j x^j\binom{i}{j}\frac{\binom{k}{j}}{\binom{2k}{j}}=\frac{\Gamma\left(k-i+\frac{1}{2}\right)i!}{\Gamma\left(k+\frac{1}{2}\right)}\left(\frac{-x}{4}\right)^i C_i^{(1/2+k-i)}\left(1-\frac{2}{x}\right),
$$

where $C_i^{(\lambda)}$ denotes the Gegenbauer (or ultraspherical) polynomial of degree i and order λ (see [1, Chapter 22]). Setting $x=2$ in the above identity yields

$$
\sum_{j=0}^{i}(-2)^j\binom{i}{j}\frac{\binom{k}{j}}{\binom{2k}{j}}=\frac{\Gamma\left(k-i+\frac{1}{2}\right)}{\Gamma\left(k+\frac{1}{2}\right)}(-1)^i\frac{i!}{2^i}C_i^{(1/2+k-i)}(0). \tag{3.17}
$$

For a non-negative integer i we have (see [1, Section 22.4]) that

$$
C_i^{(\lambda)}(0)=\frac{2^i}{i!}\frac{\sqrt{\pi}\Gamma\left(\lambda+\frac{i}{2}\right)}{\Gamma(\lambda)\Gamma\left(-\frac{i-1}{2}\right)},
$$

and so, using this identity, we can deduce that

$$
\sum_{j=0}^{i}(-2)^j\frac{\binom{k}{j}}{\binom{2k}{j}}\binom{i}{j}=\frac{\Gamma\left(k-\frac{i-1}{2}\right)\sqrt{\pi}}{\Gamma\left(k+\frac{1}{2}\right)\Gamma\left(-\frac{i-1}{2}\right)},
$$

and thus we have

$$
\begin{aligned}
b_i &= (-1)^i\frac{\ell!2^k}{(\ell+2k-i)!i!}\frac{\Gamma\left(k-\frac{i-1}{2}\right)}{\Gamma\left(-\frac{i-1}{2}\right)} \\
&= (-1)^i\frac{2^k k!\ell!}{(2k+\ell)!}\binom{2k+\ell}{i}\binom{k-\frac{i+1}{2}}{k} \\
&= (-1)^{k+i}\frac{2^k k!\ell!}{(2k+\ell)!}\binom{2k+\ell}{i}\binom{\frac{i-1}{2}}{k}.
\end{aligned}
$$

□

Another important property is that for an integer space dimension d and for k a non-negative integer the function

$$
K(\mathbf{x},\mathbf{y})=\phi_{\ell,k}(\|\mathbf{x}-\mathbf{y}\|), \quad \mathbf{x},\mathbf{y}\in\mathbb{R}^d, \tag{3.18}
$$

is the reproducing kernel of a Hilbert space which is norm equivalent to the Sobolev space $H^{\frac{d+1}{2}+k}(\mathbb{R}^d)$ [51, Chapter 10].

The native space $\mathcal{N}_\Phi(\mathbb{R}^d)$ of Φ consists of all functions $g \in L_2(\mathbb{R}^d)$ such that

$$\|g\|_\Phi^2 = \int_{\mathbb{R}^d} \frac{|\widehat{g}(\boldsymbol{\omega})|^2}{\widehat{\Phi}(\boldsymbol{\omega})} \mathrm{d}\boldsymbol{\omega} < \infty. \tag{3.19}$$

We will also need that there exist two constants $0 < c_1 \leq c_2$ such that their Fourier transforms satisfy [51]

$$c_1 \left(1 + \|\boldsymbol{\omega}\|_2^2\right)^{-\rho} \leq \widehat{\Phi}(\boldsymbol{\omega}) \leq c_2 \left(1 + \|\boldsymbol{\omega}\|_2^2\right)^{-\rho}, \quad \boldsymbol{\omega} \in \mathbb{R}^d. \tag{3.20}$$

We give explicit formulae for the original Wendland functions for $d = 3$ and $k = 1, 2, \ldots, 5$ in Table 3.1 where $\doteq$ denotes equality up to a positive constant factor. The support of all the original Wendland functions is $[0, 1]$.

k	Original Wendland function
1	$\phi_{3,1}(r) \doteq (1-r)_+^4(4r+1)$
2	$\phi_{4,2}(r) \doteq (1-r)_+^6(35r^2+18r+3)$
3	$\phi_{5,3}(r) \doteq (1-r)_+^8(32r^3+25r^2+8r+1)$
4	$\phi_{6,4}(r) \doteq (1-r)_+^{10}(429r^4+450r^3+210r^2+50r+5)$
5	$\phi_{7,5}(r) \doteq (1-r)_+^{12}(2048r^5+2697r^4+1644r^3+566r^2+108r+9)$

Table 3.1. *The original Wendland functions $\phi_{\ell,k}(r)$ for $d = 3$ and $k = 1, \ldots, 5$.*

3.2.1 Properties of the derivatives of the original Wendland functions

In this subsection we present several technical lemmas concerning derivatives of the original Wendland functions, which we will need later.

Lemma 3.3. *With spatial dimension d and smoothness parameter $k = 2, 3, \ldots$ let $\Phi_{\ell,k}$ be the original Wendland function. Then with $\mathbf{x} \in \mathbb{R}^d$ and $1 \leq i, j \leq d$ and $i \neq j$, we have*

$$\partial_{ij}\Phi_{\ell,k}(\mathbf{x})|_{\mathbf{x}=\mathbf{0}} = 0.$$

Proof. We recall that the Wendland functions are piecewise polynomials with support $[0, 1]$. With Theorem 3.2, we can write

$$\phi_{\ell,k}(r) = \sum_{i=0}^{2k+\ell} b_i\, r^i, \quad r \in [0, 1] \tag{3.21}$$

where the first k odd coefficients $\{b_{2i+1}\}_{i=0}^{k}$ vanish. With the chain rule, and with $\mathbf{x} = (x_1, \ldots, x_d)$ and $r = \|\mathbf{x}\|_2$, we have

$$\partial_{ij}\Phi_{\ell,k}(\mathbf{x}) = \frac{x_i x_j}{r^2}\left(\phi_{\ell,k}^{(2)}(r) - \frac{1}{r}\phi_{\ell,k}^{(1)}(r)\right).$$

Using (3.21), this last expression becomes

$$\begin{aligned}\partial_{ij}\Phi_{\ell,k}(\mathbf{x}) &= \frac{x_i x_j}{r^2}\left(\sum_{i=2}^{2k+\ell} b_i\,(i-1)_2\,r^{i-2} - \sum_{i=1}^{2k+\ell} i\,b_i\,r^{i-2}\right),\\ &=: \frac{x_i x_j}{r^2}\left(\sum_{i=1}^{2k+\ell} \bar{b}_i\,r^{i-2}\right),\end{aligned} \tag{3.22}$$

where $(c)_n$ denotes the Pochhammer symbol. Now the first three coefficients $\{\bar{b}_i\}_{i=1}^{3}$ are

$$\begin{aligned}\bar{b}_1 &= b_1 = 0\\ \bar{b}_2 &= (2-2)b_2 = 0\\ \bar{b}_3 &= 0,\end{aligned}$$

since the first k odd coefficients of the Wendland polynomial are zero and $k \geq 2$. Hence we can write

$$\partial_{ij}\Phi_{\ell,k}(\mathbf{x}) = x_i x_j \left(\sum_{i=4}^{2k+\ell} \bar{b}_i\,r^{i-4}\right),$$

and the result follows immediately. □

Lemma 3.4. *With spatial dimension d and smoothness parameter $k = 3, 4, \ldots$ let $\Phi_{\ell,k}$ be the original Wendland function. Then with $\mathbf{x} \in \mathbb{R}^d$ and $1 \leq i, j \leq d$ and $i \neq j$, we have*

$$\partial_{ij}\Delta^2\Phi_{\ell,k}(\mathbf{x})|_{\mathbf{x}=\mathbf{0}} = 0.$$

Proof. Once again employing the chain rule gives

$$\begin{aligned}\partial_{ij}\Delta^2\Phi_{\ell,k}(\mathbf{x}) &= \frac{x_i x_j}{r^2}\\ &\times\left(\phi_{\ell,k}^{(6)}(r) + \frac{1}{r}\phi_{\ell,k}^{(5)}(r) - \frac{7}{r^2}\phi_{\ell,k}^{(4)}(r) + \frac{12}{r^3}\phi_{\ell,k}^{(3)}(r) - \frac{15}{r^4}\phi_{\ell,k}^{(2)}(r) + \frac{15}{r^5}\phi_{\ell,k}^{(1)}(r)\right).\end{aligned}$$

With (3.21) we can rewrite this as

$$\begin{aligned}\partial_{ij}\Delta^2\Phi_{\ell,k}(\mathbf{x}) = \frac{x_i x_j}{r^2}\Bigg[&\sum_{i=6}^{2k+\ell} b_i(i-5)_6 r^{i-6} + \sum_{i=5}^{2k+\ell} b_i(i-4)_5 r^{i-6}\\ -7\sum_{i=4}^{2k+\ell} b_i(i-3)_4 r^{i-6} &+ 12\sum_{i=3}^{2k+\ell} b_i(i-2)_3 r^{i-6} - 15\sum_{i=2}^{2k+\ell} b_i(i-1)_2 r^{i-6} + 15\sum_{i=1}^{2k+\ell} i\,b_i r^{i-6}\Bigg]\\ =: &\sum_{i=1}^{2k+\ell} \tilde{b}_i r^{i-6}.\end{aligned}$$

Since $\tilde{b}_i = C(i)b_i$, the first k odd coefficients $\{\tilde{b}_{2i+1}\}_{i=0}^{k}$ are zero. Then we can determine other coefficients as

$$\begin{aligned}
\tilde{b}_2 &= 30(b_2 - b_2) = 0 \\
\tilde{b}_4 &= b_4(60 - 15(3)_2 + 12(2)_3 - 7(1)_4) = 0 \\
\tilde{b}_6 &= b_6(90 - 15(5)_2 + 12(4)_3 - 7(3)_4 + (1)_6) = 0.
\end{aligned}$$

Hence since $k = 3, 4, \ldots$, we can write

$$\partial_{ij}\Delta^2\Phi_{\ell,k}(\mathbf{x}) = x_i x_j \sum_{i=8}^{2k+\ell} \tilde{b}_i r^{i-8},$$

and the result follows immediately. □

Lemma 3.5. *With spatial dimension d and smoothness parameter $k = 2, 3, \ldots$ let $\Phi_{\ell,k}$ be the original Wendland function. Then with $\mathbf{x} \in \mathbb{R}^d$ and $1 \leq j \leq d$ we have*

$$\partial_{jj}\Phi_{\ell,k}(\mathbf{x})|_{\mathbf{x}=\mathbf{0}} < 0,$$

and is independent of j.

Proof. With the chain rule, and once again with $\mathbf{x} = (x_1, \ldots, x_d)$ and $r = \|\mathbf{x}\|_2$, we have

$$\partial_{jj}\Phi_{\ell,k}(\mathbf{x}) = \frac{x_j^2}{r^2}\left(\phi_{\ell,k}^{(2)}(r) - \frac{1}{r}\phi_{\ell,k}^{(1)}(r)\right) + \frac{1}{r}\phi_{\ell,k}^{(1)}(r).$$

With Lemma 3.3, the term in brackets is equal to zero when $\mathbf{x} = \mathbf{0}$. Using (3.21) and noting that the first k odd coefficients are zero, this last term becomes

$$\frac{1}{r}\phi_{\ell,k}^{(1)}(r) = \sum_{i=2}^{2\ell+k} i\, b_i\, r^{i-2},$$

which means that the case of $\mathbf{x} = \mathbf{0}$, which is equivalent to $r = 0$, reduces down to $2b_2$. Now combining positive factors into a generic constant C, we have from Theorem 3.2

$$\begin{aligned}
b_2 &= C(-1)^k \binom{\frac{1}{2}}{k} \\
&= C\frac{(-1)^k}{\Gamma(\frac{1}{2} - (k-1))} \\
&= C(-1)^k(-1)^{k-1} < 0,
\end{aligned}$$

where we have also used [21, 8.339.3]

$$\Gamma\left(\frac{1}{2} - n\right) = \sqrt{\pi}\frac{(-4)^n n!}{(2n)!}.$$

□

Lemma 3.6. *With spatial dimension d and smoothness parameter $k = 3, 4, \dots$ let $\Phi_{\ell,k}$ be the original Wendland function. Then with $\mathbf{x} \in \mathbb{R}^d$ and $1 \le j \le d$ we have*

$$\partial_{jj}\Delta^2\Phi_{\ell,k}(\mathbf{x})|_{\mathbf{x}=\mathbf{0}} < 0,$$

and is independent of j.

Proof. With the chain rule, and once again with $\mathbf{x} = (x_1, \dots, x_d)$ and $r = \|\mathbf{x}\|_2$, we have

$$\begin{aligned}\partial_{jj}\Delta^2\Phi_{\ell,k}(\mathbf{x}) &= \frac{x_j^2}{r^2} \\ &\times \left(\phi_{\ell,k}^{(6)}(r) + \frac{1}{r}\phi_{\ell,k}^{(5)}(r) - \frac{7}{r^2}\phi_{\ell,k}^{(4)}(r) + \frac{12}{r^3}\phi_{\ell,k}^{(3)}(r) - \frac{15}{r^4}\phi_{\ell,k}^{(2)}(r) + \frac{15}{r^5}\phi_{\ell,k}^{(1)}(r)\right) \\ &\qquad + \frac{1}{r}\left(\phi_{\ell,k}^{(5)}(r) + \frac{2}{r}\phi_{\ell,k}^{(4)}(r) - \frac{3}{r^2}\phi_{\ell,k}^{(3)}(r) + \frac{3}{r^3}\phi_{\ell,k}^{(2)}(r) - \frac{3}{r^4}\phi_{\ell,k}^{(1)}(r)\right).\end{aligned}$$

With Lemma 3.3, the first term in the previous expression is equal to zero when $\mathbf{x} = \mathbf{0}$. As before, we can write the second term as a series

$$\sum_{i=1}^{2k+\ell} \underline{b}_i\, r^{i-6}.$$

Since $k \ge 3$, $\underline{b}_1 = \underline{b}_3 = \underline{b}_5 = 0$, equating coefficients gives

$$\begin{aligned}\underline{b}_2 &= b_2(-6 + 3(1)_2) = 0 \\ \underline{b}_4 &= b_4(-12 + 3(3)_2 - 3(2)_3 + 2(1)_4) = 0,\end{aligned}$$

which means we are left with

$$\sum_{i=6}^{2k+\ell} \underline{b}_i\, r^{i-6}.$$

Hence the case of $\mathbf{x} = \mathbf{0}$, which is equivalent to $r = 0$, reduces down to $\underline{b}_6$, which is given by

$$\underline{b}_6 = ((2)_5 + 2(3)_4 - 3(4)_3 + 3(5)_2 - 18)b_6 = 1152b_6.$$

As before, combining positive factors into a generic constant C and noting that $k = 3, 4, \dots$, we have from Theorem 3.2

$$\begin{aligned}b_6 &= C(-1)^k \binom{\frac{5}{2}}{k} \\ &= C\frac{(-1)^k}{\Gamma(\frac{1}{2} - (k-3))} \\ &= C(-1)^k(-1)^{k-3} < 0.\end{aligned}$$

□

3.3 The missing Wendland functions

The missing Wendland functions are defined by (3.1) when $\alpha = k + \frac{1}{2}$ where k is a non-negative integer with

$$\mu = \ell := \left\lfloor \frac{d+1}{2} \right\rfloor + k + 1.$$

Schaback [38] extended Wendland's original approach to cover the missing Wendland functions, which are the reproducing kernels of integer order Sobolev spaces in even dimensions d. An important distinction between the original Wendland functions and the missing Wendland functions is that the missing Wendland functions, whilst still being compactly supported, now have logarithmic and square-root multipliers of polynomial components.

Schaback [38] proved that the missing Wendland functions, $\phi_{\ell,k+\frac{1}{2}}$, are of the form

$$\phi_{\ell,k+\frac{1}{2}}(r) = p_{\ell,k}\left(\frac{r^2}{2}\right) L(r) + q_{\ell,k}\left(\frac{r^2}{2}\right) S(r), \tag{3.23}$$

where

$$L(r) := \log\left(\frac{r}{1+\sqrt{1-r^2}}\right) \quad \text{and} \quad S(r) := \sqrt{1-r^2}, \tag{3.24}$$

and $p_{\ell,k}$ and $q_{\ell,k}$ are polynomials. Whilst a closed form representation for $\phi_{\ell,k+\frac{1}{2}}(r)$ was not given in [38], this can be achieved using the same techniques used in their paper. We give the closed form representation in the following theorem.

Theorem 3.7. *Let d be a given spatial dimension, k a non-negative integer and $\ell = \lfloor (d+1)/2 \rfloor + k + 1$. Then the missing Wendland functions are given by*

$$\phi_{\ell,k+\frac{1}{2}}(r) = P_{\ell,k}\left(r^2\right) L(r) + Q_{\ell,k}\left(r^2\right) S(r), \tag{3.25}$$

where

$$P_{\ell,k}(r) := \frac{(-1)^k d_{\frac{1}{2},k-\frac{1}{2}}}{\Gamma\left(k+\frac{1}{2}\right) 2^{2k-\frac{1}{2}}} \sum_{j=0}^{\lfloor \frac{\ell-1}{2} \rfloor} \binom{\ell}{2j+1} \frac{d_{\frac{1}{2},j+k+\frac{1}{2}}}{d_{1,j+k+1}\left(j+\frac{3}{2}\right)_k} r^{j+k+1}, \tag{3.26}$$

and

$$Q_{\ell,k}(r) := \frac{1}{\Gamma\left(k+\frac{1}{2}\right) 2^{k-\frac{1}{2}}} \left(\sum_{j=0}^{k-1} q_{1,j} r^j + \sum_{j=0}^{\lfloor \frac{\ell}{2} \rfloor + k} q_{2,j} r^j - \sum_{j=0}^{\lfloor \frac{\ell-1}{2} \rfloor + k} q_{3,j} r^j \right), \tag{3.27}$$

with

$$q_{1,j} := (-1)^{k-1} \sum_{n=j}^{k-1} \binom{n}{j} (-1)^{n+j} \frac{d_{n+\frac{3}{2},k-\frac{1}{2}}}{2^{k-n}} \sum_{m=0}^{\ell} \frac{(-1)^m \binom{\ell}{m}}{\left(\frac{m}{2}+1\right)_{k-n}}, \tag{3.28}$$

$$q_{2,j} := (-1)^k \sum_{n=(j-k)_+}^{\lfloor \frac{\ell}{2} \rfloor} \binom{\ell}{2n} \frac{d_{\frac{1}{2},k-\frac{1}{2}}}{2^k (n+1)_k} \frac{d_{n+k-j+1,n+k}}{d_{n+k-j+\frac{1}{2},n+k+\frac{1}{2}}}, \tag{3.29}$$

$$q_{3,j} := (-1)^k \sum_{n=(j-k)_+}^{\lfloor \frac{\ell-1}{2} \rfloor} \binom{\ell}{2n+1} \frac{d_{\frac{1}{2},k-\frac{1}{2}}}{2^k \left(n+\frac{3}{2}\right)_k} \frac{d_{n+k-j+\frac{3}{2},n+k+\frac{1}{2}}}{d_{n+k-j+1,n+k+1}} \tag{3.30}$$

where

$$d_{i,j} := \prod_{m=i}^{j} (2m).$$

and $L(r)$ and $S(r)$ are given by (3.24)*.*

Proof. We begin by applying the binomial theorem to (3.1), which with the change of variable $z := \sqrt{s^2 - r^2}$, gives

$$\phi_{\ell,k+\frac{1}{2}}(r) = \frac{1}{\Gamma\left(k+\frac{1}{2}\right) 2^{k-\frac{1}{2}}} \sum_{j=0}^{\ell} (-1)^j \binom{\ell}{j} g_{\frac{j}{2},k}(x), \tag{3.31}$$

where

$$g_{n,k}(x) := \int_0^{\sqrt{1-x^2}} \left(x^2 + z^2\right)^n z^{2k} \, \mathrm{d}z. \tag{3.32}$$

Integration by parts yields

$$g_{n,k}(r) = S(r) \sum_{i=1}^{k} \frac{(-1)^{i-1} d_{k+\frac{3}{2}-i,k-\frac{1}{2}}}{2^i (n+1)_i} \left(1-r^2\right)^{k-i} + \frac{(-1)^k d_{\frac{1}{2},k-\frac{1}{2}}}{2^k (n+1)_k} g_{n+k,0}(r). \tag{3.33}$$

From [38], we know that

$$g_{n+1,0}(x) = \frac{2n+2}{2n+3} x^2 g_{n,0}(x) + \frac{S(x)}{2n+3}.$$

In conjunction with

$$\begin{aligned} g_{0,0}(x) &= S(x) \\ g_{\frac{1}{2},0}(x) &= \frac{1}{2}\left(S(x) - x^2 L(x)\right), \end{aligned}$$

we obtain

$$g_{n,0}(x) = S(x) p_{1,n}(x^2) \tag{3.34}$$

$$g_{n-\frac{1}{2},0}(x) = L(x) p_{2,n}(x^2) + S(x) p_{3,n-1}(x^2), \tag{3.35}$$

where

$$p_{1,n}(r) := \sum_{j=0}^{n} \frac{d_{j+1,n}}{d_{j+\frac{1}{2},n+\frac{1}{2}}} r^{n-j},$$

$$p_{2,n}(r) := -\frac{d_{\frac{1}{2},n-\frac{1}{2}}}{d_{1,n}} r^n,$$

and

$$p_{3,n}(r) := \sum_{j=0}^{n} \frac{d_{j+\frac{3}{2},n+\frac{1}{2}}}{d_{j+1,n+1}} r^{n-j}.$$

Then (3.31), (3.33), (3.34) and (3.35) together lead us to

$$\phi_{\ell,k+\frac{1}{2}}(r) = \frac{S(r)}{\Gamma\left(k+\frac{1}{2}\right)2^{k-\frac{1}{2}}}\Bigg\{ \underbrace{\sum_{j=0}^{\ell}(-1)^j\binom{\ell}{j}\sum_{i=1}^{k}\frac{(-1)^{i-1}d_{k+\frac{3}{2}-i,k-\frac{1}{2}}}{2^i\left(\frac{j}{2}+1\right)_i}\left(1-r^2\right)^{k-i}}_{:=(A)}$$
$$+\underbrace{\sum_{j=0}^{\lfloor\frac{\ell}{2}\rfloor}\binom{\ell}{2j}\frac{(-1)^k d_{\frac{1}{2},k-\frac{1}{2}}}{2^k(j+1)_k}p_{1,j+k}(r^2)}_{:=(B)} - \underbrace{\sum_{j=0}^{\lfloor\frac{\ell}{2}\rfloor}\binom{\ell}{2j+1}\frac{(-1)^k d_{\frac{1}{2},k-\frac{1}{2}}}{2^k\left(j+\frac{3}{2}\right)_k}p_{3,j+k}(r^2)}_{:=(C)}\Bigg\}$$
$$-\frac{L(r)}{\Gamma\left(k+\frac{1}{2}\right)2^{k-\frac{1}{2}}}\Bigg\{\underbrace{\sum_{j=0}^{\lfloor\frac{\ell}{2}\rfloor}\binom{\ell}{2j+1}\frac{(-1)^k d_{\frac{1}{2},k-\frac{1}{2}}}{2^k\left(j+\frac{3}{2}\right)_k}p_{2,j+k+1}(r^2)}_{:=(D)}\Bigg\}.$$

Now we simplify expressions (A)-(D).

$$\begin{aligned}(A) &= \sum_{j=0}^{\ell}(-1)^j\binom{\ell}{j}\sum_{i=1}^{k}\frac{(-1)^{i-1}d_{k+\frac{3}{2}-i,k-\frac{1}{2}}}{2^i\left(\frac{j}{2}+1\right)_i}\left(1-r^2\right)^{k-i}\\
&= \sum_{j=0}^{\ell}(-1)^j\binom{\ell}{j}\sum_{n=0}^{k-1}\frac{(-1)^{k-n-1}d_{n+\frac{3}{2},k-\frac{1}{2}}}{2^{k-n}\left(\frac{j}{2}+1\right)_{k-n}}\left(1-r^2\right)^{n}\\
&= (-1)^{k-1}\sum_{i=0}^{k-1}r^{2i}\sum_{n=i}^{k-1}\binom{n}{i}(-1)^{n+i}\frac{d_{n+\frac{3}{2},k-\frac{1}{2}}}{2^{k-n}}\sum_{j=0}^{\ell}\frac{(-1)^j\binom{\ell}{j}}{\left(\frac{j}{2}+1\right)_{k-n}}.\end{aligned}$$

$$\begin{aligned}(B) &= \sum_{j=0}^{\lfloor\frac{\ell}{2}\rfloor}\binom{\ell}{2j}\frac{(-1)^k d_{\frac{1}{2},k-\frac{1}{2}}}{2^k(j+1)_k}\sum_{i=0}^{j+k}\frac{d_{i+1,j+k}}{d_{i+\frac{1}{2},j+k+\frac{1}{2}}}r^{2(j+k-i)}\\
&= \sum_{j=0}^{\lfloor\frac{\ell}{2}\rfloor}\binom{\ell}{2j}\frac{(-1)^k d_{\frac{1}{2},k-\frac{1}{2}}}{2^k(j+1)_k}\sum_{n=0}^{j+k}\frac{d_{j+k-n+1,j+k}}{d_{j+k-n+\frac{1}{2},j+k+\frac{1}{2}}}r^{2n}\\
&= \sum_{i=0}^{\lfloor\frac{\ell}{2}\rfloor+k}r^{2i}\sum_{j=(i-k)_+}^{\lfloor\frac{\ell}{2}\rfloor}\binom{\ell}{2j}\frac{(-1)^k d_{\frac{1}{2},k-\frac{1}{2}}}{2^k(j+1)_k}\frac{d_{j+k-i+1,j+k}}{d_{j+k-i+\frac{1}{2},j+k+\frac{1}{2}}}.\end{aligned}$$

$$\begin{aligned}(C) &= \sum_{j=0}^{\lfloor\frac{\ell-1}{2}\rfloor}\binom{\ell}{2j+1}\frac{(-1)^k d_{\frac{1}{2},k-\frac{1}{2}}}{2^k\left(j+\frac{3}{2}\right)_k}\sum_{i=0}^{j+k}\frac{d_{i+\frac{3}{2},j+k+\frac{1}{2}}}{d_{i+1,j+k+1}}r^{2(j+k-i)}\\
&= \sum_{j=0}^{\lfloor\frac{\ell-1}{2}\rfloor}\binom{\ell}{2j+1}\frac{(-1)^k d_{\frac{1}{2},k-\frac{1}{2}}}{2^k\left(j+\frac{3}{2}\right)_k}\sum_{n=0}^{j+k}\frac{d_{j+k-n+\frac{3}{2},j+k}}{d_{j+k-n+1,j+k+1}}r^{2n}\\
&= \sum_{i=0}^{\lfloor\frac{\ell-1}{2}\rfloor+k}r^{2i}\sum_{j=(i-k)_+}^{\lfloor\frac{\ell-1}{2}\rfloor}\binom{\ell}{2j+1}\frac{(-1)^k d_{\frac{1}{2},k-\frac{1}{2}}}{2^k\left(j+\frac{3}{2}\right)_k}\frac{d_{j+k-i+\frac{3}{2},j+k+\frac{1}{2}}}{d_{j+k-i+1,j+k+1}}.\end{aligned}$$

$$(D) = \sum_{j=0}^{\lfloor\frac{\ell}{2}\rfloor}\binom{\ell}{2j+1}\frac{(-1)^k d_{\frac{1}{2},k-\frac{1}{2}}}{2^k\left(j+\frac{3}{2}\right)_k}\frac{d_{\frac{1}{2},j+k+\frac{1}{2}}}{d_{1,j+k+1}}r^{2(j+k+1)}.$$

$\square$

We have the following closed form representation of the missing Wendland functions from [23, Corollary 4.6].

Theorem 3.8. *Let d be a given space dimension and let k be a non-negative integer and define*

$$\gamma_j := (-1)^j \frac{\binom{2k+\ell+1}{k+\ell+j}}{\binom{\ell+j-1}{\ell}}, \quad \textit{for} \quad j = 1, \dots, k+1.$$

Set

$$\ell = \left\lfloor \frac{d+1}{2} \right\rfloor + k + 1 \quad \textit{and} \quad A_{\ell,k} := \frac{(-1)^{k+1}}{\sqrt{\pi}} \frac{\ell\,(\ell+k)!}{\ell+k-\frac{1}{2}(\ell+2k+1)!}.$$

Then the missing Wendland functions have the following representation

$$\phi_{\ell,k+\frac{1}{2}} = A_{\ell,k}\left[P(r)\log\left(\frac{1+\sqrt{1-r^2}}{1-\sqrt{1-r^2}}\right) + Q(r)\sqrt{1-r^2}\right],$$

with the following cases:

- *If ℓ is even, then P and Q are polynomials of degree $\ell+2k$ given by*

$$P(r) = r^{\ell+2k+1}\sum_{j=0}^{\frac{\ell}{2}-1} \alpha_j^{(\text{even})} T_{2j+1}\left(\frac{1}{r}\right),$$

$$Q(r) = r^{\ell+2k}\left[\frac{1}{\ell}\sum_{j=1}^{k+1}\gamma_j U_{\ell-2+2j}\left(\frac{1}{r}\right) - \sum_{j=0}^{\frac{\ell}{2}-1}\beta_j^{(\text{even})} U_{2j}\left(\frac{1}{r}\right)\right],$$

  where $T_n(r)$ denotes the Chebyshev polynomial of the first kind of degree n, $U_n(r)$ denotes the Chebyshev polynomial of the second kind of degree n and where the adjusted coefficients are given, respectively, by

$$\alpha_j^{(\text{even})} := \binom{\ell+2k+1}{\frac{\ell}{2}+k-j}\binom{\ell-1}{\frac{\ell}{2}-1-j},$$

  and

$$\beta_j^{(\text{even})} := \alpha_j^{(\text{even})}\left[\Psi\left(\frac{\ell}{2}+j+1\right) - \Psi\left(\frac{\ell}{2}-j\right) + \Psi\left(\frac{\ell}{2}+k+j+2\right) - \Psi\left(\frac{\ell}{2}+k+1-j\right)\right], \quad (3.36)$$

  where $\Psi(\cdot)$ denotes the digamma function (see [1, 6.3.1]) defined by

$$\Psi(z) = \frac{\Gamma'(z)}{\Gamma(z)}. \quad (3.37)$$

- *If ℓ is odd, then P is a polynomial of degree $\ell+2k+1$ given by*

$$P(r) = r^{\ell+2k+1}\left[\frac{\alpha_0^{(\text{odd})}}{2} + \sum_{j=1}^{\frac{\ell-1}{2}}\alpha_j^{(\text{odd})} T_{2j}\left(\frac{1}{r}\right)\right],$$

and Q is a polynomial of degree $\ell + 2k - 1$ given by

$$Q(r) = r^{\ell+2k}\left[\frac{1}{\ell}\sum_{j=1}^{k+1}\gamma_j U_{\ell-2+2j}\left(\frac{1}{r}\right) - \sum_{j=0}^{\frac{\ell-1}{2}}\beta_j^{(\mathrm{odd})}U_{2j-1}\left(\frac{1}{r}\right)\right],$$

where the adjusted coefficients are given, respectively, by

$$\alpha_j^{(\mathrm{odd})} := \binom{\ell+2k+1}{\frac{\ell+1}{2}+k-j}\binom{\ell-1}{\frac{\ell-1}{2}-j},$$

and

$$\beta_j^{(\mathrm{odd})} := \alpha_j^{(\mathrm{odd})}\left[\Psi\left(\frac{\ell+1}{2}+j\right) - \Psi\left(\frac{\ell+1}{2}-j\right) + \Psi\left(\frac{\ell+1}{2}+k+j+1\right) - \Psi\left(\frac{\ell+1}{2}+k+1-j\right)\right]. \quad (3.38)$$

We give explicit formulae for the missing Wendland functions for $d = 2$ and $k = 0, 1$ and 2 in Table 3.2. The support of all the missing Wendland functions is $r \in [0, 1]$. It is

k	Missing Wendland function
0	$\phi_{2,\frac{1}{2}}(r) \doteq 3r^2L(r) + (2r^2+1)S(r)$
1	$\phi_{3,\frac{3}{2}}(r) \doteq -15r^4(6+r^2)L(r) - (81r^4+28r^2-4)S(r)$
2	$\phi_{4,\frac{5}{2}}(r) \doteq (945r^8+2520r^6)L(r) + (256r^8+2639r^6+690r^4-136r^2+16)S(r)$

Table 3.2. *The missing Wendland functions $\phi_{\ell,k+\frac{1}{2}}(r)$ for $d = 2$ and $k = 0, 1, 2$.*

proved in [38] that with $\ell = \lfloor\frac{d+1}{2}\rfloor + k + 1$ and k being any non-negative half-integer, for an integer dimension d the kernel

$$K(\mathbf{x}, \mathbf{y}) = \phi_{\ell,k+\frac{1}{2}}(\|\mathbf{x}-\mathbf{y}\|), \quad \mathbf{x}, \mathbf{y} \in \mathbb{R}^d, \quad (3.39)$$

is the reproducing kernel of a Hilbert space which is norm equivalent to the Sobolev space $H^{\frac{d}{2}+k+1}(\mathbb{R}^d)$.

Hereafter when we refer to the *Wendland functions* we will mean both the original and missing Wendland functions. With k a non-negative integer and

$$\ell = \left\lfloor\frac{d}{2}+\alpha\right\rfloor + 1$$

and $r \in [0, 1]$, $\phi_{\ell,\alpha}(r)$ with $\alpha = k$ an integer will denote the original Wendland functions and $\phi_{\ell,\alpha}$ with $\alpha = k + \frac{1}{2}$ will denote the missing Wendland functions.

Chapter Four

Fourier transform of the generalised Wendland functions

This chapter will investigate the Fourier transform of the generalised Wendland functions $\phi_{\mu,\alpha}$. Section 4.1 recalls the definition of the Fourier transform and states several results that we will require later. Section 4.2 gives the Fourier transform of the generalised Wendland functions $\phi_{\mu,\alpha}$. Section 4.3 presents the native spaces generated by these functions. Section 4.4 provides several important identities of the Fourier transform of the generalised Wendland functions $\phi_{\mu,\alpha}$. Section 4.5 provides closed form representations for the Fourier transform of the original Wendland functions $\phi_{\ell,k}$ and Section 4.6 does the same for the missing Wendland functions $\phi_{\ell,k+\frac{1}{2}}$. Section 4.7 concludes with several properties of the Fourier transform of the generalised Wendland functions $\phi_{\mu,\alpha}$.

For the moment, we deal with arbitrary $\mu > -1$ in the generalised Wendland functions, until Theorem 4.4, which will enable us to be more precise about how to choose μ.

4.1 Fourier transforms

This section provides definitions and outlines some key properties. For further information, we refer the interested reader to [41, 51].

4.1.1 Definitions and preliminaries

With the Fourier transform of $f \in L_1(\mathbb{R}^d)$ defined as

$$\widehat{f}(\mathbf{w}) := (2\pi)^{-\frac{d}{2}} \int\limits_{\mathbb{R}^d} f(\mathbf{x})\, e^{-i\mathbf{w}\cdot\mathbf{x}}\, \mathrm{d}\mathbf{x}, \quad \mathbf{w} \in \mathbb{R}^d, \tag{4.1}$$

it is well known that the Fourier transform of a radial function $\Phi \in L_1(\mathbb{R}^d) \cap C(\mathbb{R}^d)$ is also radial and is given by $\widehat{\Phi}(\mathbf{w}) = \mathcal{F}_d\phi(\|\mathbf{w}\|_2)$ where

$$\mathcal{F}_d\phi(z) := z^{1-\frac{d}{2}} \int_0^\infty \phi(y)\, y^{\frac{d}{2}}\, J_{\frac{d}{2}-1}(zy)\, \mathrm{d}y, \tag{4.2}$$

and $J_\nu(y)$ denotes the Bessel function of the first kind with order ν. In particular, we have the following result.

Lemma 4.1.

$$\mathcal{F}_d\phi(0) := \frac{1}{2^{\frac{d}{2}-1}\Gamma\left(\frac{d}{2}\right)} \int_0^\infty \phi(y)\, y^{d-1}\, \mathrm{d}y. \tag{4.3}$$

Proof. With (4.2), we need to consider

$$\lim_{z\to 0} z^{1-\frac{d}{2}} \int_0^\infty \phi(y)\, y^{\frac{d}{2}}\, J_{\frac{d}{2}-1}(z\,y)\, \mathrm{d}y. \tag{4.4}$$

Since we have [11, 10.14.4]

$$|J_\nu(x)| \le \frac{|x|^\nu}{2^\nu\Gamma(\nu+1)}, \quad x \in \mathbb{R}, \nu \ge -\frac{1}{2},$$

we can see that the absolute value of the integrand (ignoring constants) in (4.4) is dominated by

$$|\phi(y)|y^{d-1}.$$

We know that $\Phi \in L_1(\mathbb{R}^d)$, which means that

$$\int_0^\infty |\phi(y)|y^{d-1}\mathrm{d}y < \infty,$$

and hence since the dominating function is integrable, we can apply the dominated convergence theorem to interchange the limit and integral in (4.4), which with the limiting form of the Bessel function [11, 10.7.3]

$$|x|^{-\nu}J_\nu(x) \to \frac{1}{2^\nu\Gamma(\nu+1)} \quad \text{as} \quad x \to 0,$$

gives the stated result. □

Lemma 4.1 also follows immediately from

$$\mathcal{F}_d\phi(0) = (2\pi)^{-d/2}\int_{\mathbb{R}^d} \phi(\|\mathbf{x}\|_2)\, \mathrm{d}\mathbf{x} = \frac{\mathrm{vol}(\mathbb{S}^{d-1})}{(2\pi)^{d/2}} \int_0^\infty r^{d-1}\phi(r)\mathrm{d}r,$$

where $\mathbb{S}^{d-1}$ is the unit sphere in $\mathbb{R}^d$.

From the Fourier inversion theorem applied to radial functions, we know that if $\Phi \in L_1(\mathbb{R}^d)$ with $\Phi(\mathbf{x}) = \phi(\|\mathbf{x}\|_2), \phi : [0,\infty) \to \mathbb{R}$, and if $\widehat{\Phi} \in L_1(\mathbb{R}^d)$, then

$$\phi(y) = y^{1-\frac{d}{2}} \int_0^\infty \mathcal{F}_d\phi(z)\, z^{\frac{d}{2}}\, J_{\frac{d}{2}-1}(yz)\, \mathrm{d}z. \tag{4.5}$$

We also recall that if $f \in L_1(\mathbb{R}^d)$ is continuous at zero and positive definite then its Fourier transform is in $L_1(\mathbb{R}^d)$ and is non-negative [41].

For example, we can see that the Fourier transform of the Gaussian RBF is

$$\widehat{G}_{\vartheta}(z) = \frac{1}{(2\vartheta)^{\frac{d}{2}}} e^{-\frac{z^2}{4\vartheta}}, \quad z \in \mathbb{R}.$$

We note that $\widehat{G}_{\vartheta}(z)$ is the $d-$dimensional Fourier transform of

$$\mathbb{R}^d \ni \mathbf{x} \mapsto \exp\left(-\vartheta\|\mathbf{x}\|_2^2\right).$$

4.2 Fourier transform of the generalised Wendland functions

This section will present the Fourier transform of the generalised Wendland functions $\phi_{\mu,\alpha}$. First we present a hypergeometric function identity, which we will then use to derive the Fourier transform of the generalised Wendland functions $\phi_{\mu,\alpha}$.

Theorem 4.2. *Let $\mu > -1, \alpha > 0$ and $d > 0$. Then*

$$\frac{\Gamma(\mu+1)}{2^{\mu+\alpha}\Gamma(\mu+\alpha+1)} \int_0^1 \left(1-y^2\right)^{\mu+\alpha} y^{\frac{d}{2}} {}_2F_1\left(\frac{\mu}{2}, \frac{\mu+1}{2}; \mu+\alpha+1; 1-y^2\right) J_{\frac{d}{2}-1}(zy)\,\mathrm{d}y =$$
$$C_d^{\mu,\alpha} z^{\frac{d}{2}-1} {}_1F_2\left(\frac{d+1}{2}+\alpha; \frac{\mu+d+1}{2}+\alpha, \frac{\mu+d+2}{2}+\alpha; -\frac{z^2}{4}\right), \quad z > 0,$$

where

$$C_d^{\mu,\alpha} := \frac{2^{\alpha+\frac{d}{2}}\Gamma(\mu+1)\Gamma\left(\frac{d+1}{2}+\alpha\right)}{\sqrt{\pi}\,\Gamma(\mu+d+2\alpha+1)}. \tag{4.6}$$

Proof. With (3.5) and (3.1) and re-parametrising the triangle $\{(y,t) : 0 \leq y \leq 1, y \leq t \leq 1\}$ as $\{(xs,x) : 0 \leq x \leq 1, 0 \leq s \leq 1\}$, we can see that the left hand side of the equation in the Theorem statement is given by

$$\frac{1}{2^{\alpha-1}\Gamma(\alpha)} \int_0^1 \int_y^1 (1-t)^{\mu}\, t\left(t^2-y^2\right)^{\alpha-1} y^{\frac{d}{2}} J_{\frac{d}{2}-1}(zy)\,\mathrm{d}t\,\mathrm{d}y$$
$$= \frac{1}{2^{\alpha-1}\Gamma(\alpha)} \int_0^1 \int_0^1 x^{2\alpha+\frac{d}{2}}(1-x)^{\mu} s^{\frac{d}{2}} \left(1-s^2\right)^{\alpha-1} J_{\frac{d}{2}-1}(zsx)\,\mathrm{d}s\,\mathrm{d}x.$$

From [21, 6.567.1], we have that

$$\int_0^1 x^{\nu+1}\left(1-x^2\right)^{\mu} J_{\nu}(bx)\,\mathrm{d}x = 2^{\mu}\Gamma(\mu+1)b^{-(\mu+1)}J_{\nu+\mu+1}(b), \quad b > 0,$$

which means we can simplify our expression to

$$z^{-\alpha} \int_0^1 x^{\alpha+\frac{d}{2}}(1-x)^{\mu} J_{\alpha+\frac{d}{2}-1}(zx)\,\mathrm{d}x.$$

With the following identity [21, 6.569]

$$\int_0^1 x^\lambda (1-x)^{\mu-1} J_\nu(ax)\,\mathrm{d}x = \frac{\Gamma(\mu)\Gamma(\lambda+\nu+1)2^{-\nu}a^\nu}{\Gamma(\nu+1)\Gamma(\lambda+\mu+\nu+1)}$$
$$\times\, {}_2F_3\left(\frac{\lambda+\nu+1}{2}, \frac{\lambda+\nu+2}{2}; \nu+1, \frac{\lambda+\nu+\mu+1}{2}, \frac{\lambda+\nu+\mu+2}{2}; -\frac{a^2}{4}\right),$$
$$\mu > 0, \lambda+\nu > -1,$$

which is valid since $\mu+1 > 0$ and $2\alpha+d-1 > -1$ by assumption, the result follows after applying the duplication formula for the Gamma function, namely

$$\Gamma(2z) = \frac{2^{2z-1}}{\sqrt{\pi}}\Gamma(z)\Gamma\left(z+\frac{1}{2}\right), \tag{4.7}$$

and noting that in our case, the ${}_2F_3$ hypergeometric function simplifies down to a ${}_1F_2$ since the first parameters in the numerator and denominator are equal. □

Substituting (3.5) into (4.2) we can see that we get exactly the integral on the left hand side of the previous theorem, and hence this result also gives us the Fourier transform of the generalised Wendland functions $\phi_{\mu,\alpha}$, which we state next.

Theorem 4.3. *The d-dimensional Fourier transform of the generalised Wendland functions $\phi_{\mu,\alpha}$, with $\mu > -1$, $\alpha > 0$ is*

$$\mathcal{F}_d\phi_{\mu,\alpha}(z) = C_d^{\mu,\alpha}\,{}_1F_2\left(\frac{d+1}{2}+\alpha; \frac{\mu+d+1}{2}+\alpha, \frac{\mu+d+2}{2}+\alpha; -\frac{z^2}{4}\right), \quad z \ge 0,$$

where $C_d^{\mu,\alpha}$ is given by (4.7).

Next, we determine for a given dimension d, the full range of parameters μ and α for which the function $\phi_{\mu,\alpha}$ generates a d-dimensional positive definite function.

Theorem 4.4. *The generalised Wendland function $\phi_{\mu,\alpha}$ generates a positive definite function on $\mathbb{R}^d$ if and only if its parameters satisfy*

$$\mu \ge \frac{d+1}{2}+\alpha.$$

Proof. This follows directly from [29] which proves that

$${}_1F_2\left(a; a+\frac{b}{2}, a+\frac{b+1}{2}; -\frac{z^2}{4}\right) > 0, \quad z > 0,$$

for $b \ge 2a \ge 0$, for $b \ge a \ge 1$, or for $0 \le a \le 1, b \ge 1$. It is also proven that this function cannot be strictly positive for $0 \le b < a$ or $a = b, 0 < a < 1$.

In our case, $a = \frac{d+1}{2}+\alpha > 0$ since $d > 0$ and $\alpha > 0$ and hence necessary and sufficient conditions reduce to $b \ge a$ which means that

$$\mu \ge \frac{d+1}{2}+\alpha.$$

□

As a result of Theorem 4.4, we will henceforth consider

$$\mu := \frac{d+1}{2} + \alpha + \beta, \tag{4.8}$$

with β a non-negative constant. We will consider the impact of different choices of β in Section 5.3. Note that we have the following result, which is analogous to (3.6) for the original and missing Wendland functions. With μ defined by (4.8),

$$\mu \sim \alpha \text{ as } \alpha \to \infty. \tag{4.9}$$

4.3 Native Spaces

In this section, we examine the decay rate of the Fourier transforms of the generalised Wendland functions to establish the nature of the reproducing kernel Hilbert space $\mathcal{N}_{\phi_{\mu,\alpha}}$, whose reproducing kernel is the induced kernel

$$\Phi_{\mu,\alpha}(\mathbf{x},\mathbf{y}) = \Phi_{\mu,\alpha}(\mathbf{x}-\mathbf{y}) = \phi_{\mu,\alpha}(\|\mathbf{x}-\mathbf{y}\|_2) \quad \mathbf{x},\mathbf{y} \in \mathbb{R}^d. \tag{4.10}$$

Theorem 4.5. *The d-dimensional Fourier transform of the generalised Wendland functions, $\mathcal{F}_d\phi_{\mu,\alpha}$, with $\mu \geq \alpha + \frac{d+1}{2}$ satisfies*

$$\mathcal{F}_d\phi_{\mu,\alpha}(z) = \Theta\left(z^{-(d+2\alpha+1)}\right) \quad \textit{for} \quad z \to \infty.$$

Proof. We need to show that for $z \geq z_0$, there exist two positive constants, c_3 and c_4, such that

$$c_3 \leq z^{d+2\alpha+1}\mathcal{F}_d\phi_{\mu,\alpha}(z) \leq c_4. \tag{4.11}$$

From [13], we have the following asymptotic expansion for $\mathcal{F}_d\phi_{\mu,\alpha}(z)$ as $z \to \infty$ and $|\arg(z)| < \frac{\pi}{2}$

$$\begin{aligned}\mathcal{F}_d\phi_{\mu,\alpha}(z) = {} & \frac{\Gamma(\mu+d+1+2\alpha)}{\Gamma(\mu)} z^{-d-2\alpha-1}\left\{1+O(z^{-2})\right\} \\ & + \frac{\Gamma(\mu+d+1+2\alpha)}{\Gamma\left(\frac{d+1}{2}+\alpha\right)} \frac{z^{-\left(\mu+\alpha+\frac{d+1}{2}\right)}}{2^{\left(\frac{d+1}{2}+\alpha\right)-1}} \left\{\cos\left[z - \frac{\pi}{2}\left(\mu+\alpha+\frac{d+1}{2}\right)\right] + O(z^{-1})\right\}.\end{aligned}$$

Collecting terms not depending on z into constants c_5, c_6 and c_7 gives the following expression

$$z^{d+2\alpha+1}\mathcal{F}_d\phi_{\mu,\alpha}(z) = c_5\left\{1+O(z^{-2})\right\} + c_6 z^{\alpha+\frac{d+1}{2}-\mu}\left\{\cos(z-c_7) + O(z^{-1})\right\}. \tag{4.12}$$

Then for the upper bound, since $\cos(z)$ is bounded by 1 in absolute value, we can see that for $z \geq z_2$, there exists an $\epsilon_2 > 0$ such that

$$z^{d+2\alpha+1}\mathcal{F}_d\phi_{\mu,\alpha}(z) \quad \leq \quad \left(c_5 + c_6 z^{\alpha+\frac{d+1}{2}-\mu}\right)(1+\epsilon_2)$$

$$\begin{aligned} &\leq (c_5 + c_6)(1 + \epsilon_2) \\ &=: c_4, \end{aligned}$$

which is positive since all its components are also positive. We proceed similarly for the lower bound and we first consider the case where $\mu = \frac{d+1}{2} + \alpha$. For $z \geq z_1$, there exists an $\epsilon_1 > 0$ such that

$$\begin{aligned} z^{d+2\alpha+1}\mathcal{F}_d\phi_{\mu,\alpha}(z) &\geq c_5(1-\epsilon_1) - c_6(1+\epsilon_1) \\ &= c_5 - c_6 - \epsilon_1(c_5 + c_6) \\ &=: c_3. \end{aligned}$$

For small enough ϵ_1, we see that $c_3 > 0$ since

$$\begin{aligned} c_5 - c_6 &= \Gamma(\mu + d + 2\alpha + 1)\left\{\frac{1}{\Gamma\left(\frac{d+1}{2}+\alpha\right)} - \frac{1}{\Gamma\left(\frac{d+1}{2}+\alpha\right)2^{\left(\frac{d+1}{2}+\alpha\right)-1}}\right\} \\ &> 0. \end{aligned}$$

Since the second term on the right hand side of (4.12) is decaying for $\mu > \frac{d+1}{2} + \alpha$, the existence of a lower bound in this case follows similarly. Setting $z_0 := \max(z_1, z_2)$ completes the proof. $\square$

With Theorem 4.5 and the asymptotic decay of functions in Sobolev spaces (see e.g. [2]), we have the following result on the native spaces generated by the generalised Wendland functions $\phi_{\mu,\alpha}$.

Corollary 4.6. *Let $d \geq 1$ denote a fixed spatial dimension and $\alpha, \beta > 0$. The generalised Wendland function $\phi_{\frac{d+1}{2}+\alpha+\beta,\alpha}$ is reproducing in a Hilbert space which is isomorphic to the Sobolev space $H^{\frac{d+1}{2}+\alpha}\left(\mathbb{R}^d\right)$.*

With Theorem 4.5 and Corollary 4.6, we can state one more result.

Corollary 4.7. *Every Sobolev space $H^\tau(\mathbb{R}^d)$ with $\tau > (d+1)/2$ has a compactly supported and radial reproducing kernel.*

4.3.1 Norm equivalence for the scaled Wendland functions

This subsection will present an important result regarding norm equivalence between the Sobolev spaces and the native spaces generated by the scaled generalised Wendland functions.

With scaling defined by (2.1) and where Φ generates the native space $H^\tau(\mathbb{R}^d)$, the Fourier transform of Φ_δ, $\widehat{\Phi_\delta}(\boldsymbol{\omega}) = \widehat{\Phi}(\delta\boldsymbol{\omega})$, satisfies

$$c_8\left(1+\delta^2\|\boldsymbol{\omega}\|_2^2\right)^{-\tau} \leq \widehat{\Phi_\delta}(\boldsymbol{\omega}) \leq c_9\left(1+\delta^2\|\boldsymbol{\omega}\|_2^2\right)^{-\tau}, \quad \boldsymbol{\omega} \in \mathbb{R}^d. \tag{4.13}$$

We also need norm equivalence as stated in the following lemma.

Lemma 4.8. *For every $\delta \in (0, \delta_a]$ and for all $g \in H^\tau(\mathbb{R}^d)$, there exist constants $0 < c_3 \leq c_4$ such that*

$$c_{10}\|g\|_{\Phi_\delta} \leq \|g\|_{H^\tau(\mathbb{R}^d)} \leq c_{11}\delta^{-\tau}\|g\|_{\Phi_\delta}.$$

Proof. The case $\delta_a \leq 1$ was proven in [53] with $c_{10} = c_7^{1/2}$ and $c_{11} = c_8^{1/2}$. To extend this to the case where $\delta_a > 1$, note that for $\delta > 1$ we have

$$\left(1+\|\boldsymbol{\omega}\|_2^2\right)^\tau = \delta^{-2\tau}\left(\delta^2+\delta^2\|\boldsymbol{\omega}\|_2^2\right)^\tau \geq \delta_a^{-2\tau}\left(1+\delta^2\|\boldsymbol{\omega}\|_2^2\right)^\tau.$$

Together with (2.5), (4.13) and (3.19) we can see that

$$\begin{aligned}
\|g\|_{H^\tau(\mathbb{R}^d)}^2 &= \int_{\mathbb{R}^d} |\widehat{g}(\boldsymbol{\omega})|^2\left(1+\|\boldsymbol{\omega}\|_2^2\right)^\tau \mathrm{d}\boldsymbol{\omega} \\
&\geq \delta_a^{-2\tau}\int_{\mathbb{R}^d} |\widehat{g}(\boldsymbol{\omega})|^2\left(1+\delta^2\|\boldsymbol{\omega}\|_2^2\right)^\tau \mathrm{d}\boldsymbol{\omega} \\
&\geq c_7\delta_a^{-2\tau}\int_{\mathbb{R}^d} \frac{|\widehat{g}(\boldsymbol{\omega})|^2}{\widehat{\Phi_\delta}(\boldsymbol{\omega})}\mathrm{d}\boldsymbol{\omega} \\
&\geq c_7\delta_a^{-2\tau}\|g\|_{\Phi_\delta}^2.
\end{aligned}$$

For the upper bound, we can just use $\delta > 1$ directly to derive

$$\begin{aligned}
\|g\|_{H^\tau(\mathbb{R}^d)}^2 &= \int_{\mathbb{R}^d} |\widehat{g}(\boldsymbol{\omega})|^2\left(1+\|\boldsymbol{\omega}\|_2^2\right)^\tau \mathrm{d}\boldsymbol{\omega} \\
&\leq \int_{\mathbb{R}^d} |\widehat{g}(\boldsymbol{\omega})|^2\left(1+\delta^2\|\boldsymbol{\omega}\|_2^2\right)^\tau \mathrm{d}\boldsymbol{\omega} \\
&\leq c_8\|g\|_{\Phi_\delta}^2,
\end{aligned}$$

using (4.13) and (3.19). Then setting $c_{10} := c_7^{1/2}\min(1, \delta_a^{-\tau})$ and $c_{11} := c_8^{1/2}$ completes the proof. □

4.4 Identities

4.4.1 Fourier transform dimension drop

Theorem 4.9. *Let d be a given spatial dimension, let $\phi_{\mu,\alpha}$ be the generalised Wendland functions, where μ is given by* (4.8) *and $\alpha > 0$. Then*

$$\mathcal{F}_d\phi_{\mu,\alpha}(z) = \mathcal{F}_{d-1}\phi_{\mu,\alpha+\frac{1}{2}}(z). \tag{4.14}$$

Proof. A careful inspection of Theorem 4.3 reveals that the Fourier transform of the generalised Wendland functions $\phi_{\mu,\alpha}$ is a function only of $\frac{d}{2}+\alpha$ and not of d and α separately. Since

$$\frac{d}{2}+\alpha=\frac{d-1}{2}+\alpha+\frac{1}{2}$$

the d-dimensional Fourier transform of the generalised Wendland function $\phi_{\mu,\alpha}$ equals the $d-1$-dimensional Fourier transform of the generalised Wendland function $\phi_{\mu,\alpha+\frac{1}{2}}$. □

In particular, we can recursively apply the above formula and evoke (4.2) to deduce that

$$\begin{aligned}\mathcal{F}_d\phi_{\mu,\alpha}(z) &= \mathcal{F}_1\phi_{\mu,\alpha+\frac{d-1}{2}}(z)\\ &= \sqrt{z}\int_0^1 \phi_{\mu,\alpha+\frac{d-1}{2}}(y)\sqrt{y}J_{-\frac{1}{2}}(zy)\mathrm{d}y\\ &= \sqrt{\frac{2}{\pi}}\int_0^1 \phi_{\frac{d+1}{2}+\alpha,\alpha+\frac{d-1}{2}}(y)\cos(zy)\mathrm{d}y, \end{aligned} \tag{4.15}$$

where we have used the fact that

$$J_{-\frac{1}{2}}(t)=\sqrt{\frac{2}{\pi t}}\cos(t).$$

In a similar fashion we can also conclude that

$$\begin{aligned}\mathcal{F}_d\phi_{\mu,\alpha}(z) &= \mathcal{F}_2\phi_{\mu,\alpha+\frac{d-2}{2}}(z)\\ &= \int_0^1 \phi_{\mu,\alpha+\frac{d-2}{2}}(y)yJ_0(zy)\mathrm{d}y. \end{aligned} \tag{4.16}$$

We shall use both of these identities in the next section to derive explicit expressions for the Fourier transforms of the original Wendland functions.

We will need one final result regarding the Fourier transform dimension drop.

Theorem 4.10. *Let d be a given spatial dimension, let $\phi_{\mu,\alpha}$ be the generalised Wendland functions, where μ is given by* (4.8) *and $\alpha>0$. Then*

$$\mathcal{F}_d\phi_{\mu,\alpha}(z)=\mathcal{F}_{2\alpha-1}\phi_{\mu,\frac{d+1}{2}}(z).$$

Proof. This is proven in an identical fashion to Theorem 4.9. □

4.5 Closed form representations for the Fourier transform of the original Wendland functions

4.5.1 Odd spatial dimensions d

We will consider the (original) Wendland functions $\phi_{\ell,k}$, for a given odd spatial dimension d, with smoothness parameter k and $\ell = \frac{d+1}{2} + k$. We will make use of (4.15) to derive a closed form representation for the d-dimensional Fourier transform by calculating a $1-$dimensional Fourier transform with a different value of the smoothness parameter k.

Theorem 4.11. *Let d be an odd space dimension, k a positive integer and let $\ell = (d+2k+1)/2$. The $d-$dimensional Fourier transform of the original Wendland function $\phi_{\ell,k}$ is given by*

$$\mathcal{F}_d\phi_{\ell,k}(z) = \sqrt{\frac{2}{\pi}}\frac{1}{z^{d+2k+1}}\left[\sin(z)\sum_{j=0}^{\lfloor\frac{\ell}{2}\rfloor-1}\frac{\beta_{1,j}}{z^{2j+1}} + \cos(z)\sum_{j=0}^{\lfloor\frac{\ell-1}{2}\rfloor}\frac{\beta_{2,j}}{z^{2j}} + \sum_{j=0}^{\lfloor\frac{\ell-1}{2}\rfloor}\frac{\beta_{3,j}}{z^{2j}}\right], \tag{4.17}$$

where the coefficients are given by

$$\beta_{1,j} := \frac{(-1)^{j+1}2^{\ell-1}(\ell-1)!\ell!}{(\ell-2j-2)!}\sum_{m=0}^{\ell-2j-2}(-1)^m\binom{\ell-2j-2}{m}\binom{\frac{m-1}{2}+j+\ell}{\ell-1}, \tag{4.18}$$

$$\beta_{2,j} := \frac{(-1)^{j+1}2^{\ell-1}(\ell-1)!\ell!}{(\ell-2j-1)!}\sum_{m=0}^{\ell-2j-1}(-1)^m\binom{\ell-2j-1}{m}\binom{\frac{m}{2}+j+\ell-1}{\ell-1}, \tag{4.19}$$

and

$$\beta_{3,j} := 2^{\ell-1}\ell!\frac{(-1)^j(j+\ell-1)!}{(\ell-2j-1)!j!}. \tag{4.20}$$

Proof. With (4.15), we have that

$$\mathcal{F}_d\phi_{\ell,k}(z) = \sqrt{\frac{2}{\pi}}\int_0^1\phi_{\ell,\ell-1}(y)\cos(zy)dy. \tag{4.21}$$

Using Theorem 3.2 we know that, on the unit interval, the function $\phi_{\ell,\ell-1}$ is a polynomial of degree $3\ell-2$. Specifically, (3.13) yields

$$\begin{aligned}\phi_{\ell,\ell-1}(y) &= \mathcal{C}_{\text{odd}}\sum_{n=0}^{3\ell-2}(-1)^n\binom{3\ell-2}{n}\binom{\frac{n-1}{2}}{\ell-1}y^n \\ &=: \mathcal{C}_{\text{odd}}\sum_{n=0}^{3\ell-2}b_{1,n}\,y^n,\end{aligned} \tag{4.22}$$

where

$$\mathcal{C}_{\text{odd}} := \frac{(-2)^{\ell-1}(\ell-1)!\ell!}{(3\ell-2)!}.$$

Then substituting (4.22) into (4.21) with the change of variable $t := zy$ gives

$$\mathcal{F}_d\phi_{\ell,k}(z) = \sqrt{\frac{2}{\pi}}\mathcal{C}_{\text{odd}} \sum_{n=0}^{3\ell-2} \frac{b_{1,n}}{z^{n+1}} \int_0^z t^n \cos(t)\mathrm{d}t,$$

and hence we will need to consider integrals of the form

$$I_n := \int_0^z t^n \cos(t)\,\mathrm{d}t, \quad n = 0, 1, \ldots, 3\ell - 2.$$

Using integration by parts, this can be seen to satisfy the recurrence relation

$$I_n = z^n \sin(z) + nz^{n-1}\cos(z) - n(n-1)I_{n-2},$$

which together with

$$\begin{aligned} I_1 &= -1 + \cos(z) + z\sin(z) \\ I_0 &= \sin(z), \end{aligned}$$

gives

$$I_n = \sin(z)\left\{\sum_{j=0}^{\lfloor \frac{n}{2} \rfloor}(-1)^j\,(n-2j+1)_{2j}\,z^{n-2j}\right\} + \frac{\cos(z)}{z}\left\{\sum_{j=0}^{\lfloor \frac{n-1}{2} \rfloor}(-1)^j\,(n-2j)_{2j+1}\,z^{n-2j}\right\} + \left(n - 2\left\lfloor\frac{n}{2}\right\rfloor\right)(-1)^{\frac{n+1}{2}}n!,$$

where in the last line, $\left(n - 2\left\lfloor\frac{n}{2}\right\rfloor\right)$ indicates that we have a constant term only for odd powers n. Noting that the first $k = \ell - 1$ odd coefficients of $\phi_{\ell,\ell-1}(y)$ are equal to 0 gives the expression

$$\mathcal{F}_d\phi_{\ell,k}(z) = \sin(z)\underbrace{\mathcal{C}_{\text{odd}}\sum_{n=0}^{3\ell-2} b_{1,n}\sum_{j=0}^{\lfloor \frac{n}{2} \rfloor}(-1)^j\,(n-2j+1)_{2j}\,z^{-2j-1}}_{:=(A)}$$
$$+ \frac{\cos(z)}{z}\underbrace{\mathcal{C}_{\text{odd}}\sum_{n=0}^{3\ell-2} b_{1,n}\sum_{j=0}^{\lfloor \frac{n}{2} \rfloor}(-1)^j\,(n-2j)_{2j+1}\,z^{-2j-1}}_{:=(B)} + \underbrace{\mathcal{C}_{\text{odd}}\sum_{n=\ell-1}^{\lfloor \frac{2k+\ell-1}{2} \rfloor} b_{1,2n+1}(-1)^{n+1}(2n+1)!z^{-2n-2}}_{:=(C)},$$

and now we simplify expressions (A)-(C) as follows.

$$\begin{aligned} (A) &= \mathcal{C}_{\text{odd}}\sum_{j=0}^{\lfloor \frac{3\ell-2}{2} \rfloor}\frac{(-1)^j}{z^{2j+1}}\sum_{n=2j}^{3\ell-2} b_{1,n}(n-2j+1)_{2j} \\ &= \mathcal{C}_{\text{odd}}\sum_{j=\ell}^{\lfloor \frac{3\ell-2}{2} \rfloor}\frac{(-1)^j}{z^{2j+1}}\sum_{n=2j}^{3\ell-2} b_{1,n}(n-2j+1)_{2j} \end{aligned}$$

$$
\begin{aligned}
&= \mathcal{C}_{\text{odd}} \frac{1}{z^{2\ell}} \sum_{j=0}^{\lfloor \frac{\ell}{2} \rfloor -1} \frac{(-1)^{j+\ell-1}}{z^{2j+1}} \sum_{m=0}^{\ell-2j-2} b_{1,m+2j+2\ell}(m+1)_{2j+2\ell} \\
&= \frac{(-2)^{\ell-1}(\ell-1)!\ell!}{(3\ell-2)!} \frac{1}{z^{2\ell}} \sum_{j=0}^{\lfloor \frac{\ell}{2} \rfloor -1} \frac{(-1)^{j+\ell-1}}{z^{2j+1}} \\
&\qquad \sum_{m=0}^{\ell-2j-1} (-1)^m \binom{3\ell-2}{m+2j+2\ell} \binom{\frac{m-1}{2}+j+\ell}{\ell-1} \frac{\Gamma(m+2j+2\ell+1)}{\Gamma(m+1)} \\
&= \sum_{j=0}^{\lfloor \frac{\ell}{2} \rfloor -1} \frac{\beta_{1,j}}{z^{2j+1}},
\end{aligned}
$$

where we have also used the fact that the first $\ell+k-1$ derivatives at $r=1$ of the original Wendland functions $\phi_{\ell,k}$ are 0, as this property means that

$$
\sum_{i=n}^{2k+\ell} b_{1,i}\,(i-n+1)_n = 0, \quad n = 0, \ldots, \ell+k-1.
$$

Now we simplify expression (B) where we will again use that the first $\ell+k-1$ derivatives at $r=1$ of the original Wendland functions $\phi_{\ell,k}$ are 0,

$$
\begin{aligned}
(B) &= \mathcal{C}_{\text{odd}} \sum_{j=0}^{\lfloor \frac{3\ell-3}{2} \rfloor} \frac{(-1)^j}{z^{2j+2}} \sum_{n=2j+1}^{3\ell-2} b_{1,n}(n-2j)_{2j+1} \\
&= \mathcal{C}_{\text{odd}} \sum_{j=\ell-1}^{\lfloor \frac{3\ell-3}{2} \rfloor} \frac{(-1)^j}{z^{2j+1}} \sum_{n=2j+1}^{3\ell-2} b_{1,n}(n-2j)_{2j+1} \\
&= \mathcal{C}_{\text{odd}} \frac{1}{z^{2\ell}} \sum_{j=0}^{\lfloor \frac{\ell-1}{2} \rfloor} \frac{(-1)^{j+\ell-1}}{z^{2j}} \sum_{m=0}^{\ell-2j-1} b_{1,m+2j+2\ell-1}(m+1)_{2j+2\ell} \\
&= \frac{(-2)^{\ell-1}(\ell-1)!\ell!}{(3\ell-2)!} \frac{1}{z^{2\ell}} \sum_{j=0}^{\lfloor \frac{\ell-1}{2} \rfloor} \frac{(-1)^{j+\ell}}{z^{2j+1}} \\
&\qquad \sum_{m=0}^{\ell-2j-1} (-1)^{m-1} \binom{3\ell-2}{m+2j+2\ell-1} \binom{\frac{m}{2}+j+\ell-1}{\ell-1} \frac{\Gamma(m+2j+2\ell)}{\Gamma(m)} \\
&= \sum_{j=0}^{\lfloor \frac{\ell-1}{2} \rfloor} \frac{\beta_{2,j}}{z^{2j+1}}.
\end{aligned}
$$

Finally we simplify expression (C) to complete the proof.

$$
\begin{aligned}
(C) &= \mathcal{C}_{\text{odd}} \sum_{n=\ell-1}^{\lfloor \frac{2k+\ell-1}{2} \rfloor} b_{1,2n+1}(-1)^{n+1}(2n+1)!z^{-2n-2} \\
&= \frac{\mathcal{C}_{\text{odd}}}{z^{2\ell}} \sum_{j=0}^{\lfloor \frac{\ell-1}{2} \rfloor} (-1)^{j+\ell} b_{1,2j+2\ell-1}(2j+2\ell-1)!z^{-2j} \\
&= \frac{(-2)^{\ell-1}(\ell-1)!\ell!}{(3\ell-2)!z^{2\ell}} \\
&\qquad \times \sum_{j=0}^{\lfloor \frac{\ell-1}{2} \rfloor} \frac{(-1)^{j+\ell-1}}{z^{2j}} \binom{3\ell-2}{2j+2\ell-1} \binom{j+\ell-1}{\ell-1} (2j+2\ell-1)!
\end{aligned}
$$

$$= \sum_{j=0}^{\lfloor \frac{\ell-1}{2} \rfloor} \frac{\beta_{3,j}}{z^{2j}}.$$

□

We note that the existence of this representation was mentioned in [44], however the exact values of the coefficients were not given.

4.5.2 Even spatial dimensions d

In this section we assume that the space dimension d is even, i.e., where $\ell = \frac{d}{2} + k + 1$. We will consider the (original) Wendland functions $\phi_{\ell,k}$ with smoothness parameter k. We will make use of (4.16) to derive a closed form representation for the d-dimensional Fourier transform by calculating a 2−dimensional Fourier transform with a different value of the smoothness parameter k.

Theorem 4.12. *Let d be an even space dimension, k a positive integer and let $\ell = d/2 + k + 1$. The $d-$dimensional Fourier transform of the original Wendland function $\phi_{\ell,k}$ is given by*

$$\mathcal{F}_d \phi_{\ell,k}(z) = \frac{C_{\text{even}}}{z^{d+2k+1}} \Bigg[J_0(z) \sum_{j=0}^{\lfloor \frac{\ell}{2} \rfloor - 1} \frac{\gamma_{1,j+k+1}}{z^{2j-1}} + J_1(z) \sum_{j=0}^{\lfloor \frac{\ell}{2} \rfloor - 1} \frac{\gamma_{2,j+k+1}}{z^{2j}} + (J_0(z)H_1(z) - J_1(z)H_0(z)) \sum_{j=0}^{\lfloor \frac{\ell-1}{2} \rfloor} \frac{\gamma_{3,2j+2k+1}}{z^{2j-1}} \Bigg], \tag{4.23}$$

with

$$C_{\text{even}} := \frac{(-2)^{\ell-2} \ell! (\ell-2)!}{(3\ell-4)!}, \tag{4.24}$$

$$\gamma_{1,j} := (-1)^{j-1} 2^{2j} \sum_{n=2j}^{2k+\ell} \frac{(-1)^n \binom{2k+\ell}{n} \binom{\frac{n-1}{2}}{k}}{n-2j+2} \Big[\Big(\frac{n}{2} - j + 1 \Big)_j \Big]^2. \tag{4.25}$$

$$\gamma_{2,j} := (-1)^j 2^{2j} \sum_{n=2j}^{2k+\ell} (-1)^n \binom{2k+\ell}{n} \binom{\frac{n-1}{2}}{k} \Big[\Big(\frac{n}{2} - j + 1 \Big)_j \Big]^2, \tag{4.26}$$

and

$$\gamma_{3,j} := \frac{\pi}{2} (-1)^{\frac{3j-1}{2}} 2^{j+1} \binom{2k+\ell}{j} \binom{\frac{j-1}{2}}{k} \Big[\Big(\frac{1}{2} \Big)_{\frac{j+1}{2}} \Big]^2, \tag{4.27}$$

where $H_\nu(z)$ denotes the Struve function of order ν (cf. [45, Chapter 10.4]).

Proof. In this setting we are again dealing with the family $\phi_{\ell,k}$ and we are able to use (4.16) to deduce that

$$\mathcal{F}_d \phi_{\ell,k}(z) = \int_0^1 \phi_{\ell,\ell-2}(y) y J_0(zy) \, dy. \tag{4.28}$$

Using Theorem 3.2 we know that, on the unit interval, the function $\phi_{\ell,\ell-2}$ is a polynomial of degree $3\ell-4$. Specifically, (3.13) yields

$$\begin{aligned} \phi_{\ell,\ell-2}(y) &= C_{\text{even}} \sum_{j=0}^{3\ell-4} (-1)^j \binom{3\ell-4}{j} \binom{\frac{j-1}{2}}{\ell-2} y^j \qquad (4.29) \\ &=: C_{\text{even}} \sum_{j=0}^{3\ell-4} b_{2,j}\, y^j, \end{aligned}$$

where

$$C_{\text{even}} := \frac{(-1)^\ell 2^{\ell-2} \ell!(\ell-2)!}{(3\ell-4)!}.$$

To calculate this integral, we will need the following identity [36, 1.8.1.5, p.37]

$$\int_0^1 x^\mu J_\nu(ax)\,\mathrm{d}x = a^{-\mu}\left\{(\mu+\nu-1)J_v(a)s_{\mu-1,\nu-1}(a) - J_{v-1}(a)s_{\mu,\nu}(a)\right\},$$

where $s_{\mu,\nu}$ denotes the Lommel function (of the first kind). We collect some identities for the Lommel functions which we will require - for further information, we refer the reader to [45, Chapter 10.7].

$$\begin{aligned} s_{\mu+2,v}(z) &= z^{\mu+1} - \left\{(\mu+1)^2 - \nu^2\right\} s_{\mu,\nu}(z), && (4.30) \\ s_{\mu,-\nu}(z) &= s_{\mu,\nu}(z), && (4.31) \\ s_{\nu,\nu}(z) &= \Gamma\left(\nu + \frac{1}{2}\right)\sqrt{\pi}\, 2^{\nu-1} H_\nu(z), && (4.32) \\ s_{1,0}(z) &= 1 - J_0(z), && (4.33) \\ s_{2,1}(z) &= z - 2J_1(z). && (4.34) \end{aligned}$$

Then substituting (4.29) into the right hand side of (4.28), with the identities mentioned above, yields

$$\begin{aligned} \mathcal{F}_d\phi_{\ell,k}(z) &= C_{\text{even}} \sum_{j=0}^{3\ell-4} b_{2,j} z^{-j-1}\left[jJ_0(z)s_{j,1}(z) + J_1(z)s_{j+1,0}(z)\right] && (4.35) \\ &= C_{\text{even}}\left[J_0(z)\underbrace{\sum_{j=0}^{3\ell-4} \frac{b_{2,j}}{z^{j+1}} j\, s_{j,1}(z)}_{:=(A)} + J_1(z)\underbrace{\sum_{j=0}^{3\ell-4} \frac{b_{2,j}}{z^{j+1}} s_{j+1,0}(z)}_{:=(B)}\right], && (4.36) \end{aligned}$$

upon noting that $J_{-1}(z) = -J_1(z)$. To simplify this further, we will use (4.30) to derive series representations for the two types of Lommel functions that appear in (4.35). Firstly we define the following two functions

$$\begin{aligned} d_{p,i} &:= \prod_{m=p+1}^{\frac{i-1}{2}} \left((2m)^2 - 1\right) && (4.37) \\ &= \prod_{m=p+1}^{\frac{i-1}{2}} (2m-1)(2m+1) && (4.38) \end{aligned}$$

and

$$f_{p,i} := \prod_{m=p+\frac{1}{2}}^{\frac{i}{2}} (2m)^2. \tag{4.39}$$

Both $d_{p,i}$ and $f_{p,i}$ are defined for either i odd and p being an integer, or i even and p being a half-integer. Note that simply writing out the terms in both functions gives

$$\begin{aligned} d_{p,i} &= (2p+1)(2p+3)^2(2p+5)^2 \cdots (i-2)^2 i \\ f_{p,i} &= (2p+1)^2 \cdots i^2, \end{aligned}$$

from which we can immediately see that

$$f_{p,i} = i(2p+1)d_{p,i} \ , \tag{4.40}$$

which we will need later. We can now formulate the expressions that we need for the Lommel functions. We need to separate these into two cases: when j is odd, and when j is even. These follow from (4.30), (4.32), (4.33) and (4.34).

Lommel functions when j is odd

$$s_{j,1}(z) = \sum_{n=1}^{\frac{j-1}{2}} (-1)^{\frac{j-2n-1}{2}} d_{n,j}\, z^{2n} + (-1)^{\frac{j-1}{2}} \frac{\pi}{2} d_{0,j}\, H_1(z) \tag{4.41}$$

$$s_{j+1,0}(z) = \sum_{n=\frac{1}{2}}^{\frac{j}{2}} (-1)^{\frac{j-2n}{2}} f_{n+\frac{1}{2},j}\, z^{2n} - (-1)^{\frac{j-1}{2}} \frac{\pi}{2} f_{0,j}\, H_0(z). \tag{4.42}$$

Lommel functions when j is even

$$s_{j,1}(z) = \sum_{n=\frac{1}{2}}^{\frac{j-1}{2}} (-1)^{\frac{j-2n-1}{2}} d_{n,j}\, z^{2n} + 2\,(-1)^{\frac{j}{2}}\, d_{\frac{1}{2},j} J_1(z) \tag{4.43}$$

$$s_{j+1,0}(z) = \sum_{n=0}^{\frac{j}{2}} (-1)^{\frac{j-2n}{2}} f_{n+\frac{1}{2},j}\, z^{2n} - (-1)^{\frac{j}{2}} f_{\frac{1}{2},j} J_0(z). \tag{4.44}$$

Let us consider (A) in (4.36). Using (4.41), (4.43) and (4.40) gives

$$\begin{aligned} (A) &= \sum_{\text{odd}j} \frac{b_{2,j}}{z^{j+1}} \left\{ \sum_{n=1}^{\frac{j-1}{2}} (-1)^{\frac{j-2n-1}{2}} j\, d_{n,j}\, z^{2n} + (-1)^{\frac{j-1}{2}} \frac{\pi}{2} j\, d_{0,j}\, H_1(z) \right\} \\ &\quad + \sum_{\text{even}j} \frac{b_{2,j}}{z^{j+1}} \left\{ \sum_{n=\frac{1}{2}}^{\frac{j-1}{2}} (-1)^{\frac{j-2n-1}{2}} j\, d_{n,j}\, z^{2n} + 2\,(-1)^{\frac{j}{2}} j\, d_{\frac{1}{2},j} J_1(z) \right\} \\ &= \sum_{j=0}^{3\ell-4} b_{2,j} \sum_{n=1}^{\lfloor \frac{j}{2} \rfloor} (-1)^{n-1} \frac{f_{\frac{j+1}{2}-n,j}}{j-2n+2} z^{-2n} + \frac{\pi}{2} H_1(z) \sum_{\text{odd}j} \left\{ (-1)^{\frac{j-1}{2}} \frac{b_{2,j}}{z^{j+1}} f_{0,j} \right\} \\ &\quad + J_1(z) \sum_{\text{even}j} \left\{ \frac{b_{2,j}}{z^{j+1}} (-1)^{\frac{j}{2}} f_{\frac{1}{2},j} \right\} \end{aligned} \tag{4.45}$$

$$= \sum_{j=1}^{\lfloor\frac{2k+\ell}{2}\rfloor} \frac{\gamma_{1,j}}{z^{2j}} + \frac{\pi}{2} H_1(z) \sum_{\text{odd} j} \left\{ (-1)^{\frac{j-1}{2}} \frac{b_{2,j}}{z^{j+1}} f_{0,j} \right\} \tag{4.46}$$

$$+ \quad J_1(z) \sum_{\text{even} j} \frac{b_{2,j}}{z^{j+1}} (-1)^{\frac{j}{2}} f_{\frac{1}{2},j} \tag{4.47}$$

with

$$\gamma_{1,j} \;=\; (-1)^{j-1} \sum_{n=2j}^{2k+\ell} b_{2,n} \frac{f_{\frac{n+1}{2}-j,n}}{n-2j+2} \tag{4.48}$$

$$= \; (-1)^{j-1} 2^{2j} \sum_{n=2j}^{2k+\ell} \frac{(-1)^n \binom{2k+\ell}{n} \binom{\frac{n-1}{2}}{k}}{n-2j+2} \Big[\Big(\frac{n}{2} - j + 1\Big)_j \Big]^2. \tag{4.49}$$

This result can be simplified further as follows. We know that the first $k = \ell - 2$ odd coefficients $\{b_{2m+1}\}_{m=0,\ldots,\ell-2}$ vanish so we consider $\gamma_{1,j}$ for $2j - 1 \le 2\ell - 3$. Furthermore since the Pochhammer symbol appearing in (4.49) also vanishes when $n = 2p$ when $p = 0, \ldots, j-1$, we can express the coefficients $\gamma_{1,j}$ as the sum of polynomials in n of degree $2j$ with coefficients h_m as follows

$$\begin{aligned}
\gamma_{1,j} &= (-1)^{j-1} 2^{2j} \sum_{n=0}^{2k+\ell} \frac{b_{2,n}}{n-2j+2} \Big[\Big(\frac{n}{2} - j + 1\Big)_j \Big]^2 \\
&= (-1)^{j-1} 2^{2j} \sum_{n=0}^{2k+\ell} b_{2,n} \sum_{m=0}^{2j} h_m \, n^m \\
&= (-1)^{j-1} 2^{2j} \sum_{m=0}^{2j} h_m \sum_{n=0}^{2k+\ell} b_{2,n} n^m.
\end{aligned}$$

We also know that the first $\ell + k - 1 = 2\ell - 3$ derivatives of $\phi_{\ell,\ell-2}$ vanish at $r = 1$. In view of this we can deduce that

$$\sum_{n=0}^{3\ell-4} b_{2,n} \, n^p = 0, \quad p = 0, 1, \ldots, 2\ell - 3,$$

and hence

$$\gamma_{1,j} = 0, \quad \text{for} \quad j = 0, 1, \ldots, \ell - 2.$$

We proceed similarly for (B). With (4.42) and (4.44),

$$\begin{aligned}
(B) \;=\; & \sum_{\text{odd} j} \frac{b_{2,j}}{z^{j+1}} \left\{ \sum_{n=\frac{1}{2}}^{\frac{j}{2}} (-1)^{\frac{j-2n}{2}} f_{n+\frac{1}{2},j} \, z^{2n} - (-1)^{\frac{j-1}{2}} \frac{\pi}{2} f_{0,j} \, H_0(z) \right\} \\
& + \sum_{\text{even} j} \frac{b_{2,j}}{z^{j+1}} \left\{ \sum_{n=1}^{\frac{j}{2}} (-1)^{\frac{j-2n}{2}} f_{n+\frac{1}{2},j} \, z^{2n} - (-1)^{\frac{j}{2}} f_{\frac{1}{2},j} J_0(z) \right\} \\
=\; & \sum_{j=0}^{3\ell-4} b_{2,j} \sum_{n=0}^{\lfloor\frac{j}{2}\rfloor} (-1)^n f_{\frac{j-2n+1}{2},j} \, z^{-2n-1} + \frac{\pi}{2} H_0(z) \sum_{\text{odd} j} \left\{ (-1)^{\frac{j-1}{2}} \frac{b_{2,j}}{z^{j+1}} f_{0,j} \right\} \\
& - \sum_{\text{even} j} \frac{b_{2,j}}{z^{j+1}} \left\{ (-1)^{\frac{j}{2}} f_{\frac{1}{2},j} J_0(z) \right\}
\end{aligned}$$

$$
\begin{aligned}
&= \sum_{j=0}^{\lfloor\frac{2k+\ell}{2}\rfloor} \frac{\gamma_{2,j}}{z^{2j+1}} + \frac{\pi}{2}H_0(z)\sum_{\text{odd}j}\left\{(-1)^{\frac{j-1}{2}}\frac{b_{2,j}}{z^{j+1}}f_{0,j}\right\} \\
&- J_0(z)\sum_{\text{even}j}\frac{b_{2,j}}{z^{j+1}}\left\{(-1)^{\frac{j}{2}}f_{\frac{1}{2},j}\right\},
\end{aligned}
\tag{4.50}
$$

with

$$
\begin{aligned}
\gamma_{2,j} &= (-1)^j\sum_{n=2j}^{2k+\ell} b_{2,n}f_{\frac{n-2j+1}{2},n} \\
&= (-1)^j 2^{2j}\sum_{n=2j}^{2k+\ell}(-1)^n\binom{2k+\ell}{n}\binom{\frac{n-1}{2}}{k}\left[\left(\frac{n}{2}-j+1\right)_j\right]^2.
\end{aligned}
$$

As with $\gamma_{1,j}$, we can express $\gamma_{2,j}$ as

$$
\begin{aligned}
\gamma_{2,j} &= (-1)^j\sum_{n=0}^{2k+\ell} b_{2,n}\left[\left(\frac{n}{2}-j+1\right)_j\right]^2 \\
&= (-1)^j\sum_{m=0}^{2j} h_m\sum_{n=0}^{2k+\ell} b_{2,n}n^m,
\end{aligned}
$$

and hence

$$\gamma_{2,j} = 0, \quad \text{for} \quad j = 0, 1, \ldots, \ell-2.$$

Combining the above results, once again noting that the first k odd coefficients $b_{2,j}$ are 0, completes the proof. □

Note that since there are positive powers of z in two of the sums in Theorem 4.12, it is not immediately obvious that we achieve the asymptotic decay rate predicted by Theorem 4.5. To investigate this, we will need to consider the first terms ($j = 0$) in the first and third sums of Theorem 4.12. Using the asymptotic expansions of the Bessel and Struve functions ([45]), we see that as $z \to \infty$

$$
\begin{aligned}
J_0(z) &= \sqrt{\frac{2}{\pi z}}\cos\left(z-\frac{\pi}{4}\right) + O(z^{-1}) \\
J_0(z)H_1(z) - J_1(z)H_0(z) &= \frac{2}{\pi}\sqrt{\frac{2}{\pi z}}\cos\left(z-\frac{\pi}{4}\right) + O(z^{-1}),
\end{aligned}
$$

which will mean that these two $j = 0$ components will cancel out asymptotically if

$$\gamma_{1,k+1} = -\frac{2}{\pi}\gamma_{3,2k+1}.$$

With the definitions of $\gamma_{1,j}$ and $\gamma_{3,j}$ in (4.48) and (4.27) and noting that

$$\sum_{n=2k+1}^{2k+\ell}\frac{b_{2,n}f_{\frac{n+1}{2}-k-1,n}}{n-2k} = 0,$$

we can see this as follows

$$\begin{aligned}\gamma_{1,k+1} &= (-1)^k \sum_{n=2k+2}^{2k+\ell} \frac{b_{2,n} f_{\frac{n+1}{2}-k-1,n}}{n-2k} \\ &= (-1)^{k+1} b_{2,2k+1}\, f_{0,2k+1} \\ &= -\frac{2}{\pi}\gamma_{3,2k+1},\end{aligned}$$

and hence the asymptotic decay of the Fourier transform in Theorem 4.12 agrees with Theorem 4.5.

4.6 Closed form representation for the Fourier transform of the missing Wendland functions

In this section, we consider the missing Wendland functions, so $\alpha = k + \frac{1}{2}$ where $k \in \mathbb{N}$ and we once again seek a closed form representation for the Fourier transform, in other words, for

$$\mathcal{F}_d \phi_{\frac{d}{2}+k+1,k+\frac{1}{2}},$$

with an even spatial dimension d.

Theorem 4.13. *Let d be an even spatial dimension, k a positive integer and $\ell = d/2 + k + 1$. The $d-$dimensional Fourier transform of the missing Wendland function $\phi_{\ell,k+\frac{1}{2}}$ is given by*

$$\mathcal{F}_d \phi_{\ell,k+\frac{1}{2}}(z) = \sqrt{\frac{2}{\pi}} \frac{1}{z^{d+2k+2}} \left[\sin(z) \sum_{j=0}^{\lfloor \frac{\ell}{2} \rfloor - 1} \frac{\beta_{1,j}}{z^{2j+1}} + \cos(z) \sum_{j=0}^{\lfloor \frac{\ell-1}{2} \rfloor} \frac{\beta_{2,j}}{z^{2j}} + \sum_{j=0}^{\lfloor \frac{\ell-1}{2} \rfloor} \frac{\beta_{3,j}}{z^{2j}} \right], \quad (4.51)$$

where $\beta_{1,j}$, $\beta_{2,j}$ and $\beta_{3,j}$ are given by (4.18), (4.19) *and* (4.20) *respectively.*

Proof. With (4.14), we can see that

$$\begin{aligned}\mathcal{F}_d \phi_{\frac{d}{2}+k+1,k+\frac{1}{2}} &= \mathcal{F}_{d-1} \phi_{\frac{d}{2}+k+1,k+1} \\ &= \mathcal{F}_{d-1} \phi_{\frac{d-1}{2}+k+1+\frac{1}{2},k+1},\end{aligned}$$

which is just the $d-1$-dimensional Fourier transform of the original Wendland function with smoothness parameter $k+1$ (since k is an integer). Since $d-1$ is odd, the closed form representation for this is given in Theorem 4.11, which gives the stated result. □

4.6.1 Integrals leading to the result

Since the standard texts on special functions (such as [21, 36]) do not contain the integrals that we require for the Fourier transform of the missing Wendland functions, in this subsection we show that the Fourier transforms of the missing Wendland functions in even spatial dimensions d are of the form stated in Theorem 4.13. This analysis may in future lead to another closed form representation for the missing Wendland functions by use of the inverse Fourier transform to recover the missing Wendland function.

From the form of the missing Wendland functions given in Section 3.3, and the Fourier transform integral in (4.2), we can see that the Fourier transform will involve integrals of the form

$$I_n := \int_0^1 x^{2n}\sqrt{1-x^2}x^{\frac{d}{2}}J_{\frac{d}{2}-1}(xt)\,\mathrm{d}x, \quad n \geq 0$$

and

$$M_n := \int_0^1 x^{2n}\operatorname{arcsech}(x)\, x^{\frac{d}{2}}J_{\frac{d}{2}-1}(xt)\,\mathrm{d}x, \quad n \geq 0.$$

We will need to make use of the following two Bessel function integral identities ([21, 6.683.6],[21, 6.683.4])

$$\int_0^{\frac{\pi}{2}} J_\mu(z\sin\theta)\,(\sin\theta)^{\mu+1}\,(\cos\theta)^{2\rho+1}\,\mathrm{d}\theta = 2^\rho\Gamma(\rho+1)z^{-\rho-1}J_{\rho+\mu+1}(z), \tag{4.52}$$

and

$$\int_0^{\frac{\pi}{2}} J_\mu(z\sin\theta)\,(\sin\theta)^{1-\mu}\,(\cos\theta)^{2\rho+1}\,\mathrm{d}\theta = \frac{s_{\mu+v,v-\mu+1}(z)}{2^{\mu-1}z^{v+1}\Gamma(\mu)}. \tag{4.53}$$

First we consider I_n. With the substitution $x = \sin\theta$, using $\sin^2\theta = 1-\cos^2\theta$, then expanding with the binomial theorem and using (4.52) we reach

$$\begin{aligned}
I_n &= \int_0^{\frac{\pi}{2}} (\sin\theta)^{2n+\frac{d}{2}}\,\cos^2\theta J_{\frac{d}{2}-1}(t\sin\theta)\mathrm{d}\theta \\
&= \int_0^{\frac{\pi}{2}} (\sin\theta)^{\frac{d}{2}}\,\left(1-\cos^2\theta\right)^n\,\cos^2\theta J_{\frac{d}{2}-1}(t\sin\theta)\mathrm{d}\theta \\
&= \sum_{j=0}^n(-1)^j\binom{n}{j}\int_0^{\frac{\pi}{2}} J_{\frac{d}{2}-1}(z\sin\theta)\,(\sin\theta)^{\frac{d}{2}}\,(\cos\theta)^{2\left(j+\frac{1}{2}\right)+1}\,\mathrm{d}\theta \\
&= \sum_{j=0}^n(-1)^j\binom{n}{j}2^{j+\frac{1}{2}}\Gamma\left(j+\frac{3}{2}\right)t^{-j-\frac{3}{2}}J_{\frac{d}{2}+j+\frac{1}{2}}(t).
\end{aligned}$$

Now we know from [45, Chapter 9.6] that we can express a higher order Bessel function in terms of lower order Bessel functions as

$$J_{v+m}(z) = J_v(z)R_{m,v}(z) - J_{v-1}(z)R_{m-1,v+1}(z),$$

where $R_{m,v}(z)$ are the Lommel polynomials. Then since

$$\begin{aligned}
J_{\frac{1}{2}}(z) &= \sqrt{\frac{2}{\pi z}}\sin(z) \\
J_{\frac{-1}{2}}(z) &= \sqrt{\frac{2}{\pi z}}\cos(z)
\end{aligned}$$

we can reach

$$I_n = \sqrt{\frac{2}{\pi}} \sum_{j=0}^{n} (-1)^j \binom{n}{j} 2^{j+\frac{1}{2}} \Gamma\left(j+\frac{3}{2}\right) t^{-j-2} \left\{ R_{\frac{d}{2}+j,\frac{1}{2}}(z)\sin(z) - R_{\frac{d}{2}+j-1,\frac{3}{2}}(z)\cos(z) \right\}, \tag{4.54}$$

which consists only of $\sin(z)$ and $\cos(z)$ terms multiplied by polynomials in z, as required. Note that there is no pure polynomial component in this expression.

We now consider M_n. We can do this with integration by parts with $u = x^{2n}\operatorname{arcsech}(x)$ and $dv = x^{\frac{d}{2}} J_{\frac{d}{2}-1}(xt)$ where we also need that [45]

$$\int z^{v+1} J_v(tz)\mathrm{d}z = \frac{z^{v+1}}{t} J_{v+1}(tz).$$

Now we can integrate by parts, n times, using

$$\frac{\mathrm{d}}{\mathrm{d}x}\left(x^{2n}\operatorname{arcsech}(x)\right) = 2n\, x^{2n-1}\operatorname{arcsech}(x) - x^{2n-1}\left(1-x^2\right)^{-\frac{1}{2}},$$

and each time the boundary contribution is zero. So then in the end, we reach

$$\begin{aligned} M_n &= 2^n n! t^{-n} \int_0^1 \operatorname{arcsech}(x)\, x^{\frac{d}{2}+n} J_{\frac{d}{2}+n-1}(xt)\mathrm{d}x \\ &\quad + \sum_{j=1}^{n-1} (-1)^j t^{-j} 2^{j-1} \prod_{m=n-j+2}^{n} m \int_0^1 x^{2n-2j+1}(1-x^2)^{-1/2} x^{\frac{d}{2}+j-1} J_{\frac{d}{2}+j-1}(xt)\mathrm{d}x. \end{aligned} \tag{4.55}$$

Note that the second term in (4.55) can be handled in a similar fashion to I_n and hence we need only concern ourself with the first term in (4.55). We apply integration by parts again, and applying the second Bessel function identity stated above leads to (with $m := d/2+n-1$)

$$\begin{aligned} \int_0^1 \operatorname{arcsech}(x)\, x^{\frac{d}{2}+n} J_{\frac{d}{2}+n-1}(xt)\mathrm{d}x &= -\int_0^1 (1-x^2)^{-1/2} x^{\frac{d}{2}+n-1} J_{\frac{d}{2}+n}(xt)\mathrm{d}x \\ &= -\int_0^{\frac{\pi}{2}} J_{\frac{d}{2}+n}(t\sin\theta)\sin^{1-\frac{d}{2}-n}\theta \sin^{d+2n-2}\theta \mathrm{d}\theta \\ &= -\int_0^{\frac{\pi}{2}} J_{\frac{d}{2}+n}(t\sin\theta)\sin^{1-\frac{d}{2}-n}\theta (1-\cos^2\theta)^m \mathrm{d}\theta \\ &= \sum_{j=0}^{m} (-1)^{j+1}\binom{m}{j} J_{\frac{d}{2}+n}(t\sin\theta)\sin^{1-\frac{d}{2}-n}\theta\cos^{2j}\theta\mathrm{d}\theta \\ &= \sum_{j=0}^{m} (-1)^{j+1}\binom{m}{j} \frac{s_{\frac{d-}{2}+n+j,j-n+\frac{1-d}{2}}(z)}{2^{\frac{d}{2}+n-1} z^{j+1/2}\Gamma(d/2+n)}. \end{aligned}$$

Now we recall the recurrence relation that we used earlier for the Lommel function of the first kind

$$s_{\mu+2,v}(z) = z^{\mu+1} - \left\{(\mu+1)^2 - v^2\right\} s_{\mu,v}(z),$$

in conjunction with $s_{\mu,-v} = s_{\mu,v}$, because then after j such iterations, we reach the Struve function of order $\frac{d-1}{2}+n-j$ which can also be expressed as

$$H_{n+\frac{1}{2}}(z) = Y_{n+\frac{1}{2}}(z) + \frac{1}{\pi}\sum_{k=0}^{n} \frac{\Gamma(k+1/2)(\frac{z}{2})^{-2k+n-1/2}}{\Gamma(n+1-k)},$$

and $Y_{n+1}(z)$ is also $\sin(z)$ and $\cos(z)$ multiplied by a polynomial. As a result, both I_n and M_n are expressible in terms of $\sin(z)$ and $\cos(z)$ with polynomials in z, hence so is a linear combination of I_n and M_n expressions, which provides some confirmation that the Fourier transform of the missing Wendland functions in even spatial dimensions d can be expressed in terms of $\sin(z)$, $\cos(z)$ and polynomials in z.

4.7 Properties

4.7.1 When is the Fourier transform strictly decreasing

Theorem 4.14. *The Fourier transform of the generalised Wendland functions $\mathcal{F}_d\phi_{\mu,\alpha}(z)$ is strictly decreasing if and only if its parameters satisfy*

$$\mu \geq \frac{d+1}{2} + \alpha + 1.$$

In particular, note that this value of μ is one higher than the minimum required for positive definiteness.

Proof. With the following identity [11, 16.3.1]

$$\frac{\mathrm{d}}{\mathrm{d}z} {}_1F_2\left(a_1; b_1, b_2; z\right) = \frac{a_1}{b_1\, b_2} {}_1F_2\left(a_1+1; b_1+1, b_2+1; z\right)$$

applied to Theorem 4.3 yields

$$\frac{\mathrm{d}}{\mathrm{d}z}\mathcal{F}_d\phi_{\mu,\alpha}(z) = \frac{-2zC_d^{\mu,\alpha}\left(\frac{d+1}{2}+\alpha\right)}{\left(\frac{\mu+d+1}{2}+\alpha\right)\left(\frac{\mu+d+2}{2}+\alpha\right)} \times {}_1F_2\left(\frac{d+1}{2}+\alpha; \frac{\mu+d+1}{2}+\alpha, \frac{\mu+d+2}{2}+\alpha; -\frac{z^2}{4}\right),$$

and noting that $C_d^{\mu,\alpha} > 0$ and $z > 0$ we only need to determine when the hypergeometric function is strictly positive. This is identical to the proof of Theorem 4.4 except in this case all the parameters are increased by one and the result follows. □

Chapter Five

Limit of the generalised Wendland functions as $\alpha \to \infty$

This chapter will present the limiting case of the generalised Wendland functions $\phi_{\mu,\alpha}$ as $\alpha \to \infty$.

In Figure 5.1, we can see the original Wendland functions $\phi_{\ell,k}$ in $\mathbb{R}^3$ for $k = 1, \ldots, 5$, where we have normalised the functions to have value 1 at the origin. One can clearly see faster decay as $\alpha = k$ increases, which suggests the need for a change of variable when considering the limit as α approaches infinity.

Section 5.1 presents the change of variables that we will need to use to investigate the limiting behaviour of the generalised Wendland functions. Section 5.2 presents the results as $\alpha \to \infty$. Section 5.3 considers the selection of the parameter μ in the generalised Wendland functions and Section 5.4 discusses the selection of scaling factors.

5.1 Generalised Wendland functions with a change of variable

We begin this section with two technical lemmas, which will be used in the change of variable required to study the limiting behaviour of the generalised Wendland functions.

Lemma 5.1.

$$\phi_{\mu,\alpha}(0) = \frac{\Gamma(\mu+1)\Gamma(2\alpha)}{2^{\alpha-1}\Gamma(\alpha)\Gamma(\mu+2\alpha+1)}. \tag{5.1}$$

Proof. To calculate $\phi_{\mu,\alpha}(0)$ we need the value of the hypergeometric function in (3.5) at the argument 1 (since it has argument $1 - r^2$). From [1, 15.1.20] we have the identity

$${}_2F_1(a, b; c; 1) = \frac{\Gamma(c)\Gamma(c-b-a)}{\Gamma(c-b)\Gamma(c-a)} \quad , c \neq 0, -1, -2, \ldots, \; c-b-a > 0. \tag{5.2}$$

Applying (5.2) to (3.5) shows that

$$\phi_{\mu,\alpha}(0) = \frac{\Gamma(\mu+1)\,\Gamma(\alpha+\frac{1}{2})}{2^{\mu+\alpha}\,\Gamma(\frac{\mu}{2}+\alpha+\frac{1}{2})\,\Gamma(\frac{\mu}{2}+\alpha+1)}.$$

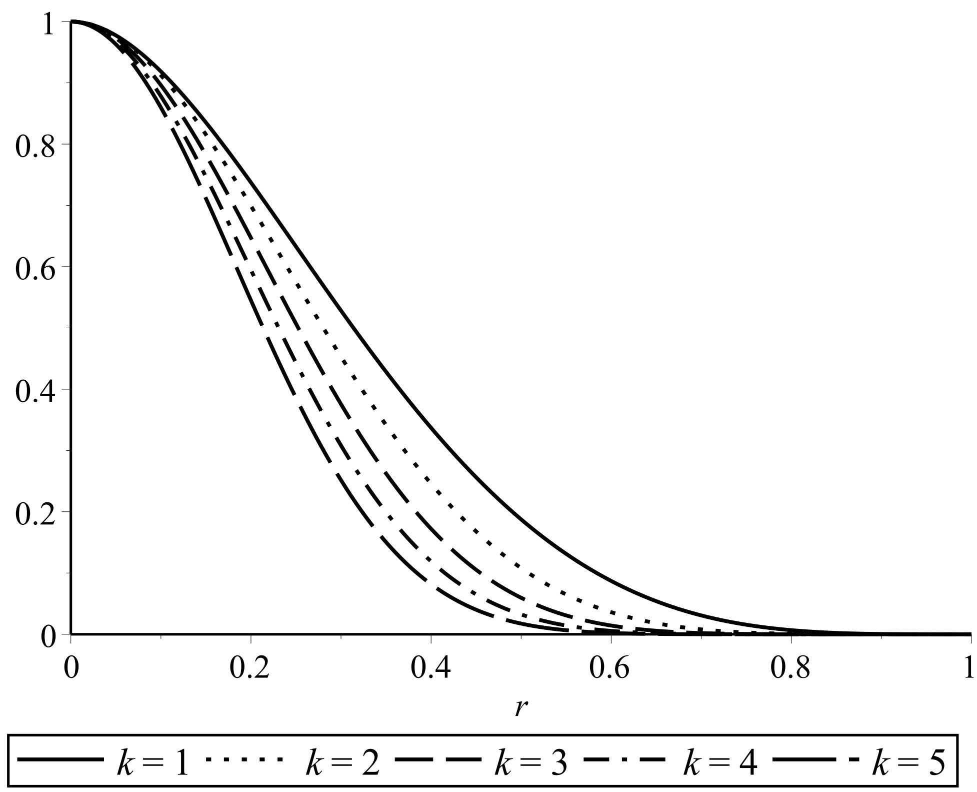

Figure 5.1. *The (original) Wendland functions $\phi_{\ell,k}(r)$ for $\ell = k+2$ and $k = 1,\ldots,5$, normalised to have value 1 at $r = 0$.*

Using (4.7) twice – firstly for $\Gamma(\frac{\mu}{2}+\alpha+\frac{1}{2})\Gamma(\frac{\mu}{2}+\alpha+1)$ and then for $\Gamma(\alpha)\Gamma\left(\alpha+\frac{1}{2}\right)$ – and with several terms cancelling out in the numerator and denominator, we get the desired result. $\square$

We will also need the following result for the area under the generalised Wendland functions $\phi_{\mu,\alpha}$.

Lemma 5.2.

$$\int_0^\infty \phi_{\mu,\alpha}(s)\mathrm{d}s = \frac{2^\alpha\,\Gamma(\mu+1)\,\Gamma(\alpha+1)}{\Gamma(\mu+2\alpha+2)}. \tag{5.3}$$

Proof. This follows from (4.3) and Theorem 4.3 on setting $d = 1$ (noting that $\phi_{\mu,\alpha}$ has no explicit d dependence). $\square$

Now we can define what we will call *normalised equal area generalised Wendland functions*. These are normalised generalised Wendland functions with a linear change of variable (which depends on α and a positive real constant ϑ) such that for a given ϑ all the normalised equal area generalised Wendland functions have area equal to the area under $\exp(-\vartheta y^2)$ over the real half-line. The value of ϑ can be chosen for the convenience of the user. We will denote the normalised equal area generalised Wendland functions by $\psi_{\mu,\alpha}$.

Theorem 5.3. *With ϑ an arbitrary positive real number, the normalised equal area Wendland functions are given by*

$$\psi_{\mu,\alpha}(y) := \frac{2^{\alpha-1}\Gamma(\alpha)\Gamma(\mu+2\alpha+1)}{\Gamma(\mu+1)\Gamma(2\alpha)} \begin{cases} \phi_{\mu,\alpha}\left(\frac{y}{\delta_{\mu,\alpha}(\vartheta)}\right) & \text{for } 0 \le y \le \delta_{\mu,\alpha}(\vartheta), \\ 0 & \text{for } y > \delta_{\mu,\alpha}(\vartheta) \end{cases}, \tag{5.4}$$

where $\alpha > 0$, μ is given by (4.8) *and*

$$\delta_{\mu,\alpha}(\vartheta) := \frac{(\mu+2\alpha+1)\,\Gamma\left(\alpha+\frac{1}{2}\right)}{2\sqrt{\vartheta}\,\Gamma(\alpha+1)}. \tag{5.5}$$

Proof. Normalisation follows from Lemma 5.1. We can verify that this definition gives us the required area, with (5.3) and (5.1), as follows.

$$\begin{aligned} \int_0^{\delta_{\mu,\alpha}(\vartheta)} \psi_{\mu,\alpha}(y)\,\mathrm{d}y &= \frac{\delta_{\mu,\alpha}(\vartheta)}{\phi_{\mu,\alpha}(0)} \int_0^1 \phi_{\mu,\alpha}(r)\,\mathrm{d}r \\ &= \frac{\sqrt{\pi}}{2\sqrt{\vartheta}} \\ &= \int_0^\infty \exp(-\vartheta y^2)\,\mathrm{d}y. \end{aligned}$$

□

In Figure 5.2 we plot the normalised equal area original Wendland functions $\psi_{\ell,k}$ for $d=3$ and $k=1,\dots,5$ with $\vartheta=1$.

We emphasise that the normalised equal area Wendland functions satisfy both $\psi_{\mu,\alpha}(0)=1$ as well as

$$\|\psi_{\mu,\alpha}\|_1 = \int_0^\infty e^{-\vartheta y^2}\,\mathrm{d}y,$$

where ϑ can be any constant.

We will also need the following results.

Lemma 5.4. *With μ given by* (4.8) *and $\alpha \ge \min\left(\frac{d}{2},1,\beta\right)$. Then*

$$\delta_{\mu,\alpha}(\vartheta) \le \frac{4\sqrt{\alpha}}{\sqrt{\vartheta}}. \tag{5.6}$$

Proof. From [46] we have the double inequality

$$\left(\frac{x}{x+s}\right)^{1-s} \le \frac{\Gamma(x+s)}{x^s\,\Gamma(x)} \le 1,$$

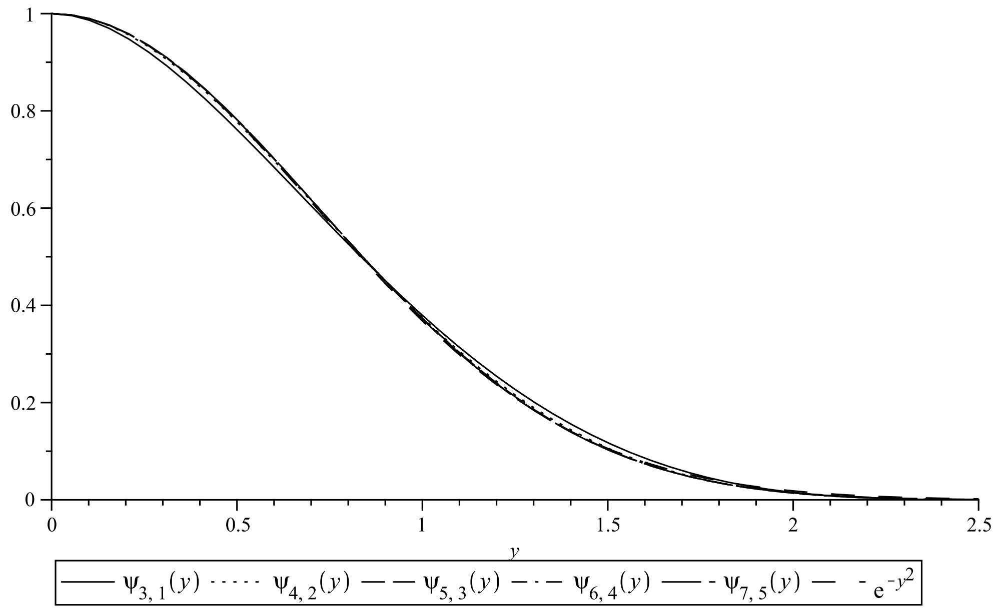

Figure 5.2. *The normalised equal area Wendland functions* $\psi_{3,1}(y)$, $\psi_{4,2}(y)$, $\psi_{5,3}(y)$, $\psi_{6,4}(y)$, $\psi_{7,5}(y)$ *with* $\alpha = 1$ *and* $\exp(-y^2)$.

for $0 < s < 1$ and $x > 0$. With $s = \frac{1}{2}$ and using $\Gamma(\alpha+1) = \alpha\Gamma(\alpha)$, this gives

$$\begin{aligned} \delta_{\mu,\alpha}(\vartheta) &= \frac{(\mu+2\alpha+1)}{2\sqrt{\vartheta}} \frac{\Gamma\left(\alpha+\frac{1}{2}\right)}{\Gamma(\alpha+1)} \\ &\leq \frac{(\mu+2\alpha+1)}{2\sqrt{\alpha\,\vartheta}} \\ &\leq \frac{\left(\frac{d}{2}+3\alpha+\beta+2\right)}{2\sqrt{\alpha\,\vartheta}} \\ &\leq \frac{4\sqrt{\alpha}}{\sqrt{\vartheta}}. \end{aligned}$$

□

Lemma 5.5. *Let* $\eta > 0$*. The function* $f_\eta : (0,\infty) \to \mathbb{R}$ *defined by*

$$f_\eta(y) := \frac{\Gamma(y+\eta)}{\Gamma(y)}, \quad y > 0, \tag{5.7}$$

is non-decreasing on $(0,\infty)$*.*

Proof. We provide a proof for the convenience of the reader. Consider $F_\eta(y) := \log f_\eta(y)$. Since $f_\eta(y) > 0$ and

$$\frac{\mathrm{d}\,F_\eta(y)}{\mathrm{d}y} = \frac{1}{f_\eta(y)} \frac{\mathrm{d}\,f_\eta(y)}{\mathrm{d}y},$$

we can consider the derivative of $F_\eta(y)$ since it will have the same sign as the derivative of $f_\eta(y)$. Now

$$\frac{\mathrm{d}\,F_\eta(y)}{\mathrm{d}y} = \psi_0(y+\eta) - \psi_0(y),$$

where ψ_0 is the digamma function with the series representation [1, 6.3.16]

$$\psi_0(y+1) = -\gamma + \sum_{n=1}^{\infty} \frac{y}{n(n+y)}, \quad y \neq -1, -2, -3, \ldots$$

where γ is the Euler-Mascheroni constant. This gives

$$\frac{\mathrm{d}\, F_\eta(y)}{\mathrm{d}y} = \sum_{n=0}^{\infty} \frac{\eta}{(n+y)(n+y+\eta)},$$

which converges and is positive on $(0, \infty)$, since $\eta > 0$. $\square$

5.2 Asymptotic behaviour as $\alpha \to \infty$

In this section, we consider the limit of the (generalised) equal area Wendland functions $\psi_{\mu,\alpha}$ as $\alpha \to \infty$. Section 5.2.1 presents the limit of the generalised equal area Wendland functions $\psi_{\mu,\alpha}$ as $\alpha \to \infty$. Section 5.2.2 provides some numerical results regarding the convergence, including graphs of the differences with the limiting Gaussian.

5.2.1 Limiting case of the normalised equal area Wendland functions $\psi_{\mu,\alpha}$ as $\alpha \to \infty$

In this section we derive the limit of the normalised equal area Wendland functions $\psi_{\mu,\alpha}$ as $\alpha \to \infty$. We start with a convergence result for the Fourier transforms.

Theorem 5.6. *Let ϑ be a positive real constant, $\alpha > \min(\frac{d}{2}, 1, \beta)$ and $\psi_{\mu,\alpha}$ be the normalised equal area generalised Wendland functions defined by* (5.4) *and* (5.5) *with μ given by* (4.8)*. Then*

$$\lim_{\alpha \to \infty} \mathcal{F}_d \psi_{\mu,\alpha}(z) = \widehat{G}_\vartheta(z) \tag{5.8}$$

uniformly for z in an arbitrary bounded subinterval of the positive numbers.

Proof. Firstly we express the Fourier transform of $\psi_{\mu,\alpha}$ in terms of the Fourier transform of $\phi_{\mu,\alpha}$. Writing $\delta_{\mu,\alpha}$ for $\delta_{\mu,\alpha}(\vartheta)$ and using the transformation $y = r\,\delta_{\mu,\alpha}$ gives, from (4.2),

$$\begin{aligned}
\mathcal{F}_d \psi_{\mu,\alpha}(z) &= z^{1-\frac{d}{2}} \int_0^{\delta_{\mu,\alpha}} \psi_{\mu,\alpha}(y)\, y^{\frac{d}{2}}\, J_{\frac{d}{2}-1}(zy)\, \mathrm{d}y \\
&= \frac{2^{\alpha-1}\Gamma(\alpha)\Gamma(\mu+2\alpha+1) z^{1-\frac{d}{2}}\, \delta_{\mu,\alpha}}{\Gamma(\mu+1)\Gamma(2\alpha)} \int_0^1 \phi_{\mu,\alpha}(r)\, \left(r\,\delta_{\mu,\alpha}\right)^{\frac{d}{2}}\, J_{\frac{d}{2}-1}(z\,r\,\delta_{\mu,\alpha})\, \mathrm{d}r \\
&= \frac{2^{\alpha-1}\Gamma(\alpha)\Gamma(\mu+2\alpha+1) z^{1-\frac{d}{2}}\, \delta_{\mu,\alpha}^{1+\frac{d}{2}}}{\Gamma(\mu+1)\Gamma(2\alpha)(\delta_{\mu,\alpha}\, z)^{1-\frac{d}{2}}} \left(\mathcal{F}_d \phi_{\mu,\alpha}\right)(\delta_{\mu,\alpha}\, z) \\
&= \frac{2^{\alpha-1}\Gamma(\alpha)\Gamma(\mu+2\alpha+1) \delta_{\mu,\alpha}^{d}}{\Gamma(\mu+1)\Gamma(2\alpha)} \left(\mathcal{F}_d \phi_{\mu,\alpha}\right)(\delta_{\mu,\alpha} z).
\end{aligned} \tag{5.9}$$

Next we use Theorem 4.3 to write the Fourier transform of $\psi_{\mu,\alpha}$ in terms of a hypergeometric function as

$$\mathcal{F}_d\psi_{\mu,\alpha}(z) = \frac{\delta_{\mu,\alpha}^d 2^{-\frac{d}{2}}\Gamma(\mu+2\alpha+1)\Gamma(\alpha)\Gamma(d+2\alpha)}{\Gamma(2\alpha)\Gamma\left(\frac{d}{2}+\alpha\right)\Gamma(\mu+d+2\alpha+1)} \times \\ {}_1F_2\left(\frac{d+1}{2}+\alpha; \frac{\mu+d+2\alpha+1}{2}, \frac{\mu+d+2\alpha+2}{2}; -\frac{\delta_{\mu,\alpha}^2 z^2}{4}\right), \quad (5.10)$$

with $\delta_{\mu,\alpha} = \delta_{\mu,\alpha}(\vartheta)$. Then the equivalent series representation is as follows

$$\begin{aligned}\mathcal{F}_d\psi_{\mu,\alpha}(z) &= 2^{-\frac{d}{2}} \sum_{n=0}^{\infty} \frac{\Gamma(d+2\alpha+2n)\Gamma(\mu+2\alpha+1)\Gamma(\alpha)}{\Gamma(2\alpha)\Gamma(\mu+2\alpha+1+d+2n)\Gamma\left(\alpha+\frac{d}{2}+n\right)} \delta_{\mu,\alpha}^{d+2n} \frac{\left(-\frac{z^2}{4}\right)^n}{n!} \\ &= 2^{-\frac{d}{2}} \sum_{n=0}^{\infty} w_n(\alpha)\left(-\frac{z^2}{4}\right)^n, \qquad (5.11)\end{aligned}$$

where

$$w_n(\alpha) := \frac{\Gamma(d+2\alpha+2n)\Gamma(\mu+2\alpha+1)\Gamma(\alpha)}{\Gamma(2\alpha)\Gamma(\mu+2\alpha+1+d+2n)\Gamma\left(\alpha+\frac{d}{2}+n\right)} \frac{\delta_{\mu,\alpha}^{d+2n}}{n!}. \quad (5.12)$$

To interchange the limit as $\alpha \to \infty$ and the infinite sum, we need to prove that this sum is dominated by an absolutely convergent series (Lebesgue's dominated convergence theorem). Using (4.7) twice together with Lemma 5.4 and the bound [11, 5.6.8]

$$\frac{\Gamma(x+a)}{\Gamma(x+b)} \le \frac{1}{x^{b-a}}, \quad x>0, b-a\ge 1, a\ge 0, \quad (5.13)$$

we have for $\alpha \ge 1$

$$\begin{aligned} w_n(\alpha) &= \frac{2^{d+2n}\Gamma\left(\frac{d}{2}+\alpha+n+\frac{1}{2}\right)\Gamma(\mu+2\alpha+1)}{\Gamma\left(\alpha+\frac{1}{2}\right)\Gamma(\mu+2\alpha+1+d+2n)} \frac{\delta_{\mu,\alpha}^{d+2n}}{n!} \\ &\le \frac{2^{d+2n}\Gamma\left(\frac{d}{2}+\frac{3\alpha}{2}+n\right)\Gamma(3\alpha)}{\Gamma\left(\frac{3\alpha}{2}\right)\Gamma(3\alpha+d+2n)} \frac{\delta_{\mu,\alpha}^{d+2n}}{n!} \\ &= \frac{2^{d+2n}\Gamma\left(\frac{d}{2}+\frac{3\alpha}{2}+n\right)2^{3\alpha-1}\Gamma\left(\frac{3\alpha}{2}\right)\Gamma\left(\frac{3\alpha+1}{2}\right)}{\Gamma\left(\frac{3\alpha}{2}\right)2^{3\alpha+d+2n-1}\Gamma\left(\frac{3\alpha+d}{2}+n\right)\Gamma\left(\frac{3\alpha+d+1}{2}+n\right)} \frac{\delta_{\mu,\alpha}^{d+2n}}{n!} \\ &= \frac{\Gamma\left(\frac{3\alpha+1}{2}\right)}{\Gamma\left(\frac{3\alpha+d+1}{2}+n\right)} \frac{\delta_{\mu,\alpha}^{d+2n}}{n!} \\ &\le \frac{1}{\left(\frac{3\alpha}{2}\right)^{\frac{d}{2}+n}} \left(\frac{4\sqrt{\alpha}}{\sqrt{\vartheta}}\right)^{d+2n} \frac{1}{n!} \\ &= \left(\frac{32}{3\vartheta}\right)^{\frac{d}{2}+n} \frac{1}{n!} \\ &=: R_n, \end{aligned}$$

where for the inequalities above we used

$$\frac{\Gamma(\mu+2\alpha+1)}{\Gamma(\mu+2\alpha+1+d+2n)} \le \frac{\Gamma(3\alpha)}{\Gamma(3\alpha+d+2n)}$$

and for $\alpha \geq 1$

$$\frac{\Gamma\left(\frac{d}{2}+\alpha+n+\frac{1}{2}\right)}{\Gamma\left(\alpha+\frac{1}{2}\right)} \leq \frac{\Gamma\left(\frac{d}{2}+\frac{3\alpha}{2}+n\right)}{\Gamma\left(\frac{3\alpha}{2}\right)},$$

both of which follow from Lemma 5.5.

The ratio test shows that $\sum_n R_n \left(-\frac{z^2}{4}\right)^n$ is absolutely convergent. Therefore we can take the limit as $\alpha \to \infty$ inside the infinite sum, giving

$$\lim_{\alpha\to\infty} \mathcal{F}_d \psi_{\mu,\alpha}(z) = 2^{-\frac{d}{2}} \sum_{n=0}^{\infty} \lim_{\alpha\to\infty} w_n(\alpha) \left(-\frac{z^2}{4}\right)^n.$$

Using the following asymptotic result from [11]

$$\frac{\Gamma(x+a)}{\Gamma(x+b)} \sim x^{a-b}, \tag{5.14}$$

we can see that

$$\lim_{\alpha\to\infty} w_n(\alpha) = \frac{1}{n!\vartheta^{\frac{d}{2}+n}}$$

and hence

$$\begin{aligned}
\lim_{\alpha\to\infty} \mathcal{F}_d \psi_{\mu,\alpha}(z) &= (2\vartheta)^{-\frac{d}{2}} \sum_{n=0}^{\infty} \frac{\left(-\frac{z^2}{4\vartheta}\right)^n}{n!} \\
&= (2\vartheta)^{-\frac{d}{2}} e^{-\frac{z^2}{4\vartheta}} \\
&= \widehat{G}_\vartheta(z),
\end{aligned}$$

which proves pointwise convergence. Uniform convergence follows since the interval is bounded. $\square$

We are now ready to state the main result of this subsection.

Theorem 5.7. *Let ϑ be a positive real constant, $\alpha > \min(\frac{d}{2}, 1, \beta)$ and $\psi_{\mu,\alpha}$ be the normalised equal area generalised Wendland functions $\psi_{\mu,\alpha}$ defined by* (5.4) *and* (5.5) *with μ given by* (4.8). *Then*

$$\lim_{\alpha\to\infty} \psi_{\mu,\alpha}(y) = G_\vartheta(y) \tag{5.15}$$

with the convergence being uniform for $y \in [0,\infty)$.

Proof. It follows from (4.5) that for a fixed y

$$\begin{aligned}
|\psi_{\mu,\alpha}(y) - G_\vartheta(y)| &= y^{1-\frac{d}{2}} \left| \int_0^\infty \left(\mathcal{F}_d \psi_{\mu,\alpha}(z) - \widehat{G}_\vartheta(z)\right) z^{\frac{d}{2}} J_{\frac{d}{2}-1}(yz)\, \mathrm{d}z \right| \\
&\leq \frac{2^{1-\frac{d}{2}}}{\Gamma(\frac{d}{2})} \int_0^\infty |\mathcal{F}_d \psi_{\mu,\alpha}(z) - \widehat{G}_\vartheta(z)| z^{d-1}\, \mathrm{d}z, \qquad (5.16)
\end{aligned}$$

where we have used the following bound on the Bessel function [11, 10.14.4]

$$|J_v(x)| \le \frac{|\frac{x}{2}|^v}{\Gamma(v+1)}, \quad v \ge -\frac{1}{2}, \quad x \in \mathbb{R}.$$

Since the right hand side of (5.16) is independent of y, the result follows if we can show that

$$D_{\vartheta,\alpha} := \int_0^\infty |\mathcal{F}_d \psi_{\mu,\alpha}(z) - \widehat{G}_\vartheta(z)| z^{d-1}\, \mathrm{d}z \to 0 \quad \text{as} \quad \alpha \to \infty.$$

Now for arbitrary $Z > 0$ we have, because $\mathcal{F}_d \psi_{\mu,\alpha}$ and $\widehat{G}_\vartheta$ are non-negative,

$$\begin{aligned} D_{\vartheta,\alpha} &\le \int_0^Z |\mathcal{F}_d \psi_{\mu,\alpha}(z) - \widehat{G}_\vartheta(z)| z^{d-1}\, \mathrm{d}z + \int_Z^\infty \mathcal{F}_d \psi_{\mu,\alpha}(z)\, z^{d-1}\, \mathrm{d}z + \int_Z^\infty \widehat{G}_\vartheta(z)\, z^{d-1}\, \mathrm{d}z \\ &= \int_0^Z |\mathcal{F}_d \psi_{\mu,\alpha}(z) - \widehat{G}_\vartheta(z)| z^{d-1}\, \mathrm{d}z + \int_0^Z \left(\widehat{G}_\vartheta(z) - \mathcal{F}_d \psi_{\mu,\alpha}(z)\right) z^{d-1}\, \mathrm{d}z \\ &\qquad + 2\int_Z^\infty \widehat{G}_\vartheta(z)\, z^{d-1}\, \mathrm{d}z \\ &\le 2\int_0^Z |\mathcal{F}_d \psi_{\mu,\alpha}(z) - \widehat{G}_\vartheta(z)| z^{d-1}\, \mathrm{d}z + 2\int_Z^\infty \widehat{G}_\vartheta(z)\, z^{d-1}\, \mathrm{d}z, \end{aligned} \tag{5.17}$$

where we used the positivity of $\mathcal{F}_d \psi_{\ell,k}$ and $\widehat{G}_\alpha$, and

$$\int_0^\infty \mathcal{F}_d \psi_{\ell,k}(z)\, z^{d-1}\, \mathrm{d}z = \int_0^\infty \widehat{G}_\alpha(z)\, z^{d-1}\, \mathrm{d}z = 2^{\frac{d}{2}-1}\Gamma\left(\frac{d}{2}\right),$$

which follow from (4.3) with $\mathcal{F}_d$ replaced by $\mathcal{F}_d^{-1}$.

Given an arbitrary $\epsilon > 0$, we now choose Z sufficiently large to ensure that

$$\int_Z^\infty \widehat{G}_\vartheta(z)\, z^{d-1}\, \mathrm{d}z < \frac{\epsilon}{4}.$$

For the first term in (5.17), we note that from Theorem 5.6, the integrand converges to zero uniformly for z in a bounded interval, thus there exists $\alpha_1 \in \mathbb{R}_+$ such that

$$\int_0^Z |\mathcal{F}_d \psi_{\mu,\alpha}(z) - \widehat{G}_\vartheta(z)| z^{d-1}\, \mathrm{d}z < \frac{\epsilon}{4} \quad \forall \ \alpha \ge \alpha_1,$$

and hence

$$D_{\vartheta,\alpha} < \frac{\epsilon}{2} + \frac{\epsilon}{2} = \epsilon$$

for all $\alpha \ge \alpha_1$, which completes the proof. □

An interpretation of Theorem 5.7 in terms of probability distributions is that

$$\lim_{\alpha\to\infty} \frac{1}{\sqrt{2\pi}\,\sigma} \tilde{\phi}_{\mu,\alpha}\left(\frac{y}{\delta_{\mu,\alpha}\left(\frac{1}{2\sigma^2}\right)}\right) = \frac{1}{\sqrt{2\pi}\,\sigma} \exp\left(-\frac{y^2}{2\sigma^2}\right), \quad y \ge 0 \tag{5.18}$$

where the limit on the right hand side is the right half of the Gaussian probability density with mean 0 and variance σ^2.

We note that since

$$\delta_{\ell,k}(\vartheta) \sim \frac{3}{2}\sqrt{\frac{\alpha}{\vartheta}}, \tag{5.19}$$

from (5.14), we could have used the right hand side of this expression instead of $\delta_{\ell,k}(\vartheta)$ to define a change of variable to study the limiting case.

Since the original and missing Wendland functions are simply special cases of the generalised Wendland functions, and there were no restrictions on α in Theorem 5.7, this result will also hold for the original and missing Wendland functions.

We note that the similarity of the normalised (original) Wendland functions to a Gaussian has been mentioned in [30] and of the normalised equal area (original) Wendland functions to a Gaussian in [15], in both cases for $\mathbb{R}^3$ with $k = 1$. No theoretical explanations were given for these observations.

5.2.2 Numerical results

In this section we present numerical results regarding the differences between the appropriately scaled original and missing Wendland functions and the Gaussian limit established in Theorem 5.7. We also consider an interpolation example using both the original Wendland functions $\phi_{\ell,k}$, normalised to have value 1 at the origin, and the normalised equal area original Wendland functions $\psi_{\ell,k}$.

Difference with the limiting Gaussian

Let the differences between the normalised equal area Wendland functions and the limiting Gaussian be

$$E_{\ell,k}(y) := \psi_{\ell,k}(y) - \exp(-\vartheta y^2)$$

and let

$$\epsilon_{\ell,k} := \sup_{y \geq 0} |E_{\ell,k}(y)|,$$

Note that the change of variable used to define $\psi_{\ell,k}$ depends on the parameter ϑ. Figure 5.3 shows plots of $E_{\ell,k}(y)$ with $\vartheta = 1$. The upper plots are for $d = 2$ and $k = 1.5$ and $k = 5.5$ and the lower plots are for $d = 3$ and $k = 2$ and $k = 6$.

In the absence of theoretical rates of convergence, we show numerical results. Figure 5.4 shows $\epsilon_{\ell,k}$ with $\vartheta = 1$ for $k = 1, \ldots, 50$ and $d = 3, 5, 7$ and 9 for the original Wendland functions. Figure 5.5 shows $\epsilon_{\ell,k}$ with $\vartheta = 1$ for $k = 0.5, \ldots, 49.5$ and $d = 2, 4, 6$ and 8 for the missing Wendland functions. Since ϑ is just a scaling factor, the results do not vary

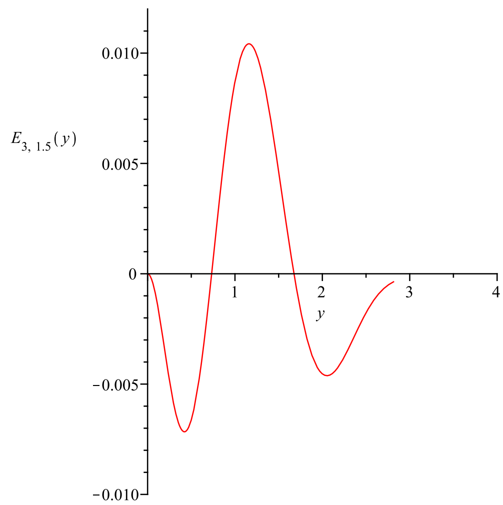

(a) $d = 2, k = 1.5$

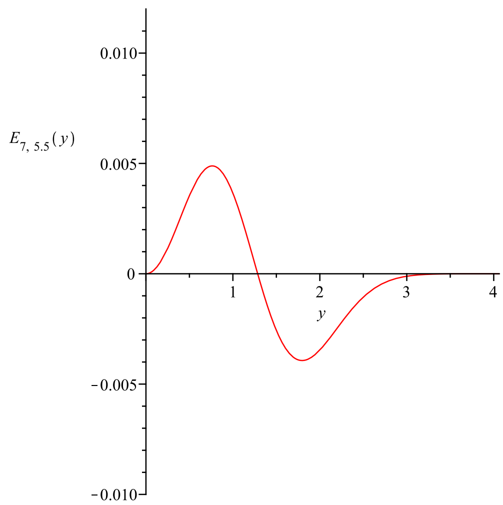

(b) $d = 2, k = 5.5$

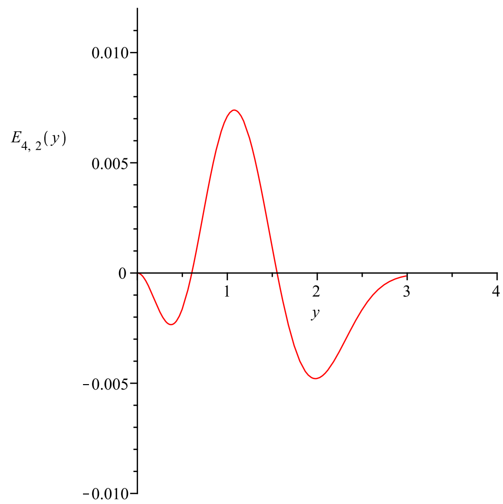

(c) $d = 3, k = 2$

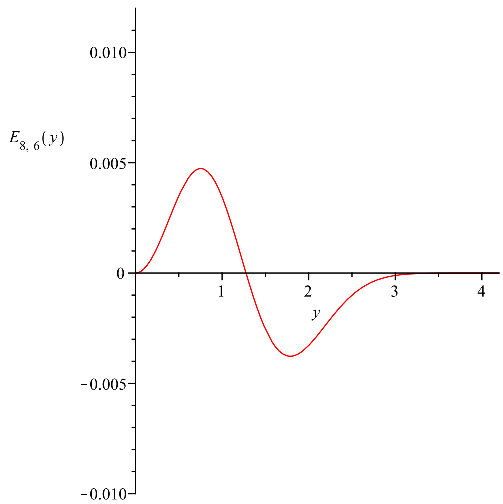

(d) $d = 3, k = 6$

Figure 5.3. *$E_{\ell,k}(y)$ with $\alpha = 1$ and $0 \leq y \leq \delta_{\ell,k}(1)$. Subplots (a) and (b) are for the missing Wendland functions and subplots (c) and (d) are for the original Wendland functions.*

in an essential way for different values of ϑ.

In all cases, we see convergence of $\epsilon_{\ell,k}$ to zero as the smoothness parameter k increases. This is consistent with the theoretical convergence results. Note that $\epsilon_{\ell,k}$ is not monotonically decreasing in k. We also remark that $\epsilon_{\ell,k}$ is reached at different values of y as k increases.

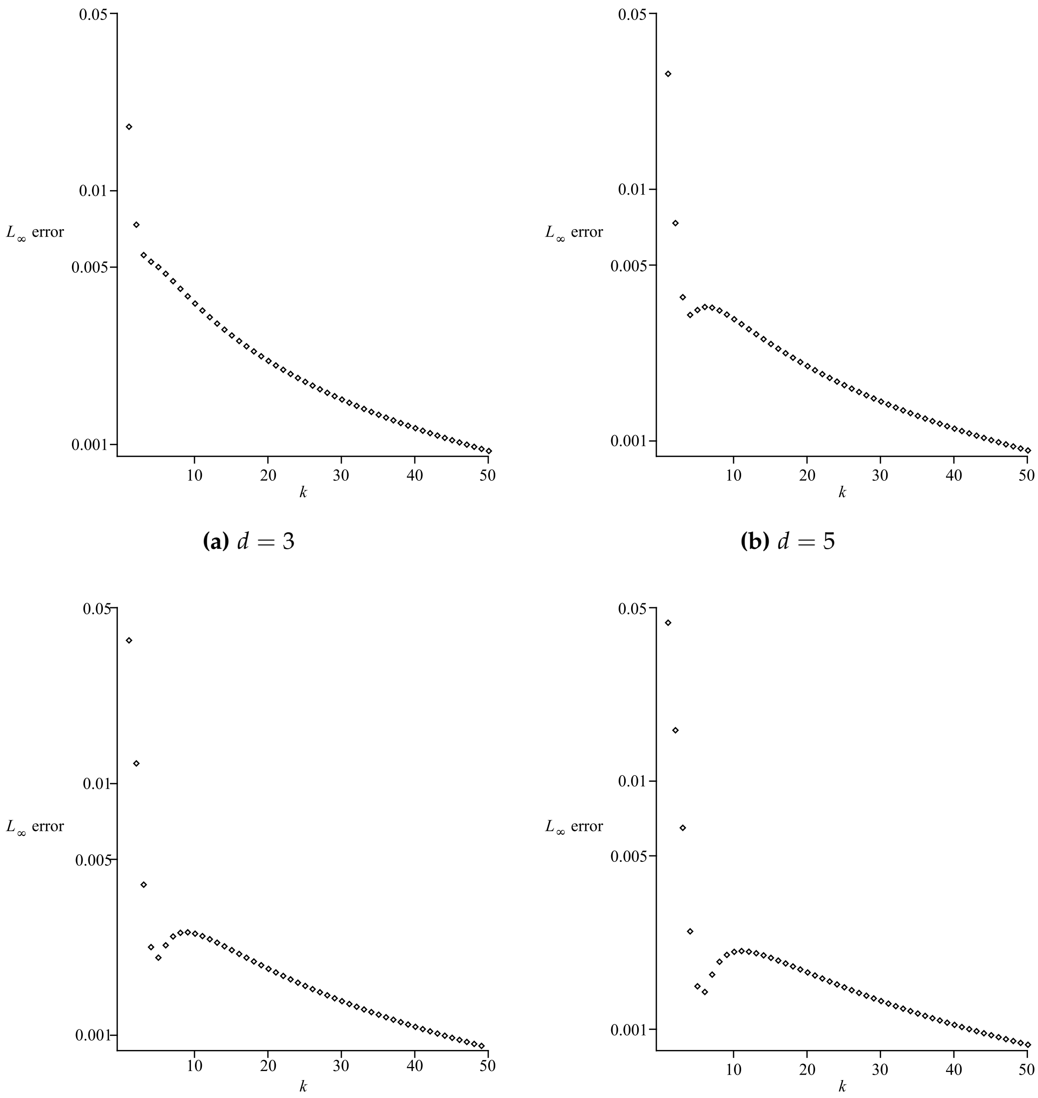

(a) $d = 3$

(b) $d = 5$

(c) $d = 7$

(d) $d = 9$

Figure 5.4. *$\epsilon_{\ell,k}$ on a logarithmic scale with $\vartheta = 1$, $k = 1, \ldots, 50$ and $d = 3, 5, 7, 9$ for the original Wendland functions.*

An interpolation example

We consider an example, in which we show results obtained with both the Wendland functions $\phi_{\ell,k}$, normalised to have value 1 at the origin, and the normalised equal area Wendland functions $\psi_{\ell,k}$ for different values of k. The aim of the example is to approximate the 2-dimensional Franke-like function (the Franke function [16] rescaled to $[0,5]^2$). For $k = 1, \ldots, 5$ we consider interpolation, using the Wendland functions $\phi_{\ell,k}$, normalised to have value 1 at the origin, and the normalised equal area Wendland functions $\psi_{\ell,k}$ with $\vartheta = 2$. We use 9×9 and 17×17 equally spaced grids as the centres. The number of centres is thus $n = 81$ and $n = 289$. The L_2 error was estimated

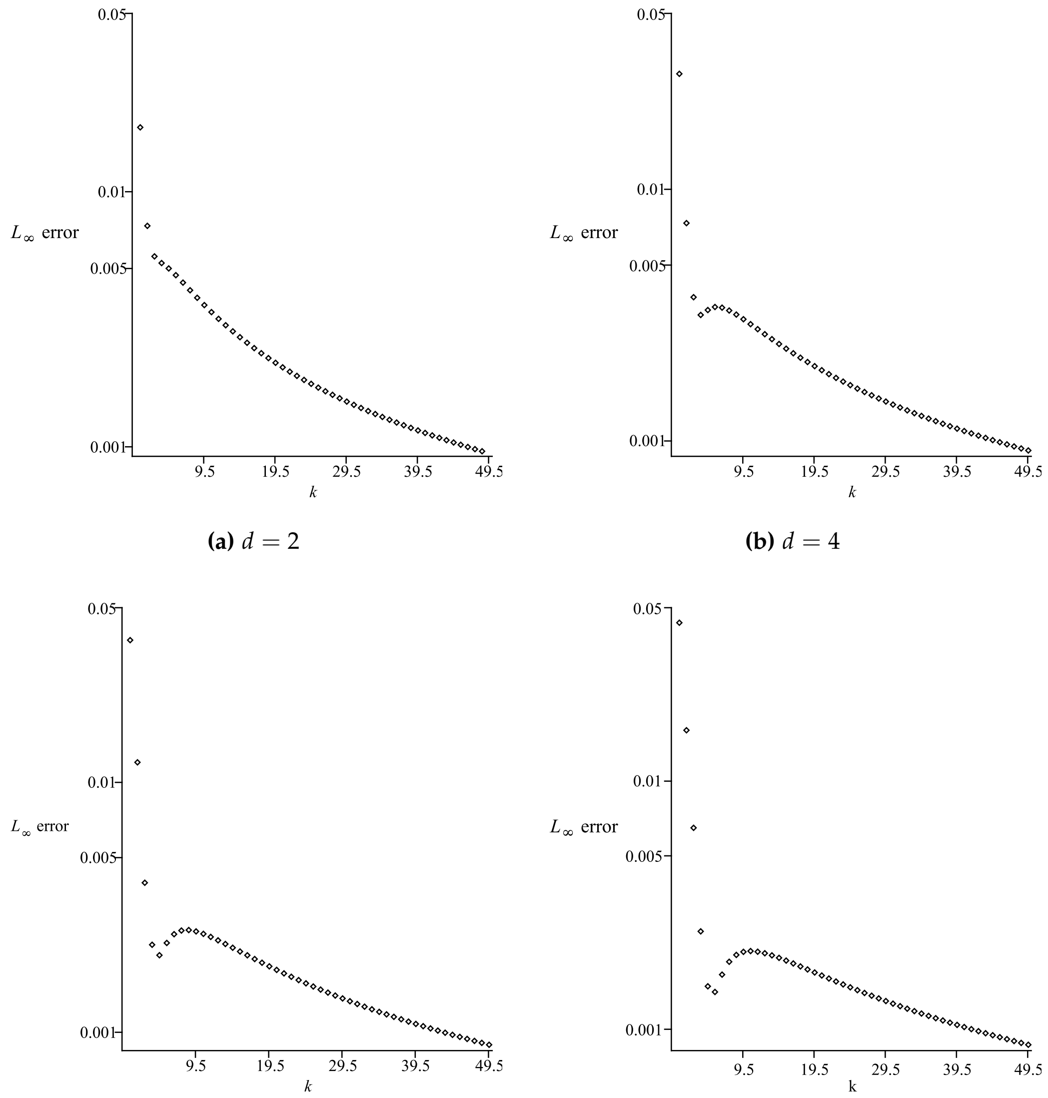

(a) $d = 2$ **(b)** $d = 4$

(c) $d = 6$ **(d)** $d = 8$

Figure 5.5. *$\epsilon_{\ell,k}$ on a logarithmic scale with $\vartheta = 1$, $k = 0.5, \ldots, 49.5$ and $d = 2, 4, 6, 8$ for the missing Wendland functions.*

using Gaussian quadrature with a 120×120 tensor product grid of Gauss-Legendre points and the L_∞ error was estimated by using a 360×360 equally spaced grid. Table 5.1 shows the L_2 and L_∞ errors, as well as the 2-norm condition numbers of the interpolation matrices. We also show the results with the limiting Gaussian of $\exp(-2\,y^2)$, denoted by $k = \infty$.

We see from the right-hand part of Table 5.1 that once the argument is properly scaled to give approximately constant effective support, increasing the smoothness has remarkably little effect on the error. On the other hand the condition number increases rapidly as the smoothness increases and is very large for the Gaussian limit. Taken together, these observations suggest that any benefit gained from the higher smoothness is likely to be offset by the increased condition numbers of the matrices.

The results with the Wendland functions $\phi_{\ell,k}$, normalised to have value 1 at the origin, are in the left-hand part of Table 5.1. We can see that the condition number is decreasing as k increases, which is due to the decreasing magnitude of the non-zero elements away from the diagonal. This is due to the fact that as k increases the Wendland functions $\phi_{\ell,k}$, normalised to have value 1 at the origin, decay more rapidly with respect to r, as illustrated in Figure 5.1.

		RBF: $\phi_{\ell,k}$			RBF: $\psi_{\ell,k}$				
N	k	L_2 error	L_∞ error	κ	L_2 error	L_∞ error	κ	$\lambda_{\min}$	$\lambda_{\max}$
81	1	2.25e-1	6.96e-1	1.71	1.89e-1	5.89e-1	1.76e1	1.55e-1	2.74
	2	2.61e-1	7.95e-1	1.22	1.86e-1	5.78e-1	3.14e1	9.62e-2	3.02
	3	3.00e-1	8.90e-1	1.07	1.87e-1	5.79e-1	4.96e1	6.50e-2	3.22
	4	3.36e-1	9.73e-1	1.02	1.87e-1	5.80e-1	5.56e1	5.98e-2	3.30
	5	3.63e-1	1.03	1.01	1.87e-1	5.81e-1	6.37e1	5.29e-2	3.37
	∞				1.89e-1	5.89e-1	9.40e1	4.03e-2	3.78
289	1	7.75e-2	2.26e-1	4.87e1	8.20e-2	2.45e-1	4.77e2	2.25e-2	10.74
	2	7.48e-2	2.00e-1	5.64e1	7.98e-2	2.11e-1	3.89e3	3.08e-3	11.97
	3	7.47e-2	1.98e-1	3.00e1	7.88e-2	2.00e-1	1.23e4	1.04e-3	12.78
	4	7.59e-2	2.12e-1	1.24e1	7.71e-2	2.04e-1	9.88e4	1.33e-4	13.09
	5	7.75e-2	2.33e-1	6.85	7.61e-2	2.09e-1	3.77e5	3.55e-5	13.39
	∞				7.23e-2	1.90e-1	2.13e9	7.04e-9	15.00

Table 5.1. *Results from the example in Section 5.2.2 showing L_2 and L_∞ errors, 2-norm condition numbers κ and minimum and maximum eigenvalues ($\lambda_{\min}$ and $\lambda_{\max}$) when using the Wendland RBFs $\phi_{\ell,k}$, normalised to have value 1 at the origin, and the normalised equal area Wendland RBFs $\psi_{\ell,k}$ with $\vartheta = 2$.*

5.3 On the selection of the parameter μ

We recall from (4.8) that $\mu = \frac{d+1}{2} + \alpha + \beta$, where β is a non-negative constant. We are now better able to understand the effect of choosing different values of β. For a given spatial dimension d, higher values of β are equivalent to higher values of the smoothness parameter α, and hence we will see faster decay of the generalised Wendland functions as we select higher values of β. Consequently there appears little benefit to selecting

$\beta > 0$, as this will lead to reduced overlap between the basis functions as well as higher degree polynomials which will increase computational complexity.

5.4 Implications for selecting scaling parameters

In Figure 5.1 we saw that the (original) normalised Wendland functions exhibit faster decay with respect to r as the smoothness parameter k increases. This suggests the need for a change of variable, not only to have a well-defined limit as considered in this paper, but perhaps also in practical applications. Without a change of variable, in the case of interpolation we could have a nearly diagonal interpolation matrix and consequently high errors between the interpolation points.

The number of interpolation points that fall within the support of an RBF is also related to the stationary approach to interpolation (e.g. [12, Section 12.2]), in which the goal is to keep the number of points in the support of each RBF approximately equal across different sets of centres. However here it is not the centres that are changing, but rather the basis functions that change with k.

In Figure 5.2 we saw the (original) normalised equal area Wendland functions, whilst formally having support $[0, \delta_{\ell,k}(\alpha)]$ that is different for each k, appear nearly identical. As a result, if the user wishes to compare the results using Wendland functions of different smoothness, the normalised equal area Wendland functions may be a more appropriate choice of RBF.

We saw in Section 5.2.2 that whilst the normalised equal area Wendland functions with different k might appear comparable, and give similar accuracy, the increasing support as k increases causes decreased sparsity of the interpolation matrix, and consequently an increased condition number of the linear system. This leads us to conclude that there may be little benefit from considering high values of the smoothness parameter k.

Chapter Six

Solving PDEs with Wendland functions

This chapter will review theoretical results concerning the construction of approximate solutions to elliptic PDEs and the Stokes problem with Wendland functions.

Section 6.1 covers approximation theory for Galerkin approximation, and Section 6.2 does the same in the case of collocation. This chapter should be viewed as operating in a single scale (single level) framework.

6.1 Galerkin approximation for elliptic PDEs

6.1.1 PDEs with Neumann and/or Robin boundary conditions

In this section, we consider a second order PDE which has homogeneous Neumann and/or Robin boundary conditions. For example, such a PDE with Neumann boundary conditions is given by

$$\mathcal{L}u = f \quad \text{in } \Omega, \tag{6.1a}$$

$$\frac{\partial u}{\partial \mathbf{n}} = 0 \quad \text{on } \partial\Omega, \tag{6.1b}$$

where $\mathcal{L}$ is a second order elliptic differential operator, $\mathbf{n}$ denotes the outward unit normal vector and $\partial\Omega$ denotes the boundary of the domain $\Omega \subseteq \mathbb{R}^d$. We now assume that $\langle \mathcal{L}u, u \rangle$ is equivalent to $\|u\|^2_{H_1(\mathbb{R}^d)}$, as in the case where $\mathcal{L} = -\Delta + I$. The weak formulation is given by

$$a(u,v) = \langle f, v \rangle_{L_2(\Omega)} \quad \forall\, v \in V, \tag{6.2}$$

where $V = H^1(\Omega)$. We assume that $\mathcal{L}$ and f are such that $a(u,v)$ is a strictly coercive and continuous bilinear form defined on $V \times V$ and $\langle f, v \rangle_{L_2(\Omega)}$ is a continuous linear form defined on V. By the Lax-Milgram theorem, (6.2) has a unique solution $u \in V$. We will also require $u \in H^2(\Omega)$ with spatial dimension $d \leq 3$.

Galerkin approximation seeks to find an approximation to (6.2) in a finite dimensional subspace $V_N \subseteq V$. In other words, the Galerkin approximation $\widetilde{u}_N$ is the solution of

$$\widetilde{u}_N \in V_N : a(\widetilde{u}_N, v) = \langle f, v \rangle_{L_2(\Omega)} \quad \forall\, v \in V_N. \tag{6.3}$$

We will consider Ω to be a bounded domain with a Lipschitz boundary, which means that we can apply the extension operator to use norms in $\mathbb{R}^d$ as stated in Lemma 2.1. For further information on weak formulation of PDEs and Galerkin approximation, we refer the reader to [7].

Since the PDE does not have Dirichlet boundary conditions, we can use the entire Sobolev space $H^1(\Omega)$ rather than the subspace $\mathring{H}^1(\Omega)$ consisting of functions with zero boundary values, which can occur with pure Dirichlet boundary conditions.

We will consider finite dimensional subspaces $V_N \subseteq V$ of the form

$$V_N := \text{span}\left\{\Phi\left(\cdot - \mathbf{x}_j\right) : 1 \leq j \leq N\right\},$$

where $\Phi : \mathbb{R}^d \to \mathbb{R}$ is at least a C^1-function and there are N centres $\{\mathbf{x}_j : 1 \leq j \leq N\}$. In this case our approximation takes the form

$$\widetilde{u}_N = \sum_{j=1}^{N} c_j \Phi(\cdot - \mathbf{x}_j),$$

and the weak formulation with this approximation given by

$$a(\widetilde{u}_N, v) = \langle f, v \rangle_{L_2(\Omega)} \quad \forall\, v \in V_N,$$

results in a linear system

$$\mathbf{Ac} = \mathbf{f},$$

where the entries of the *stiffness matrix* are given by

$$A_{ij} = a(\Phi(\cdot - \mathbf{x}_i), \Phi(\cdot - \mathbf{x}_j)) \tag{6.4}$$

and

$$f_i = \int_\Omega f(\mathbf{x}) \Phi(\mathbf{x} - \mathbf{x}_i)\, \mathrm{d}\mathbf{x}.$$

We have the following result from [49].

Theorem 6.1. *If $u \in H^2(\Omega), d \leq 3$, is the solution to the variational problem* (6.2) *and $\widetilde{u}_N \in V_N$ is the solution of* (6.3)*, where V_N is generated with a point set X satisfying $h \leq h_0$ for h_0 small enough and a kernel Φ satisfying* (3.20)*, then the error can be bounded by*

$$\|u - \widetilde{u}_N\|_{H^1(\Omega)} \leq Ch\|u\|_{H^2(\Omega)}.$$

Lemma 6.2. *Consider the adjoint variational problem*

$$a(v, w) = \langle g, v \rangle_{L_2(\Omega)} \quad \forall\, v \in V. \tag{6.5}$$

If the adjoint problem satisfies the regularity estimate

$$\|w\|_{H^2(\Omega)} \leq C\|g\|_{L_2(\Omega)}, \tag{6.6}$$

then we have the following error bound

$$\|u - \widetilde{u}_N\|_{L_2(\Omega)} \leq Ch\|u - \widetilde{u}_N\|_{H^1(\Omega)} \leq Ch^2\|u\|_{H^2(\Omega)}.$$

Proof. With $\widetilde{u}_N$ as defined in (6.3), let w be the solution to the adjoint problem

$$a(v, w) = \langle u - \widetilde{u}_N, v\rangle_{L_2(\Omega)} \quad \forall\, v \in V,$$

and let the Galerkin approximation be given by $\widetilde{w}$. Then since the bilinear form $a(\cdot, \cdot)$ is bounded, $u \in H^2(\Omega)$, and with Theorem 6.1 we have, for $\widetilde{w} \in V_N$,

$$\begin{aligned}
\|u - \widetilde{u}_N\|^2_{L_2(\Omega)} &= \langle u - \widetilde{u}_N, u - \widetilde{u}_N\rangle_{L_2(\Omega)} \\
&= a(u - \widetilde{u}_N, w) = a(u - \widetilde{u}_N, w - \widetilde{w}) \\
&\leq C\|u - \widetilde{u}_N\|_{H^1(\Omega)}\, \|w - \widetilde{w}\|_{H^1(\Omega)} \\
&\leq Ch\|u - \widetilde{u}_N\|_{H^1(\Omega)}\, \|w\|_{H^2(\Omega)} \\
&\leq Ch\|u - \widetilde{u}_N\|_{H^1(\Omega)}\, \|u - \widetilde{u}_N\|_{L_2(\Omega)},
\end{aligned}$$

where for the second last step, we use the regularity estimate (6.6) and the result follows with another application of Theorem 6.1. □

We note that (6.6) is known to hold [7, p.139]

- if Ω has a smooth boundary and the problem has pure Dirichlet or pure Neumann boundary conditions;
- if $d = 2$ and Ω is convex and the problem has pure Dirichlet or pure Neumann boundary conditions.

6.1.2 PDEs with Dirichlet boundary conditions

In this section we will consider a PDE with Dirichlet boundary conditions and we seek error estimates similar to those in the previous section. For ease of description, we will consider the following boundary value problem

$$-\Delta u = f \quad \text{in } \Omega, \tag{6.7a}$$

$$u = g \quad \text{on } \partial\Omega, \tag{6.7b}$$

where Δ denotes the Laplacian in $\mathbb{R}^d$. Nitsche [34] proposed minimising the functional $J(v-u)$ where

$$J(w) := \int_{\Omega} |\nabla w|^2 - 2 \int_{\partial\Omega} w\,(\nabla w \cdot \mathbf{n}) + \beta_N \int_{\partial\Omega} w^2,$$

for all $v \in V_N$ with u being the solution of (6.7) and where $\mathbf{n}$ denotes the outward unit normal vector and ∇ the gradient operator. The parameter $\beta_N > 0$ depends only on the subspace V_N. The approximation $\widetilde{u}_N$ is given by

$$J(\widetilde{u}_N - u) := \inf_{v \in V_N} J(v-u).$$

With f and g from (6.7), we can compute $\widetilde{u}_N$ since

$$J(v-u) = J(v) + J(u) - 2\left(\int_{\Omega} fv + \int_{\partial\Omega} g\,(\beta_N v - \nabla v \cdot \mathbf{n}) \right).$$

Then the variational form to approximate (6.7) becomes: find $\widetilde{u}_N \in V_N$ such that for all $v \in V_N$

$$a_D(\widetilde{u}_N, v) = \ell_D(v), \tag{6.8}$$

where we use the subscript D to denote the Dirichlet boundary conditions and

$$a_D(u,v) := \int_{\Omega} \nabla u \cdot \nabla v - \int_{\partial\Omega} v\,(\nabla u \cdot \mathbf{n}) - \int_{\partial\Omega} u\,(\nabla v \cdot \mathbf{n}) + \beta_N \int_{\partial\Omega} uv \tag{6.9a}$$

$$\ell_D(v) := \int_{\Omega} fv - \int_{\partial\Omega} g\,(\nabla v \cdot \mathbf{n}) + \beta_N \int_{\partial\Omega} vg. \tag{6.9b}$$

It can be shown that the variational form using Nitsche's method leads to variational consistency, in the sense that if u is sufficiently regular, then [5, p. 119]

$$a_D(u,v) = \ell_D(v), \quad \forall\, v \in V_N.$$

If there exists a positive constant C_N such that

$$\|\nabla v \cdot \mathbf{n}\|_{L_2(\partial\Omega)} \le \frac{C_N}{\sqrt{\delta}} \|\nabla v\|_{L_2(\Omega)}, \quad \forall\, v \in V_N, \tag{6.10}$$

with δ being the support of the radial basis functions, then selecting

$$\beta_N = \frac{c_{12}}{\delta}, \tag{6.11}$$

with $c_{12} > 2C_N^2$ will ensure that the bilinear form $a_D(\cdot,\cdot)$ is symmetric positive definite. This choice of c_{12} will also ensure that a_D is coercive on V_N since

$$a_D(v,v) \;=\; \|\nabla v\|^2_{L_2(\Omega)} - 2\int_{\partial\Omega} v\,(\nabla v \cdot \mathbf{n}) + \beta_N \|v\|^2_{L_2(\partial\Omega)}$$

$$
\begin{aligned}
&\geq \|\nabla v\|_{L_2(\Omega)}^2 - \frac{2C_N}{\delta^{1/2}}\|v\|_{L_2(\partial\Omega)}\|\nabla v\|_{L_2(\Omega)} + \beta_N\|v\|_{L_2(\partial\Omega)}^2 \\
&\geq \frac{1}{2}\|\nabla v\|_{L_2(\Omega)}^2 + \left(\beta_N - \frac{2C_N^2}{\delta}\right)\|v\|_{L_2(\partial\Omega)}^2 \\
&\geq C\|v\|_{H^1(\Omega)}^2, \ \forall\, v \in V_N,
\end{aligned}
$$

where we have used the Cauchy-Schwarz and Friedrichs inequalities, (6.10) and $2xy \leq x^2 + y^2$. We recall that the Friedrichs inequality [27] states that

$$
\int_\Omega |u|^2 \leq C\left(\int_\Omega |\nabla u|^2 + \int_{\partial\Omega} |u|^2\right),
$$

for Ω being a bounded domain for which the Gauss-Green formula holds.

Continuity follows since

$$
\begin{aligned}
|a_D(u,v)| &\leq |u|_{H^1(\Omega)}|v|_{H^1(\Omega)} + C_N/\delta\left(\|v\|_{L_2(\partial\Omega)}\|\nabla u\|_{L_2(\Omega)} + \right. \\
&\qquad \left. \|u\|_{L_2(\partial\Omega)}\|\nabla v\|_{L_2(\Omega)}\right) + \beta_N\|u\|_{L_2(\partial\Omega)}\|v\|_{L_2(\partial\Omega)} \\
&\leq |u|_{H^1(\Omega)}|v|_{H^1(\Omega)} + C\left(\|v\|_{L_2(\Omega)}\|\nabla u\|_{L_2(\Omega)} + \right. \\
&\qquad \left. \|u\|_{L_2(\Omega)}\|\nabla v\|_{L_2(\Omega)}\right) + \beta_N\|u\|_{L_2(\Omega)}\|v\|_{L_2(\Omega)} \\
&\leq C\|u\|_{H^1(\Omega)}\|v\|_{H^1(\Omega)}, \quad \forall\, u,v \in V_N,
\end{aligned}
$$

where we have used the Cauchy-Schwarz inequality, (6.10) and the Sobolev trace embedding theorem.

Nitsche also proved that the optimal error estimates of Theorem 6.1 and Lemma 6.2 hold in this setting if, in addition to the requirement of selecting β_N satisfying (6.11), there exists a $s_u \in V_N$ such that for $u \in H^2(\Omega)$, the following error bounds hold for $k \in \{0,1\}$

$$
\|u - s_u\|_{H^k(\Omega)} \leq Ch^{2-k}\|u\|_{H^2(\Omega)}, \tag{6.12a}
$$

$$
\|u - s_u\|_{H^k(\partial\Omega)} \leq Ch^{3/2-k}\|u\|_{H^2(\Omega)}. \tag{6.12b}
$$

For the Wendland functions, this requirement is known to hold [49].

Note that the most challenging aspects of Nitsche's method are the derivation of the weak form and the selection of the stabilisation parameter β_N. Both the weak form and the choice of the parameter β_N depend on the PDE as well as the Dirichlet boundary conditions.

6.2 Collocation

In this section, we consider symmetric collocation with Wendland functions for solving elliptic PDEs and symmetric collocation with Wendland functions for solving the classical stationary Stokes problem.

6.2.1 Symmetric collocation for elliptic PDEs

In this section we consider the following Dirichlet PDE

$$\mathcal{L}u(\mathbf{x}) = f(\mathbf{x}), \quad \mathbf{x} \text{ in } \Omega, \tag{6.13}$$

with

$$u(\mathbf{x}) = g(\mathbf{x}), \quad \mathbf{x} \text{ on } \partial\Omega, \tag{6.14}$$

where $\Omega \subseteq \mathbb{R}^d$ is a bounded $C^{1,1}$ domain (as defined in [19, p.94]) with a $C^{k,s}$-boundary $\partial\Omega$, with $k \in \mathbb{N}_0$ and $s \in [0,1)$. $\mathcal{L}$ is an elliptic second order differential operator of the form

$$\mathcal{L}u = a^{ij}(x)D_{ij}u + b^i(x)D_iu + c(x)u,$$

with coefficients $a^{ij} \in C^0(\bar{\Omega}), b^i, c \in L^\infty$, where $i,j = 1,\ldots,d$, defined on $\Omega \subseteq \mathbb{R}^d$. Suppose that Φ is a kernel that satisfies condition (3.20) for some $\rho = \tau > 2 + d/2$. This assumption ensures that we may apply $\mathcal{L}$ to Φ twice and still have a continuous function. We choose interior and boundary point sets as $X = X_1 \cup X_2$ where $X_1 = \{x_1,\ldots,x_n\} \subseteq \Omega$ and $X_2 = \{x_{n+1},\ldots,x_N\} \subseteq \partial\Omega$. We construct our approximation $\widetilde{u}$ as

$$\widetilde{u} = \sum_{j=1}^{n} \alpha_j \mathcal{L}_2 \Phi(\cdot - \mathbf{x}_j) + \sum_{j=n+1}^{N} \alpha_j \Phi(\cdot - \mathbf{x}_j), \tag{6.15}$$

where the 2 subscript on $\mathcal{L}$ indicates that this operator acts with respect to its second argument.

Without loss of generality, we will only consider the case where the RBF centres coincide with the collocation points. Then solving (6.13) and (6.14) by collocation on the set X means to select $\widetilde{u}$ such that the collocation equations

$$\mathcal{L}u(\mathbf{x}_j) = \mathcal{L}\widetilde{u}(\mathbf{x}_j) = f(\mathbf{x}_j), \quad \mathbf{x}_j \in X_1, \tag{6.16}$$

$$u(\mathbf{x}_j) = \widetilde{u}(\mathbf{x}_j) = g(\mathbf{x}_j), \quad \mathbf{x}_j \in X_2, \tag{6.17}$$

are satisfied.

The resulting linear system is of the form

$$\mathbf{A}\mathbf{c} = \mathbf{f},$$

where $\mathbf{A}$ is the collocation matrix

$$\mathbf{A} = \begin{bmatrix} A_{\mathcal{L}\mathcal{L}_2} & A_{\mathcal{L}\mathcal{B}_2} \\ A_{\mathcal{B}\mathcal{L}_2} & A_{\mathcal{B}\mathcal{B}_2} \end{bmatrix}, \tag{6.18}$$

with entries given by

$$\begin{aligned}
(A_{\mathcal{L}\mathcal{L}_2})_{ij} &= \mathcal{L}\mathcal{L}_2\Phi(\mathbf{x},\boldsymbol{\xi})|_{\mathbf{x}=\mathbf{x}_i,\xi=\xi_j}, \mathbf{x}_i, \boldsymbol{\xi}_j \in X_1 \\
(A_{\mathcal{L}\mathcal{B}_2})_{ij} &= \mathcal{L}\Phi(\mathbf{x},\boldsymbol{\xi})|_{\mathbf{x}=\mathbf{x}_i,\xi=\xi_j}, \mathbf{x}_i \in X_1, \boldsymbol{\xi}_j \in X_2 \\
(A_{\mathcal{B}\mathcal{L}_2})_{ij} &= \mathcal{L}_2\Phi(\mathbf{x},\boldsymbol{\xi})|_{\mathbf{x}=\mathbf{x}_i,\xi=\xi_j}, \mathbf{x}_i \in X_2, \boldsymbol{\xi}_j \in X_1 \\
(A_{\mathcal{B}\mathcal{B}_2})_{ij} &= \Phi(\mathbf{x},\boldsymbol{\xi})|_{\mathbf{x}=\mathbf{x}_i,\xi=\xi_j}, \mathbf{x}_i, \boldsymbol{\xi}_j \in X_2.
\end{aligned}$$

The vector $\mathbf{f}$ consists of the entries $f(\mathbf{x}_i)$, $\mathbf{x}_i \in X_1$, followed by $g(\mathbf{x}_i)$, $\mathbf{x}_i \in X_2$. We note that $u, \widetilde{u} \in H^\tau(\Omega)$. Under the assumption that the functionals $\{\lambda_1, \ldots, \lambda_N\}$ given by

$$\begin{aligned}
\lambda_j(u) &:= \delta_{\mathbf{x}_j} \circ \mathcal{L}(u) = (\mathcal{L}u)(\mathbf{x}_j), \quad j = 1, \ldots, n \\
\lambda_j(u) &:= \delta_{\mathbf{x}_j} \circ (u) = u(\mathbf{x}_j), \quad j = n+1, \ldots, N
\end{aligned}$$

are linearly independent, the symmetric collocation matrix is nonsingular and there exists an unique approximation satisfying the collocation conditions (6.16) and (6.17) [51, Section 16.3].

The error between the solution and the approximate solution depends on the mesh norms of the interior and boundary centres, as given in the following lemma.

Lemma 6.3. *Assume that the exact solution of* (6.13) *belongs to* $H^\tau(\Omega)$ *with* $\tau > 2 + d/2$. *Let* h_1 *be the mesh norm of the interior collocation points* X_1 *and* h_2 *be the mesh norm of the boundary collocation points, let* Φ *be a positive definite kernel satisfying* (3.20) *and let* $\widetilde{u}$ *be the approximate solution obtained by symmetric collocation. Then we have the following error bounds:*

$$\|u - \widetilde{u}\|_{L_2(\Omega)} \leq c h_1^{\tau-2} \|u - \widetilde{u}\|_{H^\tau(\Omega)} \leq c h_1^{\tau-2} \|u\|_{H^\tau(\Omega)},$$

and

$$\|u - \widetilde{u}\|_{L_2(\partial\Omega)} \leq C h_2^{\tau-1/2} \|u - \widetilde{u}\|_{H^\tau(\Omega)}.$$

Proof. From [19, Theorem 9.17], there exists a constant C (independent of u), such that

$$\|u\|_{H^2(\Omega)} \leq C \|\mathcal{L}u\|_{L_2(\Omega)}.$$

Since $\|u\|_{L_2(\Omega)} \leq \|u\|_{H^2(\Omega)}$ and with [18], we have

$$\|\mathcal{L}u - \mathcal{L}\widetilde{u}\|_{L_2(\Omega)} \leq C h_1^{\tau-2} \|u\|_{H^\tau(\Omega)},$$

which proves the first result. The second result is from [18, Theorem 3.10]. □

6.2.2 Symmetric collocation for the Stokes problem

In this subsection we investigate symmetric collocation approximation with Wendland compactly supported radial basis functions (RBFs) to solve the Stokes problem

$$-\nu\Delta\mathbf{u} + \nabla p = \mathbf{f} \quad \text{in } \Omega, \tag{6.19}$$

$$\nabla\cdot\mathbf{u} = 0 \quad \text{in } \Omega, \tag{6.20}$$

$$\mathbf{u} = \mathbf{g} \quad \text{on } \partial\Omega, \tag{6.21}$$

where the region $\Omega \subseteq \mathbb{R}^d$, the viscosity ν, $\mathbf{f} : \Omega \to \mathbb{R}^d$ and $\mathbf{g} : \Omega \to \mathbb{R}^d$ are given and we seek an approximate solution to the velocity $\mathbf{u} : \Omega \to \mathbb{R}^d$ and the pressure $p : \Omega \to \mathbb{R}$.

Function spaces

First we define divergence-free approximation spaces in Ω and in $\mathbb{R}^d$. With the divergence of $\mathbf{u} : \Omega \to \mathbb{R}^d$ defined as

$$\nabla\cdot\mathbf{u} := \sum_{j=1}^{d} \partial_j u_j \ ,$$

we define

$$\mathbf{H}^\tau(\Omega; \mathrm{div}) := \{\mathbf{u} \in \mathbf{H}^\tau(\Omega) : \nabla\cdot\mathbf{u} = 0\},$$

and

$$\widetilde{\mathbf{H}}^\tau(\mathbb{R}^d; \mathrm{div}) := \left\{\mathbf{f} \in \mathbf{H}^\tau(\mathbb{R}^d; \mathrm{div}) : \int_{\mathbb{R}^d} \frac{\|\widehat{\mathbf{f}}(\boldsymbol{\omega})\|_2^2}{\|\boldsymbol{\omega}\|_2^2} \left(1 + \|\boldsymbol{\omega}\|_2^2\right)^{\tau+1} \mathrm{d}\boldsymbol{\omega} < \infty\right\},$$

with norm

$$\|\mathbf{f}\|^2_{\widetilde{\mathbf{H}}^\tau(\mathbb{R}^d;\mathrm{div})} := (2\pi)^{-d/2} \int_{\mathbb{R}^d} \frac{\|\widehat{\mathbf{f}}(\boldsymbol{\omega})\|_2^2}{\|\boldsymbol{\omega}\|_2^2} \left(1 + \|\boldsymbol{\omega}\|_2^2\right)^{\tau+1} \mathrm{d}\boldsymbol{\omega}.$$

We note that $\widetilde{\mathbf{H}}^\tau(\mathbb{R}^d; \mathrm{div})$ is a subspace of $\mathbf{H}^\tau(\mathbb{R}^d; \mathrm{div})$. We will also need that for $\Omega \subseteq \mathbb{R}^d$ being a simply connected domain with $C^{\lceil\tau\rceil,1}$ boundary for $d = 2, 3$ and with $\tau \geq 0$, there exists a continuous operator

$$\widetilde{\boldsymbol{\mathcal{E}}}_{\mathrm{div}} : \mathbf{H}^\tau(\Omega; \mathrm{div}) \to \widetilde{\mathbf{H}}^\tau(\mathbb{R}^d; \mathrm{div}),$$

such that $\widetilde{\boldsymbol{\mathcal{E}}}_{\mathrm{div}}\mathbf{u}|\Omega = \mathbf{u}$ for all $\mathbf{u} \in \mathbf{H}^\tau(\Omega; \mathrm{div})$ [52, Proposition 3.8]. This operator is defined as

$$\widetilde{\boldsymbol{\mathcal{E}}}_{\mathrm{div}}\mathbf{u} := \nabla \times \mathcal{E}_S \mathcal{T}\mathbf{u}, \tag{6.22}$$

where $\mathcal{E}_S$ is the classical Stein extension operator defined in Lemma 2.1 and $\mathcal{T}$ is a bounded operator $\mathcal{T} : \mathbf{H}^\tau(\Omega; \mathrm{div}) \to \mathbf{H}^{\tau+1}(\Omega)$ with $\tau = k + \theta$ for $k \in \mathbb{N}_0$ and $\theta \in [0, 1]$ [52, p. 3167].

To measure the pressure, which is determined only up to a constant, we will use the norm

$$\|p\|_{H^\tau(\Omega)/\mathbb{R}} := \inf_{c\in\mathbb{R}} \|p+c\|_{H^\tau(\Omega)}.$$

Symmetric collocation approximation

We consider a single-scale approximant to the combined velocity and pressure vector $\mathbf{v} := (\mathbf{u}, p) : \mathbb{R}^d \to \mathbb{R}^{d+1}$, following [31, 17, 52]. Then (6.19)-(6.21) become

$$\left(\mathcal{L}^S\mathbf{v}\right)_i := -\nu \sum_{j=1}^{d} \partial_{jj} v_i + \partial_i v_{d+1} \;=\; f_i \quad \text{in } \Omega, \tag{6.23}$$

$$\sum_{j=1}^{d} \partial_j v_j \;=\; 0 \quad \text{in } \Omega, \tag{6.24}$$

$$v_i \;=\; g_i \quad \text{on } \partial\Omega, \tag{6.25}$$

where $1 \le i \le d$. We seek a meshfree, kernel-based collocation method with an analytically divergence-free approximation space. We use the notation $\phi_{\tau+1}$ and $\phi_{\tau-1}$ to denote the functions to be used in our matrix-valued kernel. We will mainly be interested in the case where both $\phi_{\tau+1}$ and $\phi_{\tau-1}$ are original Wendland functions which, for a given spatial dimension d, have native space norms equivalent to the Sobolev spaces $H^{\tau+1}(\mathbb{R}^d)$ and $H^{\tau-1}(\mathbb{R}^d)$, respectively. Their Fourier transforms satisfy

$$c_{1,\tau+1}(1+\|\boldsymbol{\omega}\|_2^2)^{-\tau-1} \le \widehat{\phi_{\tau+1}}(\|\boldsymbol{\omega}\|_2) \le c_{2,\tau+1}(1+\|\boldsymbol{\omega}\|_2^2)^{-\tau-1}, \tag{6.26}$$

and

$$c_{1,\tau-1}(1+\|\boldsymbol{\omega}\|_2^2)^{-\tau+1} \le \widehat{\phi_{\tau-1}}(\|\boldsymbol{\omega}\|_2) \le c_{2,\tau-1}(1+\|\boldsymbol{\omega}\|_2^2)^{-\tau+1}, \tag{6.27}$$

and we define $\bar{C}_1 := \min(c_{1,\tau+1}, c_{1,\tau-1})$ and $\bar{C}_2 := \max(c_{2,\tau+1}, c_{2,\tau-1})$. Then we define the matrix-valued kernel

$$\mathbf{\Psi} := \begin{pmatrix} \mathbf{\Phi}_{\tau+1} & 0 \\ 0 & \phi_{\tau-1} \end{pmatrix} : \mathbb{R}^d \to \mathbb{R}^{(d+1)\times(d+1)}, \tag{6.28}$$

where $\mathbf{\Phi}_{\tau+1} := (-\Delta\mathbf{I} + \nabla\nabla^T)\phi_{\tau+1}$, with $\mathbf{I}$ denoting the identity matrix. We note that $\mathbf{\Phi}_{\tau+1}$ is also positive definite (cf. [31]) and hence due to the tensor product construction of $\mathbf{\Psi}$, it is positive definite as well. This choice for $\mathbf{\Phi}_{\tau+1}$ is known to lead to divergence-free interpolants [31]. We also note that

$$\widehat{\mathbf{\Phi}_{\tau+1}}(\boldsymbol{\omega}) = \left(\|\boldsymbol{\omega}\|_2^2\mathbf{I} - \boldsymbol{\omega}\boldsymbol{\omega}^T\right)\widehat{\phi_{\tau+1}}(\boldsymbol{\omega}). \tag{6.29}$$

We will consider the case where the collocation points are the same as the RBF centres. We denote the interior centres by $X_1 := \{\mathbf{x}_1, \dots, \mathbf{x}_N\}$ and the boundary centres by $X_2 := \{\mathbf{x}_{N+1}, \ldots, \mathbf{x}_M\}$ and their union by $X = X_1 \cup X_2$, with mesh norms h_1 and h_2, respectively. Since (6.24) is automatically satisfied, this means that our approximant and collocation conditions will consist of dN terms from (6.23) and $d(M-N)$ terms from (6.25). Then with $\mathcal{L}_2^S$ denoting the operator $\mathcal{L}^S$ acting as a function of the second argument, applied to rows of $\mathbf{\Psi}$, our approximant takes the form

$$\mathbf{S}_X\mathbf{v}(\mathbf{x}) = \sum_{i=1}^{d}\sum_{j=1}^{N} \alpha_{i,j} \left(\mathcal{L}_2^S \mathbf{\Psi}\left(\mathbf{x}-\mathbf{x}_j\right)\right)_i + \sum_{i=1}^{d}\sum_{j=N+1}^{M} \alpha_{i,j}\mathbf{\Psi}\left(\mathbf{x}-\mathbf{x}_j\right)_i, \tag{6.30}$$

where the notation $\mathbf{\Psi}_i$ means column i of the matrix $\mathbf{\Psi}$. The coefficients $\alpha_{i,j}$, $1 \le i \le d$, $1 \le j \le M$ are determined by the collocation conditions

$$\begin{aligned} \left(\mathcal{L}^S \mathbf{S}_X \mathbf{v}(\mathbf{x}_j)\right)_i &= f_i(\mathbf{x}_j), \quad 1 \le i \le d,\ j = 1, \ldots, N, && (6.31)\\ \left(\mathbf{S}_X \mathbf{v}(\mathbf{x}_j)\right)_i &= g_i(\mathbf{x}_j), \quad 1 \le i \le d,\ j = N+1, \ldots, M. && (6.32) \end{aligned}$$

From [17, 52], we know that if $\phi_{\tau+1}, \phi_{\tau-1}$ are positive definite and if $\mathbf{\Phi}_{\tau+1} \in W_1^2(\mathbb{R}^d) \cap C^2(\mathbb{R}^d)$, then the native space of the kernel $\mathbf{\Psi}$ given by (6.28) is

$$\mathcal{N}_{\mathbf{\Psi}}(\mathbb{R}^d) = \mathcal{N}_{\mathbf{\Phi}_{\tau+1}}(\mathbb{R}^d) \times \mathcal{N}_{\phi_{\tau-1}}(\mathbb{R}^d),$$

with norm

$$\begin{aligned} \|\mathbf{f}\|^2_{\mathcal{N}_{\mathbf{\Psi}}}(\mathbb{R}^d) &= \|\mathbf{f_u}\|^2_{\mathcal{N}_{\mathbf{\Phi}_{\tau+1}}(\mathbb{R}^d)} + \|f_p\|^2_{\mathcal{N}_{\phi_{\tau-1}}(\mathbb{R}^d)} \\ &= (2\pi)^{-d/2}\int_{\mathbb{R}^d}\left[\frac{\|\widehat{\mathbf{f}}_{\mathbf{u}}(\boldsymbol{\omega})\|_2^2}{\|\boldsymbol{\omega}\|_2^2\widehat{\phi_{\tau+1}}(\boldsymbol{\omega})} + \frac{|\widehat{f}_p(\boldsymbol{\omega})|^2}{\widehat{\phi_{\tau-1}}(\boldsymbol{\omega})}\right]\mathrm{d}\boldsymbol{\omega}, \end{aligned} \tag{6.33}$$

where $\mathbf{f} = (\mathbf{f_u}, f_p)^T$ with $\mathbf{f_u} : \mathbb{R}^d \to \mathbb{R}^d$ and $f_p : \mathbb{R}^d \to \mathbb{R}$. We recall that the generalised interpolant satisfies [51, Chapter 16]

$$\|\boldsymbol{\mathcal{E}}\mathbf{v} - \mathbf{S}_X\boldsymbol{\mathcal{E}}\mathbf{v}\|_{\mathcal{N}_{\mathbf{\Psi}}(\mathbb{R}^d)} \le \|\boldsymbol{\mathcal{E}}\mathbf{v}\|_{\mathcal{N}_{\mathbf{\Psi}}(\mathbb{R}^d)}.$$

With (6.26) and (6.27), upon defining the extension operator for the velocity-pressure vector $\mathbf{v}$ as

$$\boldsymbol{\mathcal{E}}\mathbf{v} := \left(\widetilde{\boldsymbol{\mathcal{E}}}_{\mathrm{div}}\mathbf{u}, \mathcal{E}_{\mathrm{S}}p\right), \tag{6.34}$$

where $\mathcal{E}_{\mathrm{S}}$ is the classical Stein extension operator as defined in Lemma 2.1, then the native space of our approximant given by (6.30) is

$$\boldsymbol{\mathcal{E}} : \mathbf{H}^{\tau}(\Omega; \mathrm{div}) \times H^{\tau-1}(\Omega) \to \mathcal{N}_{\mathbf{\Psi}}(\mathbb{R}^d) = \widetilde{\mathbf{H}}^{\tau}(\mathbb{R}^d; \mathrm{div}) \times H^{\tau-1}(\mathbb{R}^d).$$

Once again we can define interpolants with scaled kernels. In this case, we define the matrix-valued kernel

$$\mathbf{\Psi}_\delta := \begin{pmatrix} \mathbf{\Phi}_{\tau+1,\delta} & 0 \\ 0 & \phi_{\tau-1,\delta} \end{pmatrix} : \mathbb{R}^d \to \mathbb{R}^{(d+1)\times(d+1)}, \tag{6.35}$$

where $\mathbf{\Phi}_{\tau+1,\delta} := (-\Delta\mathbf{I} + \nabla\nabla^T)\phi_{\tau+1,\delta}$ and the scaled basis functions are defined as in (2.1). Then the native space of the kernel $\mathbf{\Psi}_\delta$ is given by

$$\mathcal{N}_{\mathbf{\Psi}_\delta}(\mathbb{R}^d) = \mathcal{N}_{\mathbf{\Phi}_{\tau+1,\delta}}(\mathbb{R}^d) \times \mathcal{N}_{\phi_{\tau-1,\delta}}(\mathbb{R}^d),$$

with norm

$$\begin{aligned} \|\mathbf{f}\|^2_{\mathcal{N}_{\mathbf{\Psi}_\delta}(\mathbb{R}^d)} &= \|\mathbf{f_u}\|^2_{\mathcal{N}_{\mathbf{\Phi}_{\tau+1,\delta}}(\mathbb{R}^d)} + \|f_p\|^2_{\mathcal{N}_{\phi_{\tau-1,\delta}}(\mathbb{R}^d)} \\ &= (2\pi)^{-d/2} \int_{\mathbb{R}^d} \left[\frac{\|\widehat{\mathbf{f}}_\mathbf{u}(\boldsymbol{\omega})\|_2^2}{\|\boldsymbol{\omega}\|_2^2 \widehat{\phi_{\tau+1,\delta}}(\boldsymbol{\omega})} + \frac{|\widehat{f_p}(\boldsymbol{\omega})|^2}{\widehat{\phi_{\tau-1,\delta}}(\boldsymbol{\omega})} \right] \mathrm{d}\boldsymbol{\omega}. \end{aligned} \tag{6.36}$$

We will need norm equivalence as stated in the following lemma.

Lemma 6.4. *For every $\delta \in (0, \delta_a]$ where $\phi_{\tau+1}$ and $\phi_{\tau-1}$ generate $H^{\tau+1}(\mathbb{R}^d)$ and $H^{\tau-1}(\mathbb{R}^d)$, respectively, we have $\mathcal{N}_{\mathbf{\Psi}_\delta}(\mathbb{R}^d) = \mathcal{N}_{\mathbf{\Psi}}(\mathbb{R}^d)$ and for every $\mathbf{f} \in \mathcal{N}_{\mathbf{\Psi}}(\mathbb{R}^d)$ there exist positive constants c_{15} and c_{16} such that*

$$c_{15}^{1/2}\|\mathbf{f}\|_{\mathcal{N}_{\mathbf{\Psi}_\delta}(\mathbb{R}^d)} \le \|\mathbf{f}\|_{\mathcal{N}_{\mathbf{\Psi}}(\mathbb{R}^d)} \le c_{16}^{1/2}\delta^{-\tau-1}\|\mathbf{f}\|_{\mathcal{N}_{\mathbf{\Psi}_\delta}(\mathbb{R}^d)}.$$

Proof. With $\mathbf{f} = (\mathbf{f_u}, f_p)^T$, by using the same arguments as in Lemma 4.8, we have

$$c_{1,\tau-1}\min(1, \delta_a^{-\tau-1})\|f_p\|_{\mathcal{N}_{\psi_{\tau-1,\delta}}(\mathbb{R}^d)} \le \|f_p\|_{\mathcal{N}_{\psi_{\tau-1}}(\mathbb{R}^d)} \le c_{2,\tau-1}\delta^{-\tau-1}\|f_p\|_{\mathcal{N}_{\psi_{\tau-1,\delta}}(\mathbb{R}^d)}.$$

Similarly, we can show

$$c_{1,\tau+1}\min(1, \delta_a^{-\tau-1})\|\mathbf{f_u}\|_{\mathcal{N}_{\blacksquare_{\tau+1,\delta}}(\mathbb{R}^d)} \le \|\mathbf{f_u}\|_{\mathcal{N}_{\blacksquare_{\tau+1}}(\mathbb{R}^d)} \le c_{2,\tau+1}\delta^{-\tau-1}\|\mathbf{f_u}\|_{\mathcal{N}_{\blacksquare_{\tau+1,\delta}}(\mathbb{R}^d)}.$$

With (6.36) and setting $c_{15} := \min(c_{1,\tau-1}, c_{1,\tau+1})\min(1, \delta^{-\tau-1})$ and $c_{16} := \max(c_{2,\tau-1}, c_{2,\tau+1})$, we get the final result. □

We require one further result from [43].

Theorem 6.5. *Let $m \in \mathbb{N}_0$ and let $\Omega \subseteq \mathbb{R}^d$ be a $C^{m+1,1}$ smooth domain with outer normal vector $\mathbf{n}$. For each $\mathbf{f} \in \mathbf{H}^m(\Omega)$ and $\mathbf{g} \in \mathbf{H}^{m+3/2}(\partial\Omega)$ with $\int_{\partial\Omega} \mathbf{g} \cdot \mathbf{n}\, \mathrm{d}S = 0$, the nonhomogeneous Stokes problem* (6.19)-(6.21) *has a unique solution $\mathbf{u} \in \mathbf{H}^{m+2}(\Omega)$ and $p \in H^{m+1}(\Omega)$ and*

$$\|\mathbf{u}\|_{\mathbf{H}^{m+2}(\Omega)} + \|p\|_{H^{m+1}(\Omega)/\mathbb{R}} \le C\left(\|\mathbf{f}\|_{\mathbf{H}^m(\Omega)} + \|\mathbf{g}\|_{\mathbf{H}^{m+3/2}(\partial\Omega)}\right). \tag{6.37}$$

Theorem 6.6. *Let $\tau > 2 + d/2$. Assume that $\Omega \subseteq \mathbb{R}^d$ is a bounded, simply connected region with a $C^{\lceil\tau\rceil,1}$ boundary. Let $\mathbf{f} \in \mathbf{H}^{\tau-2}(\Omega)$ and $\mathbf{g} \in \mathbf{H}^{\tau-1/2}(\partial\Omega)$ satisfy $\int_{\partial\Omega} \mathbf{g} \cdot \mathbf{n}\, \mathrm{d}S = 0$. Suppose the kernel $\mathbf{\Psi}$ is chosen such that $\mathcal{N}_{\mathbf{\Psi}}(\mathbb{R}^d) = \widetilde{\mathbf{H}}^\tau(\mathbb{R}^d; \mathrm{div}) \times H^{\tau-1}(\mathbb{R}^d)$. Then the approximation $\mathbf{S}_X\mathbf{v}$ given by* (6.30) *to the Stokes problem* (6.19)-(6.21) *satisfies the error bound*

$$\|\mathbf{v} - \mathbf{S}_X\mathbf{v}\|_{\mathbf{L}_2(\Omega)} \le C\,\bar{h}^{\tau-2}\|\boldsymbol{\mathcal{E}}\mathbf{v} - \mathbf{S}_X\boldsymbol{\mathcal{E}}\mathbf{v}\|_{\mathcal{N}_{\mathbf{\Psi}}(\mathbb{R}^d)}, \tag{6.38}$$

where $\bar{h} := \max(h_1, h_2)$ and the extension operator $\boldsymbol{\mathcal{E}}$ is given by (6.34).

Proof. With the definition of the Sobolev space norms in (2.4) and assuming that we choose the representer for the pressure p such that $\|p\|_{H^1(\Omega)/\mathbb{R}} = \|p\|_{H^1(\Omega)}$, and with the notation $\mathbf{S}_X\mathbf{v} = (\mathbf{S}_{X,u}\mathbf{u}, S_{X,p}p)$ gives

$$\begin{aligned}
\|\mathbf{v} - \mathbf{S}_X\mathbf{v}\|_{\mathbf{L}_2(\Omega)} &\leq \|\mathbf{u} - \mathbf{S}_{X,u}\mathbf{u}\|_{\mathbf{L}_2(\Omega)} + \|p - S_{X,p}p\|_{L_2(\Omega)} \\
&\leq \|\mathbf{u} - \mathbf{S}_{X,u}\mathbf{u}\|_{\mathbf{H}^2(\Omega)} + \|p - S_{X,p}p\|_{H^1(\Omega)} \\
&= \|\mathbf{u} - \mathbf{S}_{X,u}\mathbf{u}\|_{\mathbf{H}^2(\Omega)} + \|p - S_{X,p}p\|_{H^1(\Omega)/\mathbb{R}} \\
&\leq C\|\mathcal{L}^S\mathbf{v} - \mathcal{L}^S\mathbf{S}_X\mathbf{v}\|_{\mathbf{L}_2(\Omega)} + \|\mathbf{u} - \mathbf{S}_{X,u}\mathbf{u}\|_{\mathbf{H}^{3/2}(\partial\Omega)}, \qquad (6.39)
\end{aligned}$$

where the last line follows from (6.37) applied to $\mathbf{v} - \mathbf{S}_X\mathbf{v}$ with $m = 0$. We now extend the function $\mathbf{v}$ to $\boldsymbol{\mathcal{E}}\mathbf{v} \in \widetilde{\mathbf{H}}^\tau(\mathbb{R}^d) \times H^{\tau-1}(\mathbb{R}^d)$ and note that the generalised interpolant $\mathbf{S}_X\mathbf{v}$ coincides with $\mathbf{S}_X\boldsymbol{\mathcal{E}}\mathbf{v}$. We now consider the two terms in the right hand side of (6.39) separately. From (2.6) and [52], we have

$$\|\mathcal{L}^S\mathbf{v} - \mathcal{L}^S\mathbf{S}_X\mathbf{v}\|_{\mathbf{L}_2(\Omega)} \leq Ch_1^{\tau-2}\|\boldsymbol{\mathcal{E}}\mathbf{v} - \mathbf{S}_X\boldsymbol{\mathcal{E}}\mathbf{v}\|_{\mathcal{N}_{\mathbf{\Psi}}(\mathbb{R}^d)}.$$

From (2.7), we have

$$\|\mathbf{u} - \mathbf{S}_{X,u}\mathbf{u}\|_{\mathbf{H}^{3/2}(\partial\Omega)} \leq Ch_2^{\tau-2}\|\mathbf{u} - \mathbf{S}_{X,u}\mathbf{u}\|_{\mathbf{H}^\tau(\Omega)}. \qquad (6.40)$$

Now we can write

$$\begin{aligned}
\|\mathbf{u} - \mathbf{S}_{X,u}\mathbf{u}\|_{\mathbf{H}^\tau(\Omega)} &\leq \|\mathbf{u} - \mathbf{S}_{X,u}\mathbf{u}\|_{\mathbf{H}^\tau(\Omega)} + \|p - S_{X,p}p\|_{H^{\tau-1}(\Omega)} \\
&\leq \|\widetilde{\boldsymbol{\mathcal{E}}}_{\mathrm{div}}\mathbf{u} - \mathbf{S}_{X,u}\widetilde{\boldsymbol{\mathcal{E}}}_{\mathrm{div}}\mathbf{u}\|_{\widetilde{\mathbf{H}}^\tau(\mathbb{R}^d;\mathrm{div})} + \|\mathcal{E}p - S_{X,p}\mathcal{E}_S p\|_{H^{\tau-1}(\mathbb{R}^d)} \\
&\leq C\|\boldsymbol{\mathcal{E}}\mathbf{v} - \mathbf{S}_X\boldsymbol{\mathcal{E}}\mathbf{v}\|_{\mathcal{N}_{\mathbf{\Psi}}(\mathbb{R}^d)},
\end{aligned}$$

and the stated result follows. □

Chapter Seven

Multiscale algorithms for Galerkin approximation of elliptic PDEs

This chapter will cover theoretical results and numerical experiments regarding two multiscale algorithms for Galerkin approximation of elliptic PDEs on bounded domains.

7.1 Framework

In this chapter, we will use (scaled) compactly supported radial basis functions to construct multiscale approximate solutions to PDEs, that is, we form the solution over multiple levels. We will work with a given domain $\Omega \subseteq \mathbb{R}^d$.

At each level i, we denote the mesh norm by h_i. The selection of point sets with mesh norms decreasing in a specific way will be one of the requirements for convergence of our algorithms.

At each level, we will also require a scaled version of the kernel $\Phi : \mathbb{R}^d \to \mathbb{R}$. For our unscaled kernel we will use a Wendland compactly supported radial basis function. With a (level-specific) scaling parameter $\delta > 0$, we can define the scaled kernels with (2.1).

Appropriate selection of the scaling parameters will also prove to be one of the important ingredients for convergence of our multiscale algorithms.

7.2 Multiscale Galerkin approximations

In this section, we consider a multiscale algorithm for constructing a Galerkin approximation where we use the residual from the previous level as the target for each subsequent level. We define the approximation at level i as $\widetilde{u}_i := \widetilde{u}_{N_i}$ with centres N_i and the approximation space at level i as $V_i := V_{N_i}$. The algorithm is given in Algorithm 1. The bilinear form $a(\cdot,\cdot)$ used in this algorithm is the unmodified bilinear form in the case of a PDE with Neumann or Robin boundary conditions and the Nitsche's method bilinear form $a_D(\cdot,\cdot)$ in the case of a PDE with Dirichlet boundary conditions.

Algorithm 1 Multiscale Galerkin approximation

Input n: number of levels

$\{X_i\}_{i=1}^n$: the set of nested centres for each level i, with mesh norms at each level given by h_i satisfying $c\mu h_i \leq h_{i+1} \leq \mu h_i$ with fixed $\mu \in (0,1), c \in (0,1]$ and h_1 sufficiently small

$\{\delta_i\}_{i=1}^n$: the scale parameters to use at each level, satisfying $\delta_i = \nu h_i$, ν a fixed constant.

Set $\widetilde{u}_0 = 0$.

for $i = 1$ to n **do**

With the level-specific approximation subspace $V_i := \text{span}\,\{\Phi_{\delta_i}(\cdot - \mathbf{x}), \mathbf{x} \in X_i\}$ solve the Galerkin approximation given by

$$\text{Find } s_i \in V_i \;:\; a(s_i, v) = \langle f, v\rangle_{L_2(\Omega)} - a(\widetilde{u}_{i-1}, v)\ \forall\, v \in V_i.$$

Update the solution according to

$$\widetilde{u}_i \;=\; \widetilde{u}_{i-1} + s_i.$$

end for

Output Approximate solution at level n, $\widetilde{u}_n$.

The error at level n, $e_n := u - \widetilde{u}_n$.

The algorithm as stated uses the same bilinear form at each level and it is the approximation space V_i which changes. However the Nitsche's method bilinear form $a_D(\cdot,\cdot)$ will vary at each level since the value of C_N^2 is proportional to δ^{-1} and hence so is β_N. This means that we will need to select the value of β_N corresponding to the last level and to use this for all previous levels. This will also mean that we will need to know the number of levels in advance.

Henceforth we will simply refer to the bilinear form as $a(\cdot,\cdot)$. This should cause no confusion as we have the same error bounds in both cases, as well as coercivity and continuity, and the multiscale algorithm follows the same steps in both cases. We require one more lemma before we can analyse the convergence of the multiscale algorithm.

Lemma 7.1. *Let $\Omega \subseteq \mathbb{R}^d$ be a bounded domain with a Lipschitz boundary. Let Φ be at least a C^1 function and let Φ_j be defined by* (2.1) *with scale factor δ_j. Then for Algorithm 1 and for a* *given level $i > 1$, we have the following bound on the $H^1(\Omega)$ error between subsequent levels.*

$$\|e_i\|_{H^1(\Omega)} \leq C\|e_{i-1}\|_{H^1(\Omega)},$$

where e_i is defined in Algorithm 1.

Proof. We will firstly show that s_i is the Galerkin approximation of e_{i-1}. We have

$$\begin{aligned} a(s_i, w) &= \langle f, w\rangle_{L_2(\Omega)} - a(\widetilde{u}_{i-1}, w), \ w \in V_i \\ &= a(u, w) - a(\widetilde{u}_{i-1}, w) \\ &= a(u - \widetilde{u}_{i-1}, w) \\ &= a(e_{i-1}, w), \end{aligned}$$

where we have used the variational form of the PDE and the linearity in the first argument of the bilinear form $a(\cdot, \cdot)$. Hence on setting $w = s_i$ we obtain

$$a(e_{i-1} - s_i, s_i) = 0.$$

Upon noting that $e_i = e_{i-1} - s_i$, it follows easily that

$$a(e_i, e_i) = a(e_{i-1}, e_{i-1}) - a(s_i, s_i),$$

and since the bilinear form a is continuous and coercive

$$\|e_i\|^2_{H^1(\Omega)} + \|s_i\|^2_{H^1(\Omega)} \leq C\|e_{i-1}\|^2_{H^1(\Omega)},$$

from which the result follows. $\square$

The following theorem and corollaries are our main results for the convergence of the multiscale Galerkin approximation. For the error analysis, we will need the norm

$$\|u\|^2_{\Psi_j} := \int_{\mathbb{R}^d} |\widehat{u}(\boldsymbol{\omega})|^2 \left(1 + \delta_j^2\|\boldsymbol{\omega}\|_2^2\right) \mathrm{d}\boldsymbol{\omega}. \tag{7.1}$$

As in Lemma 4.8, this norm satisfies

$$c_{17}\|u\|_{\Psi_j} \leq \|u\|_{H^1(\mathbb{R}^d)} \leq c_{18}\delta_j^{-1}\|u\|_{\Psi_j}. \tag{7.2}$$

Theorem 7.2. *Let $\Omega \subseteq \mathbb{R}^d$ be a bounded domain with a Lipschitz boundary. Then for Algorithm 1 there exists a constant $\alpha_1 > 0$ such that*

$$\|\mathcal{E}_S e_i\|_{\Psi_{i+1}} \leq \alpha_1\|\mathcal{E}_S e_{i-1}\|_{\Psi_i} \quad \textit{for} \quad i = 1, 2, \ldots$$

where $\mathcal{E}_S e_i$ is the extension operator defined in Lemma 2.1 applied to e_i. The constant α_1 satisfies $\alpha_1 < 1$ if in Algorithm 1 ν is sufficiently small and μ is sufficiently large.

Proof. Using (7.1), we can write

$$\|\mathcal{E}_S e_i\|^2_{\Psi_{i+1}} = \int\limits_{\mathbb{R}^d} |\widehat{\mathcal{E}_S e_i}(\boldsymbol{\omega})|^2 \left(1 + \delta^2_{i+1}\|\boldsymbol{\omega}\|^2_2\right) \,\mathrm{d}\boldsymbol{\omega} =: (I_1 + I_2)\,,$$

with

$$I_1 := \int\limits_{\|\boldsymbol{\omega}\|_2 \le \frac{1}{\delta_{i+1}}} |\widehat{\mathcal{E}_S e_i}(\boldsymbol{\omega})|^2 \left(1 + \delta^2_{i+1}\|\boldsymbol{\omega}\|^2_2\right) \,\mathrm{d}\boldsymbol{\omega},$$

$$I_2 := \int\limits_{\|\boldsymbol{\omega}\|_2 \ge \frac{1}{\delta_{i+1}}} |\widehat{\mathcal{E}_S e_i}(\boldsymbol{\omega})|^2 \left(1 + \delta^2_{i+1}\|\boldsymbol{\omega}\|^2_2\right) \,\mathrm{d}\boldsymbol{\omega}.$$

Now we consider the first integral where we can use that $\delta_{i+1}\|\boldsymbol{\omega}\|_2 \le 1$ and then Lemmas 6.2 and 4.8.

$$\begin{aligned} I_1 &\le 2 \int\limits_{\|\boldsymbol{\omega}\|_2 \le \frac{1}{\delta_{i+1}}} |\widehat{\mathcal{E}_S e_i}(\boldsymbol{\omega})|^2 \,\mathrm{d}\boldsymbol{\omega} \\ &\le 2\,\|\mathcal{E}_S e_i\|^2_{L_2(\mathbb{R}^d)} \le C\,\|e_i\|^2_{L_2(\Omega)} \le C h_i^2\,\|e_i\|^2_{H^1(\Omega)} \\ &\le C\,h_i^2\,\|e_{i-1}\|^2_{H^1(\Omega)} \le C\left(\frac{h_i}{\delta_i}\right)^2 \|\mathcal{E}_S e_{i-1}\|^2_{\Psi_i} \\ &= C\nu^{-2}\,\|\mathcal{E}_S e_{i-1}\|^2_{\Psi_i}, \end{aligned}$$

where we have also used Lemma 7.1. For I_2, since $\delta_{i+1}\|\boldsymbol{\omega}\|_2 \ge 1$, we have

$$\left(1 + \delta^2_{i+1}\|\boldsymbol{\omega}\|^2_2\right) \le 2\delta^2_{i+1}\|\boldsymbol{\omega}\|^2_2 \le 2\delta^2_{i+1}\left(1 + \|\boldsymbol{\omega}^2_2\|\right).$$

Then again using Lemma 7.1 shows that

$$\begin{aligned} I_2 &\le 2\delta^2_{i+1}\|\mathcal{E}_S e_i\|^2_{H^1(\mathbb{R}^d)} \le C\delta^2_{i+1}\|e_i\|^2_{H^1(\Omega)} \\ &\le C\delta^2_{i+1}\|e_{i-1}\|^2_{H^1(\Omega)} \le C\left(\frac{\delta_{i+1}}{\delta_i}\right)^2 \|\mathcal{E}_S e_{i-1}\|^2_{\Psi_i} \\ &\le C\mu^2\|\mathcal{E}_S e_{i-1}\|^2_{\Psi_i}. \end{aligned} \tag{7.3}$$

Combining our results for I_1 and I_2 and now writing C_1 and C_2 for the two constants appearing in the bounds of the expressions for I_1 and I_2 respectively, we have

$$\|\mathcal{E}_S e_i\|^2_{\Psi_{i+1}} \le \left(\nu^{-2}C_1 + \mu^2 C_2\right)\,\|\mathcal{E}_S e_{i-1}\|^2_{\Psi_i},$$

and the result follows with

$$\alpha_1 := \left(\nu^{-2}C_1 + \mu^2 C_2\right)^{1/2}. \tag{7.4}$$

□

Corollary 7.3. *There exists a constant $C_3 > 0$ such that*

$$\|u - \widetilde{u}_n\|_{L_2(\Omega)} \leq C_3 \alpha_1^n \|u\|_{H^1(\Omega)} \quad \textit{for} \quad n = 1, 2, \ldots \tag{7.5}$$

Thus $\widetilde{u}_n$ resulting from Algorithm 1 converges linearly to u in the L_2-norm if $\alpha_1 < 1$.

Proof. Using Lemmas 6.2 and 4.8 again, we can see that

$$\begin{aligned}
\|u - \widetilde{u}_n\|_{L_2(\Omega)} &= \|e_n\|_{L_2(\Omega)} \leq C h_n \|e_n\|_{H^1(\Omega)} \\
&\leq C h_n \|\mathcal{E}_S e_n\|_{H^1(\mathbb{R}^d)} \leq C\, h_n\, \delta_{n+1}^{-1} \|\mathcal{E}_S e_n\|_{\Psi_{n+1}} \\
&\leq C \|\mathcal{E}_S e_n\|_{\Psi_{n+1}},
\end{aligned}$$

since

$$\frac{h_n}{\delta_{n+1}} = \frac{h_n}{\nu h_{n+1}} \leq \frac{1}{c\mu\nu}.$$

Now we can apply Theorem 7.2 n times, and noting that $\widetilde{u}_0 = 0$, leads to

$$\|u - \widetilde{u}_n\|_{L_2(\Omega)} \leq C \alpha_1^n \|\mathcal{E}_S u\|_{\Psi_1} \leq C \alpha_1^n \|\mathcal{E}_S u\|_{H^1(\mathbb{R}^d)} \leq C \alpha_1^n \|u\|_{H^1(\Omega)}.$$

□

7.2.1 Condition numbers

In this subsection, we present upper and lower bounds for the eigenvalues of the multiscale Galerkin algorithm. Since the Galerkin approximation matrix is symmetric and positive definite, we know that the condition number is given by

$$\kappa(\mathbf{A}) = \frac{\lambda_{\max}(\mathbf{A})}{\lambda_{\min}(\mathbf{A})}, \tag{7.6}$$

where $\lambda_{\max}(\mathbf{A})$ and $\lambda_{\min}(\mathbf{A})$ denote the maximum and minimum eigenvalues of $\mathbf{A}$ with entries given by (6.4).

Theorem 7.4. *Let Φ be a positive definite kernel generating $H^\tau(\mathbb{R}^d)$ with $\tau > d/2$. Let $\Phi_i := \Phi(\cdot - \mathbf{x}_i)$ and assume that there exists a constant $c_{19} > 0$, depending only on Φ and Ω, such that*

$$\gamma^T (\mathbf{F} - c_{19}\mathbf{G})\, \gamma \geq 0, \quad \forall\, \alpha \in \mathbb{R}^N, \tag{7.7}$$

which means that $\mathbf{F} - c_{19}\mathbf{G}$ is positive semi-definite and where

$$\begin{aligned}
F_{i,j} &= \left\langle \Phi_i, \Phi_j \right\rangle_{H^1(\Omega)}, \\
G_{i,j} &= \left\langle \Phi_i, \Phi_j \right\rangle_{H^1(\mathbb{R}^d)}.
\end{aligned}$$

Then the condition number of $\mathbf{A}$ *can be bounded by*

$$\kappa(\mathbf{A}) \leq C \left(\frac{1}{q_X}\right)^{4\tau-2},$$

where the constant C *is independent of the point set* X.

Proof. Since $v = \sum_{i=1}^{N} \gamma_i \Phi_i$ and with the coercivity of $a(\cdot,\cdot)$ and (7.7), we have

$$\begin{aligned} a(v,v) &\geq C\|v\|_{H^1(\Omega)}^2 = C\gamma^T \mathbf{F}\gamma^T \\ &\geq C\gamma^T \mathbf{G}\gamma \geq C\lambda_{\min}(\mathbf{G})\|\gamma\|_2^2, \end{aligned}$$

where $\lambda_{\min}(\mathbf{G})$ is the minimum eigenvalue of $\mathbf{G}$. From [50], we know that $\langle \Phi_i, \Phi_j \rangle_{H^1(\mathbb{R}^d)}$ is a radial function given by

$$\Upsilon\left(\mathbf{x}_i, \mathbf{x}_j\right) := -\left(\Delta\Phi\right) \star \Phi(\mathbf{x}_i - \mathbf{x}_j) + \Phi \star \Phi(\mathbf{x}_i - \mathbf{x}_j),$$

where Δ again denotes the Laplace operator and $\star$ denotes convolution defined as $f \star g(x) := \int f(y) g(x-y)\,\mathrm{d}y$. From [51, Theorem 12.3] we know that we can use $\widehat{\Upsilon}$ to derive a lower bound on the minimum eigenvalue of $\mathbf{G}$. Then we have

$$\widehat{\Upsilon}(\mathbf{z}) = \left(1 + \|\mathbf{z}\|^2\right) \widehat{\Phi}^2(\mathbf{z}).$$

From [51, Theorem 10.35], we know that $\widehat{\Phi}(\mathbf{z}) \geq C\|\mathbf{z}\|^{-2\tau}$ and hence $\widehat{\Upsilon}(\mathbf{z}) \geq C\|\mathbf{z}\|^{-4\tau+2}$. Then using [51, Theorem 12.3] we reach

$$\lambda_{\min}(\mathbf{G}) \geq C q_X^{4\tau-d-2}.$$

With the continuity of $a(\cdot,\cdot)$, [48, Theorem 14.2] and the non-negativity of norms, we also have the following bound on the maximum eigenvalue

$$\begin{aligned} a(v,v) &\leq C\|v\|_{H^1(\Omega)}^2 \leq C\|v\|_{H^1(\mathbb{R}^d)}^2 = C\gamma^T \mathbf{G}\gamma \\ &\leq C q_X^{-d} \|\gamma\|_2^2. \end{aligned}$$

These two bounds, in conjunction with (7.6), complete the proof. □

We will consider (7.7) further with the scaled RBFs $\Phi_i := \Phi_\delta(\cdot - \mathbf{x}_i)$, where Φ is the C^6 Wendland function given by

$$\Phi_{5,3}(\mathbf{x}) = (1 - \|\mathbf{x}\|)_+^8 \left(32\|\mathbf{x}\|^3 + 25\|\mathbf{x}\|^2 + 8\|\mathbf{x}\| + 1\right), \tag{7.8}$$

which is positive definite on $\mathbb{R}^2$ [51]. Now since the support of the radial basis functions is fixed, $\|\Phi_i\|_{H^1(\mathbb{R}^d)}$ is fixed and is independent of the point set X and Ω and we can express this as

$$\|\Phi_i\|_{H^1(\mathbb{R}^d)}^2 = \int_0^{2\pi}\int_0^{\delta} r\left(\phi_\delta^2(r) + \delta^2\left(\frac{\mathrm{d}}{\mathrm{d}r}\phi_\delta(r)\right)^2\right)\mathrm{d}r\,\mathrm{d}\theta. \tag{7.9}$$

In the case of the unit square, which will be used for the numerical experiments in Section 7.4, note that $\|\Phi_i\|_{H^1(\Omega)}$ is minimised when the RBF centre is located on a corner. This can be easily verified since moving the centre in any direction (in Ω) will keep the original area inside Ω and lead to additional area being inside Ω and the integrand is non-negative. Then we can then bound $\|\Phi_i\|^2_{H^1(\Omega)}$ by

$$\begin{aligned}\|\Phi_i\|^2_{H^1(\Omega)} &\geq \int_0^{\frac{\pi}{2}}\int_0^{\delta} r\left(\phi_\delta^2(r)+\delta^2\left(\frac{\mathrm{d}}{\mathrm{d}r}\phi_\delta(r)\right)^2\right)\mathrm{d}r\,\mathrm{d}\theta \\ &= \frac{1}{4}\|\Phi_i\|^2_{H^1(\mathbb{R}^d)},\end{aligned} \tag{7.10}$$

where we have also used equations from [12, Appendix D].

This means that

$$\rho_i := \frac{\|\Phi_i\|_{H^1(\mathbb{R}^d)}}{\|\Phi_i\|_{H^1(\Omega)}} \leq 2.$$

As a result, if $\delta \leq q_X$, which means that there is no overlap between the various RBFs and **F** and **G** are diagonal, or if **F** and **G** are diagonally dominant, then (7.7) will hold since then we know that positive diagonal entries will ensure at least positive semi-definiteness. Whilst we have been unable to prove that (7.7) holds in full generality for the unit square, it is supported by extensive numerical testing. The numerical experiments in Section 7.4 also provide empirical evidence since Corollary 7.6 holds, which depends on Theorem 7.4.

We have the following theorem on the condition number of the multiscale algorithm.

Theorem 7.5. *Let Φ be a positive definite kernel generating $H^\tau(\mathbb{R}^d)$. Then the condition number of the Galerkin approximation matrices from Algorithm 1 can be bounded by*

$$\kappa(\mathbf{A}) \leq C\left(\frac{\delta}{q_X}\right)^{4\tau-2}, \tag{7.11}$$

with a constant $C>0$ independent of X and of the scaling parameter δ.

Proof. At each level, we now introduce the point set $X/\delta = \{\mathbf{x_1}/\delta, \ldots, \mathbf{x}_M/\delta\}$, which obviously has separation distance

$$q_{X/\delta} = \frac{q_X}{\delta},$$

and since $a(\cdot,\cdot)$ is bilinear, the Galerkin approximation matrix at each level is

$$\begin{aligned}\mathbf{A}_{X,\delta} &= \left(a(\Phi_\delta(\cdot,\mathbf{x_i}),\Phi_\delta(\cdot,\mathbf{x_j}))\right) \\ &= \left(\delta^{-2d}a\left(\Phi\left(\frac{\cdot-\mathbf{x}_i}{\delta}\right),\Phi\left(\frac{\cdot-\mathbf{x}_j}{\delta}\right)\right)\right) = \delta^{-2d}\mathbf{A}_{X/\delta,1}.\end{aligned}$$

Then the result follows with Theorem 7.4. □

Corollary 7.6. *If the point sets are quasi-uniform, which means that h_j/q_j is bounded above by a constant, then the condition numbers of the Galerkin approximation matrices from Algorithm 1 are bounded above by a constant.*

Proof. Algorithm 1 takes $\delta_j = \nu h_j$ with a constant $\nu > 1$. With the assumption of quasi-uniformity, $h_j \leq c q_j$ and the result follows with Theorem 7.5. □

We note that since we only require the bilinear form $a(\cdot,\cdot)$ to be continuous and coercive, these theorems on the condition number will apply for PDEs with Robin and/or Neumann boundary conditions as well as PDEs with Dirichlet boundary conditions.

7.3 Nested multiscale Galerkin approximations

In this section we will consider another multiscale Galerkin algorithm that was proposed in [50]. This essentially extends Algorithm 1 and hence we can consider a PDE either with or without Dirichlet boundary conditions. We refer to this as a *nested* multiscale algorithm because it contains inner and outer iterations. We will also see that this has a connection to multigrid methods from the finite elements literature. The details are given in Algorithm 2.

From [50] we have the following theorem regarding convergence.

Theorem 7.7. *Let u^* denote the best approximation to u from $V_1 + \ldots + V_n$ with respect to the norm $\|\cdot\|_{H^1(\Omega)}$. Then there exists $c \in (0,1)$ such that*

$$\|u^* - \widetilde{u}\|_{H^1(\Omega)} \leq c^K \|u\|_{H^1(\Omega)},$$

where $\widetilde{u}_K$ is the approximation from Algorithm 2.

Note however that this does not mean that we have linear convergence of the approximation from Algorithm 2 to the true solution u. The convergence of the approximation from Algorithm 2 to the true solution u is given in the following theorem.

Theorem 7.8. *Let $\Omega \subseteq \mathbb{R}^d$ be a bounded domain with Lipschitz boundary. Let Φ be a kernel generating $H^1(\mathbb{R}^d)$ and Φ_j be defined by* (2.1) *with scale factor δ_j. Then for Algorithm 2 there exist constants $\alpha_2 > 0$ and $C_4 > 0$ such that*

$$\|u - \widetilde{u}_{n(K+1)}\|_{L_2(\Omega)} \leq C_4 \alpha_1^{n+K(n-1)} \alpha_2^K \|u\|_{H^1(\Omega)}, \quad K = 1, 2, \ldots$$

with α_1 given by (7.4). *The constants α_1 and α_2 satisfy $\alpha_1 < 1$ and $\alpha_2 < 1$ if in Algorithm 2 ν is sufficiently small and μ is sufficiently large.*

Algorithm 2 Nested multiscale Galerkin approximation

Input K: number of outer levels

n: number of inner levels

$\{X_i\}_{i=1}^{n}$: the set of centres for each inner level i, with mesh norms at each inner level given by h_i satisfying $c\mu h_i \leq h_{i+1} \leq \mu h_i$ with fixed $\mu \in (0,1), c \in (0,1]$ and h_1 sufficiently small

$\{\delta_i\}_{i=1}^{n}$: the scale parameters to use at each inner level, satisfying $\delta_i = \nu h_i$, ν a fixed constant.

Set $\widetilde{u}_0 = 0$.

for $k = 0$ to K **do**

for $i = 1$ to n **do**

With the level-specific approximation subspace $V_i := \operatorname{span}\{\Phi_i(\cdot - \mathbf{x}), \mathbf{x} \in X_i\}$, solve for the Galerkin approximation given by

$$s_{kn+i} \in V_i \,:\, a(s_{kn+i}, v) = \langle f, v \rangle_{L_2(\Omega)} - a(\widetilde{u}_{kn+i-1}, v)$$

for all $v \in V_i$. Update the solution according to

$$\widetilde{u}_{kn+i} \quad = \quad \widetilde{u}_{kn+i-1} + s_{kn+i}.$$

end for

end for

Output Approximate solution at level n, $\widetilde{u}_{n(K+1)}$

The error at level $n(K+1)$, $e_{n(K+1)} := u - \widetilde{u}_{n(K+1)}$.

Proof. Since there are $K+1$ outer iterations (since the outer level index starts at 0) and n inner iterations, we have $(K+1)n$ iterations in total, of which $K(n-1)+n$ iterations are with subsequently decreasing scale parameters for which we can use Theorem 7.2. The remaining K iterations involve the subsequent error estimation for $K > 0$ and $i = 1$ since in this case, we have an increasing scale parameter for which Theorem 7.2 does not apply. With the proof of Theorem 7.2, we can derive a similar result with increasing scale parameters. In this case, we need to change the right hand side of (7.3) and the following line to

$$\left(\frac{\delta_{i+1}}{\delta_i}\right) \leq \mu^{-2},$$

and then we can define

$$\alpha_2 := \left(\nu^{-2} C_1 + \mu^{-2} C_2\right)^{1/2}. \tag{7.12}$$

Note that $\alpha_2 > \alpha_1$ since $\mu < 1$ by definition and the constants are all positive which will mean a lower rate of convergence as compared to Algorithm 1. The remainder of the proof follows the same steps as the proofs of Corollary 7.3 and we leave the details to the reader. □

Note that the original justification for proposing this nested multiscale algorithm was that the errors from Algorithm 1 appeared to be dominated by a global behaviour, suggesting the need to go back and fit on a coarse set of centres with a large support. This is a similar idea used in the multigrid method in the finite element literature [7, Chapter 6.3]. As stated in [12, Chapter 44.3], this additional outer iteration is known from Kaczmarz iteration, which is frequently used in the multigrid literature as a smoother [28, 24].

7.4 Numerical experiments

In this section, we present the results from applying the multiscale and nested multiscale algorithms to various PDEs.

7.4.1 Multiscale Algorithm

In this subsection we consider two PDEs, the first without Dirichlet boundary conditions and the second with Dirichlet boundary conditions.

The first problem is the Helmholtz-like equation with natural boundary conditions:

$$\begin{aligned} -\Delta u + u &= f \quad \text{in} \quad \Omega, \\ \frac{\partial}{\partial \mathbf{n}} u &= 0 \quad \text{on} \quad \partial\Omega. \end{aligned}$$

We take $\Omega = [-1,1]^2$ and $f(x,y) = \cos(\pi x)\cos(\pi y)$. The outer unit normal vector is denoted by $\mathbf{n}$. The exact solution is given by

$$u(x,y) = \frac{\cos(\pi x)\cos(\pi y)}{2\pi^2 + 1}.$$

We again use the C^6 Wendland radial basis function given by (7.8). We used five levels for the approximation, with equally spaced point sets at each level. The number of points, N, and the mesh norms, h, are given in Table 7.1. We note that the mesh norms decrease by almost exactly one half at each level and hence we select $\mu = \frac{1}{2}$. The L_2 and L_∞ errors and condition numbers (κ) of the stiffness matrix are given in Table 7.2. The L_2 error was estimated using Gaussian quadrature with a 300×300 tensor product grid

Level	1	2	3	4	5
N	25	81	289	1089	4225
h	3.5e-1	1.75e-1	8.75e-2	4.37e-2	2.19e-2

Table 7.1. *The number of equally spaced points used at each level and the associated mesh norm for the multiscale Galerkin approximation example*

of Gauss-Lobatto points and the L_∞ error was estimated with the same tensor product grid.

Level	1	2	3	4	5
δ_j	2	1	0.5	0.25	0.125
$\|e_j\|_2$	8.00e-4	2.15e-4	1.06e-4	7.01e-5	5.18e-5
$\|e_j\|_\infty$	1.72e-3	7.27e-4	3.76e-4	2.15e-4	1.40e-4
κ_j	1.61e+3	3.13e+3	4.16e+3	4.58e+3	4.71e+3

Table 7.2. *The scaling factors, approximation errors and condition numbers of the stiffness matrices for the multiscale Galerkin algorithm with Neumann boundary conditions*

The second example uses the Poisson problem

$$\begin{aligned} -\Delta u &= f \quad \text{in} \quad \Omega, \\ u &= 0 \quad \text{on} \quad \partial\Omega. \end{aligned}$$

We take $\Omega = [-1,1]^2$ and $f(x,y) = \sin(\pi x)\cos\left(\frac{\pi}{2}y\right)$. The exact solution is given by

$$u(x,y) = \frac{\sin(\pi x)\cos\left(\frac{\pi}{2}y\right)}{1.25\pi^2}.$$

We again use the C^6 Wendland function as the kernel, with the same 5 levels as for the first example. To verify that (6.10) holds, we first check for the basis functions. For the boundary norm, since $\Omega = [-1,1]^2$, without loss of generality, we consider the case $x = -1$ boundary of the domain only. Then we have boundary integrals of the form [12, Appendix D]

$$\begin{aligned} \|\nabla\Phi_\delta \cdot \mathbf{n}\|^2_{L_2(\partial\Omega)} &= \int_{-\delta}^{\delta} \left(\frac{\partial\phi_\delta}{\partial y}\right)^2 \mathrm{d}y \\ &= \delta^2 \int_{-\delta}^{\delta} \left(\frac{22y}{\delta^2}\left(\frac{16y^2}{\delta^2} + \frac{7y}{\delta} + 1\right)\left(1 - \frac{y}{\delta}\right)^7\right)^2 \mathrm{d}y \\ &= \frac{603969552384\delta}{11305}. \end{aligned}$$

For the interior, we have

$$\begin{aligned}
\|\nabla\Phi_\delta\|^2_{L_2(\Omega)} &= \delta^2 \int\limits_{\Theta}\int\limits_{0}^{\delta} r\left(\frac{d}{dr}\phi_\delta(r)\right)^2 \mathrm{d}r\mathrm{d}\theta \\
&= \delta^2 \int\limits_{\Theta}\int\limits_{0}^{\delta} r\left(\frac{22r}{\delta^2}\left(\frac{16r^2}{\delta^2}+\frac{7r}{\delta}+1\right)\left(1-\frac{r}{\delta}\right)^7\right)^2 \mathrm{d}r\mathrm{d}\theta \\
&= \frac{2453\delta^2}{4845}\int\limits_{\Theta}\mathrm{d}\theta,
\end{aligned}$$

where Θ specifies the support of ϕ in Ω and hence this last expression is finite and does not depend on δ.

In practical applications, we need to select a value of β_N satisfying $\beta_N > 2C_N^2/\delta$. In [22], it is proposed to estimate $C_N/\sqrt{\delta}$ as the maximum eigenvalue of the generalised eigenvalue problem,

$$\mathbf{B}\mathbf{v} = \lambda\mathbf{D}\mathbf{v}, \tag{7.13}$$

where

$$B_{ij} = \int\limits_{\partial\Omega} \left(\nabla\Phi_i\cdot\mathbf{n}\right)\left(\nabla\Phi_j\cdot\mathbf{n}\right), \tag{7.14}$$

and

$$D_{ij} = \int\limits_{\Omega} \nabla\Phi_i\cdot\nabla\Phi_j, \tag{7.15}$$

where i and j run over the indices of all the radial basis functions with support overlapping the boundary. The extra calculation involved in this step is not significant since the entries of $\mathbf{B}$ are required for the construction of the stiffness matrix and the set of centres overlapping the boundary will generally be small compared to the entire set of centres. The maximum eigenvalue can also be efficiently computed with a simultaneous Rayleigh-quotient minimisation method [26].

Level	1	2	3	4	5
δ_j	2	1	0.5	0.25	0.125
$\|e_j\|_2$	8.13e-3	1.45e-3	3.23e-4	8.22e-5	2.22e-5
$\|e_j\|_\infty$	1.06e-2	2.35e-3	6.50e-4	1.96e-4	5.96e-5
κ_j	5.63e+5	1.00e+6	8.06e+5	4.57e+5	2.37e+5

Table 7.3. *The scaling factors, approximation errors and condition numbers of the stiffness matrices for the multiscale Galerkin algorithm with Dirichlet boundary conditions*

The results are in Table 7.3 and support the theoretical findings above. We note that whilst [50] did not find convergence after the third level with a similar algorithm, this may be due to the approximations used to calculate the integrals, rather than the algorithm itself. The potential for errors in integration to affect the performance of Galerkin techniques are well known [42, 7]. To estimate the integrals, we used the MATLAB functions `quad2d` and `quad` with an absolute tolerance value of $1e^{-10}$. We also estimated the non-zero integration range both to speed up the calculations as well as to reduce numerical error which can result if for example, we integrate over the entire domain $[-1,1]^2$ whilst the function only has a very small support.

7.4.2 Nested multiscale algorithm

In this subsection, we consider the same example as in Section 7.4.1, however now with Algorithm 2 with $K = 2$ and $n = 2$. We use the first two levels of the example described in Section 7.4.1 as the inner iteration. We also use the same kernel. Our choice of K and n leads to a 6 level algorithm. A similar example was considered in [50, Section 5], however a lack of information regarding the exact approximation spaces used for the inner and outer level iterations means we have not been able to compare our results. The results from this 6 level nested algorithm are in Table 7.4.

Level	1	2	3	4	5	6
N	25	81	25	81	25	81
$\|e_j\|_2$	8.00e-4	2.15e-4	2.05e-4	2.09e-4	1.99e-4	2.03e-4
$\|e_j\|_\infty$	1.72e-3	7.27e-4	4.33e-4	7.00e-4	4.17e-4	6.74e-4
κ_j	1.61e+3	3.13e+3	1.61e+3	3.13e+3	1.61e+3	3.13e+3

Table 7.4. *The number of centres, scaling factors, approximation errors and condition numbers of the stiffness matrices for the nested multiscale Galerkin algorithm*

The results indicate erratic convergence and approximation errors far inferior to those using Algorithm 1. This is not surprising since Theorem 7.10 indicates convergence of our approximation to the best approximation to u from $V_1 + V_2$ whilst in Algorithm 1 our approximation is formed from $V_1 + \ldots + V_5$.

7.5 Analysis of convergence

In this section we will focus on estimation of the convergence and verifying approximation orders. Similarly to [53], we will also rewrite the convergence results in terms of mesh norms, which is the usual form of convergence results for radial basis function approximations [51, 12].

7.5.1 Multiscale Galerkin algorithm

We consider Algorithm 1 with $h_1 = \mu$ and $h_{j+1} = \mu h_j$. Since μ is a constant, we can rewrite (7.4) as

$$\alpha_1 = c_{20}\mu.$$

Then with Corollary 7.3 we have

$$\|e_n\|_{L_2(\Omega)} := \|u - \widetilde{u}_n\|_{L_2(\Omega)} \le C h_n^{1-\sigma} \|u\|_{H^1(\Omega)}, \tag{7.16}$$

with

$$\sigma := -\log c_{20} / \log \mu. \tag{7.17}$$

Hence we can either express our convergence in terms of an exponent of h_n or equivalently α_1^n.

It is of interest that the error bounds do not depend on the kernel used for the approximation spaces. Typically with a kernel which generates $H^\tau(\mathbb{R}^d)$, we see error bounds proportional to h^τ. Since our kernel for the error analysis generates $H^1(\mathbb{R}^d)$, we have h_n^1. Henceforth, we analyse the convergence in terms of α_1. We can calculate estimates of α_1, which we denote by $\widetilde{\alpha}_1$, as follows

$$\widetilde{\alpha}_{1,n} := \frac{\|e_n\|_{L_2(\Omega)}}{\|e_{n-1}\|_{L_2(\Omega)}}.$$

	C^2 WF	C^6 WF
$\widetilde{\alpha}_{1,2}$	0.128	0.268
$\widetilde{\alpha}_{1,3}$	0.318	0.494
$\widetilde{\alpha}_{1,4}$	0.507	0.662
$\widetilde{\alpha}_{1,5}$	0.618	0.739

Table 7.5. *The estimated convergence rates $\widetilde{\alpha}_{1,n}$ using the results for the L_2 norm errors from the first example in Section 7.4.1 with the C^2 and C^6 Wendland functions.*

We can see that the estimated values of α_1 are higher with the C^6 Wendland function, which indicates that we should not necessarily expect faster convergence with a smoother Wendland function and consequently we should not expect an error bound proportional to h^τ.

7.5.2 Nested multiscale Galerkin algorithm

In this subsection, we will focus on considering convergence of the nested multiscale Galerkin algorithm in terms of α_1 and α_2. Note that a bound for the error at level

$n(K+1)$ in terms of the mesh norm at level $n(K+1)$, such as in (7.16), will not be possible here because the mesh norm at level $n(K+1)$ only depends on n and not on K. In other words, increasing K has no effect on the final mesh norm.

An additional benefit of considering the nested multiscale algorithm is more estimates of α_1, particularly for repeated applications of the inner iterations (when $K > 1$). Table 7.6 gives the estimates of α_1 and α_2 from considering successive L_2 norm error estimates in Section 7.4.2. Successive error estimates will be of the form

$$\frac{\|e_i\|_{L_2(\Omega)}}{\|e_{i-1}\|_{L_2(\Omega)}}.$$

By definition of our nested multiscale algorithm, for $i = n+1, 2n+1, \ldots$ we have an estimate for α_2 and in all other cases, an estimate for α_1.

Table 7.4.2 presents the estimated convergence rates $\widetilde{\alpha}_{1,n}$ and $\widetilde{\alpha}_{2,n}$ using the results for the L_2 norm errors from the example in Section 7.4.2.

Level	$\widetilde{\alpha}_{1,n}$	$\widetilde{\alpha}_{2,n}$
2	0.268	
3		0.953
4	1.021	
5		0.954
6	1.022	

Table 7.6. *The estimated convergence rates $\widetilde{\alpha}_{1,n}$ and $\widetilde{\alpha}_{2,n}$ using the results for the L_2 norm errors from the example in Section 7.4.2.*

Interestingly, the difficulties with convergence, at least in this example, are not due to α_2 which is seen to be less than 1 in all cases. This is empirical evidence of the effectiveness of the smoothing nature of the inner iterations, in that after the inner iterations, the errors are again of a global nature and hence a return to a coarse grid is justified. Convergence is affected by the repeated application of the inner iterations for which $\widetilde{\alpha}_{1,n}$ is always greater than 1. Empirically, this appears to suggest that the more localised features have already been captured in the approximate solution.

This also implies that the angles between the approximation subspaces are close to zero since the linear convergence rate in Theorem 7.7 can be bounded above by the angle between the subspaces. This is covered next.

Angles between subspaces

For our analysis of the convergence of the nested multiscale algorithm, we require the following definition of the angle between subspaces.

Definition 7.9. *Let $\mathcal{H}_1$ and $\mathcal{H}_2$ be closed subspaces of a Hilbert space $\mathcal{H}$ with $U := \mathcal{H}_1 \cap \mathcal{H}_2$. Then the angle θ between $\mathcal{H}_1$ and $\mathcal{H}_2$ is given by*

$$\cos\theta = \sup\left\{\langle u, v\rangle : u \in \mathcal{H}_1 \cap U^\perp, v \in \mathcal{H}_2 \cap U^\perp \text{ and } \|u\|, \|v\| \leq 1\right\}.$$

It is well known [39, 9] that Algorithm 2 converges linearly in the following sense.

Theorem 7.10. *Let u^* be the best approximation to u from $V_1 + \ldots + V_j$ with respect to $\|\cdot\|_{H^1(\Omega)}$. Let $\widetilde{u}$ be the approximation from Algorithm 2. Let θ_j be the angle between V_j and $\cap_{i=j+1}^k V_i$. Then*

$$\|u^* - \widetilde{u}_K\|_{H^1(\Omega)} \leq c^K \|u\|_{H^1(\Omega)},$$

where

$$c^2 \leq 1 - \prod_{j=1}^{n-1} \sin^2\theta_j.$$

This means that we need to estimate $\sin\theta_j$ to obtain upper bounds for the convergence rate. We follow a similar approach to [4]. We firstly define modified sets of centres as $\widetilde{X}_1 = X_1$ and

$$\widetilde{X}_i = X_i \backslash \bigcup_{j=1}^{i-1} X_j, \quad i \geq 2,$$

and the corresponding approximation spaces as

$$\widetilde{V}_i = \operatorname{span}\left\{\Phi_{\delta_i}(\cdot - \mathbf{x}), \mathbf{x} \in \widetilde{X}_i\right\}.$$

Then we need to find the supremum of the inner product of $u \in \widetilde{V}_i$ and $v \in \mathcal{A}_{i+1}$ where

$$\mathcal{A}_{i+1} = \bigcup_{j=i+1}^{K} \widetilde{V}_j = \operatorname{span}\left\{\Phi_{\delta_j}(\cdot - \mathbf{x}_j), \mathbf{x}_j \in \bigcup_{j=i+1}^{K} \widetilde{X}_j\right\},$$

with $\|u\| = \|v\| = 1$. With the matrix $\mathbf{K}^{\{12\}}$ given by

$$K_{i,j}^{\{12\}} = \left\langle \Phi_{\delta_i}(\cdot - \mathbf{x}_i), \Phi_{\delta_j}(\cdot - \mathbf{x}_j)\right\rangle, \mathbf{x}_i \in \widetilde{X}_i, \mathbf{x}_j \in \bigcup_{j=i+1}^{K} \widetilde{X}_j,$$

and with coefficient vectors μ and ν for u and v respectively, we seek the supremum of $\mu\mathbf{K}^{\{12\}}\nu$. We also define matrices $\mathbf{K}^{\{1\}}$ and $\mathbf{K}^{\{2\}}$ as

$$K_{ij}^{\{1\}} = \left\langle \Phi_{\delta_i}(\cdot - \mathbf{x}_i), \Phi_{\delta_j}(\cdot - \mathbf{x}_j)\right\rangle, \mathbf{x}_i \in \widetilde{X}_i, \mathbf{x}_j \in \widetilde{X}_i,$$

and

$$K^{\{2\}}_{ij} = \left\langle \Phi_{\delta_i}(\cdot, \mathbf{x}_i), \Phi_{\delta_j}(\cdot, \mathbf{x}_j) \right\rangle, \mathbf{x}_i \in \bigcup_{j=i+1}^{K} \widetilde{X}_j, \mathbf{x}_j \in \bigcup_{j=i+1}^{K} \widetilde{X}_j.$$

Let the Cholesky decomposition of $\mathbf{K}^{\{1\}}$ be $\mathbf{L}_1^T\mathbf{L}_1$. This is well-defined since $\mathbf{K}^{\{1\}}$ is strictly positive definite and symmetric. Then $\|u\|^2 = \mu^T\mathbf{L}_1^T\mathbf{L}_1\mu$ and letting $\gamma_1 = \mathbf{L}_1\mu$ gives $\|u\|^2 = \gamma_1^T\gamma_1$. We can follow a similar approach with $\mathbf{K}^{\{2\}}$ which gives $\|v\|^2 = \gamma_2^T\gamma_2$ with $\mathbf{K}^{\{2\}} = \mathbf{L}_2^T\mathbf{L}_2$ and $\gamma_2 = \mathbf{L}_2\nu$. However in this case since $\mathbf{K}^{\{2\}}$ is the union of radial basis functions with (possibly) different scaling factors, we cannot be sure that $\mathbf{K}^{\{2\}}$ is positive definite. In our example, $\mathbf{K}^{\{2\}}$ was always positive definite and we do not dwell further on this. Sufficient conditions for an interpolation matrix constructed with several scaling factors to be positive definite can be found in [6, (11)] which also requires the Fourier transform of a Wendland function [8] to compute a lower bound on the minimum eigenvalue as given in [51, Theorem 12.3].

Then we have

$$\begin{aligned} \langle u, v\rangle &= \mu^T\mathbf{K}^{\{12\}}\nu \\ &= \mu^T\mathbf{L}_1^T(\mathbf{L}_1^{-1})^T\mathbf{K}^{\{12\}}\mathbf{L}_2^{-1}\mathbf{L}_2\nu \\ &= \gamma_1^T\mathbf{M}\gamma_2, \end{aligned}$$

with $\mathbf{M} := (\mathbf{L}_1^{-1})^T\mathbf{K}^{\{12\}}\mathbf{L}_2^{-1}$. The supremum of the inner product is given by the largest singular value of $\mathbf{M}$. We denote this supremum by $\sin\widetilde{\theta}_j$ and the results with $\{\widetilde{V}_i\}_{i=1}^5$ are in Table 7.7. We note that since $\widetilde{X}_i \subseteq X_i$, $\sin\widetilde{\theta}_i$ is a lower bound on $\sin\theta_i$. We chose to estimate $\sin\widetilde{\theta}_i$ since by removing nested centres from later levels, we had less difficulties with singular matrices.

i	1	2	3	4
$\sin\widetilde{\theta}_i$	9.85e-3	2.68e-2	4.15e-2	6.99e-2

Table 7.7. *The estimates of* $\sin\widetilde{\theta}_i$ *with the approximation spaces* $\{\widetilde{V}_i\}_{i=1}^5$.

Chapter Eight

Multiscale algorithms for collocation of PDEs

This chapter will cover theoretical results and numerical experiments of several multiscale algorithms for collocation of elliptic PDEs and the Stokes problem on bounded domains. We again denote the mesh norm at level i by h_i.

8.1 Multiscale symmetric collocation of elliptic PDEs on bounded domains

We formally state our multiscale algorithm for the symmetric collocation approximation of (6.13) and (6.14), which is stated as Algorithm 3.

The following theorem and corollaries are our main results for the convergence of the multiscale symmetric collocation algorithm.

Theorem 8.1. *Let $\Omega \subseteq \mathbb{R}^d$ be a bounded domain with $C^{k,s}$-boundary. Let Φ be a kernel generating $H^\tau(\mathbb{R}^d)$ with $\tau > 2 + d/2$ and Φ_j be defined by* (2.1) *with scale factor δ_j. Then for Algorithm 3 there exists a constant $\alpha_3 > 0$ such that*

$$\|\mathcal{E}_S e_j\|_{\Phi_{j+1}} \leq \alpha_3 \|\mathcal{E}_S e_{j-1}\|_{\Phi_j} \quad \textit{for} \quad j = 1, 2, \ldots$$

where $\mathcal{E}_S e_j$ is the extension operator defined in Lemma 2.1 applied to the error at level j defined in Algorithm 3. The constant α_3 satisfies $\alpha_3 < 1$ if in Algorithm 3 ν is sufficiently small and μ is sufficiently large.

Proof. With (4.13), we can write

$$\|\mathcal{E}_S e_j\|^2_{\Phi_{j+1}} \leq \frac{1}{c_8} \int\limits_{\mathbb{R}^d} |\widehat{\mathcal{E}_S e_j}(\omega)|^2 \left(1 + \delta_{j+1}^2 \|\omega\|_2^2\right)^\tau \mathrm{d}\omega =: \frac{1}{c_8}\left(I_1 + I_2\right)$$

with

$$I_1 := \int\limits_{\|\omega\|_2 \leq \frac{1}{\delta_{j+1}}} |\widehat{\mathcal{E}_S e_j}(\omega)|^2 \left(1 + \delta_{j+1}^2 \|\omega\|_2^2\right)^\tau \mathrm{d}\omega,$$

Algorithm 3 Multiscale symmetric collocation approximation

Input n: number of levels

$\{X_{1,i}, X_{2,i}\}_{i=1}^{n}$: the interior and boundary collocation points for each level i, with mesh norms at each level given by $\{h_{1,i}, h_{2,i}\}_{i=1}^{n}$ satisfying

$c\mu\bar{h}_i \leq \bar{h}_{i+1} \leq \mu\bar{h}_i$, where $\bar{h}_i := \max(h_{1,i}, h_{2,i})$, with fixed $\mu \in (0,1), c \in (0,1]$ and h_1 sufficiently small

$\{\delta_i\}_{i=1}^{n}$: the scale parameters to use at each level, satisfying

$\delta_i = \nu\bar{h}_i^{1-(4+d)/(2\tau)}$, where ν is a fixed constant.

Set $\widetilde{u}_0 = 0, f_0 = f, g_0 = g$.

for $i = 1$ to n **do**

With the scaled kernel Φ_{δ_i}, solve the unsymmetric collocation linear system

$$\begin{aligned}\mathcal{L}s_i(\mathbf{x}) &= f_{i-1}(\mathbf{x}) \quad \forall \quad \mathbf{x} \in X_{1,i} \\ s_i(\mathbf{x}) &= g_{i-1}(\mathbf{x}) \quad \forall \quad \mathbf{x} \in X_{2,i}.\end{aligned}$$

Update the solution and residual according to

$$\begin{aligned}\widetilde{u}_i &= \widetilde{u}_{i-1} + s_i \\ f_i &= f_{i-1} - \mathcal{L}s_i \\ g_i &= g_{i-1} - s_i\end{aligned}$$

end for

Output Approximate solution at level n, $\widetilde{u}_n$.

The error at level n, $e_n := u - \widetilde{u}_n$.

$$I_2 := \int\limits_{\|\boldsymbol{\omega}\|_2 \geq \frac{1}{\delta_{j+1}}} |\widehat{\mathcal{E}_S e_j}(\boldsymbol{\omega})|^2 \left(1 + \delta_{j+1}^2 \|\boldsymbol{\omega}\|_2^2\right)^{\tau} \, \mathrm{d}\boldsymbol{\omega}.$$

Now we consider the first integral where we can use $\delta_{j+1}\|\boldsymbol{\omega}\|_2 \leq 1$ and then Lemma 6.3 and (4.13). This is valid since $s_j \in V_j$ is the approximate solution with symmetric collocation of $\mathcal{L}e_{j-1} = f_{j-1}$. Then we have

$$\begin{aligned}I_1 &\leq 2^{\tau} \int\limits_{\|\boldsymbol{\omega}\|_2 \leq \frac{1}{\delta_{j+1}}} |\widehat{\mathcal{E}_S e_j}(\boldsymbol{\omega})|^2 \, \mathrm{d}\boldsymbol{\omega} \\ &\leq 2^{\tau} \, \|\mathcal{E}_S e_j\|_{L_2(\mathbb{R}^d)}^2 \leq C \, \|e_j\|_{L_2(\Omega)}^2 \\ &\leq C \, h_{1,j}^{2\tau-4} \, \|e_{j-1}\|_{H^{\tau}(\Omega)}^2 \\ &\leq C h_{1,j}^{2\tau-4} \, \delta_j^{-2\tau} \|\mathcal{E}_S e_{j-1}\|_{\Phi_j}^2\end{aligned}$$

$$\leq \quad C\nu^{-2\tau} \|\mathcal{E}_S e_{j-1}\|^2_{\Phi_j},$$

where we have also used Lemma 6.3. For the second integral I_2, we note that

$$\delta_{j+1}/\delta_j = (\bar{h}_{j+1}/\bar{h}_j)^{1-(4+d)/(2\tau)} \leq \mu^{1-(4+d)/(2\tau)},$$

and since $\delta_{j+1}\|\boldsymbol{\omega}\|_2 \geq 1$, we have that

$$\left(1+\delta_{j+1}^2\|\boldsymbol{\omega}\|_2^2\right)^{\tau} \leq 2^{\tau}\delta_{j+1}^{2\tau}\|\boldsymbol{\omega}\|_2^{2\tau} \leq 2^{\tau}\mu^{2\tau-4-d}\left(1+\delta_j^2\|\boldsymbol{\omega}\|_2^2\right)^{\tau}.$$

Then again using (4.13) shows that

$$\begin{aligned} I_2 &\leq 2^{\tau}\, c_9\, \mu^{2\tau-4-d}\|\mathcal{E}_S e_j\|^2_{\Phi_j} \\ &\leq 2^{\tau}\, c_9\, \mu^{2\tau-4-d}\|\mathcal{E}_S e_{j-1}\|^2_{\Phi_j}, \end{aligned}$$

where in the second last step we have used that since the interpolant at X_j to e_{j-1} is the same as the interpolant to $\mathcal{E}_S e_{j-1}$ (both functions take the same values on $X_j \subseteq \Omega$), we have

$$\begin{aligned} \|e_j\|_{H^\tau(\Omega)} &= \|e_{j-1} - s_j e_{j-1}\|_{H^\tau(\Omega)} \\ &= \|\mathcal{E}_S e_{j-1} - s_j\mathcal{E}_S e_{j-1}\|_{H^\tau(\Omega)} \\ &\leq \|\mathcal{E}_S e_{j-1} - s_j\mathcal{E}_S e_{j-1}\|_{H^\tau(\mathbb{R}^d)} \\ &\leq C\delta_j^{-\tau-1}\|\mathcal{E}_S e_{j-1} - s_j\mathcal{E}_S e_{j-1}\|_{\mathcal{N}_{\Phi_j}(\mathbb{R}^d)} \\ &\leq C\delta_j^{-\tau}\|\mathcal{E}_S e_{j-1}\|_{\mathcal{N}_{\Phi_j}(\mathbb{R}^d)}. \end{aligned}$$

Combining our results for I_1 and I_2 and now writing C_5 and C_6 for the two constants appearing in the bounds of the expressions for I_1 and I_2 respectively, we have that

$$\|\mathcal{E}_S e_j\|^2_{\Phi_{j+1}} \leq \left(\nu^{-2\tau}C_5/c_8 + \mu^{2\tau-4-d}C_6/c_8\right)\, \|\mathcal{E}_S e_{j-1}\|^2_{\Phi_j},$$

and the result follows with

$$\alpha_3 := \left(\nu^{-2\tau}C_5/c_8 + \mu^{2\tau-4-d}C_6/c_8\right)^{1/2}.$$

□

Corollary 8.2. *There exist constants $C_7 > 0$ and $C_8 > 0$ such that for the solutions of the multiscale symmetric collocation from Algorithm 3 we have the following error bounds*

$$\|u - \widetilde{u}_n\|_{L_2(\Omega)} \leq C_7\alpha_3^n\|u\|_{H^\tau(\Omega)} \quad \textit{for} \;\; n = 1, 2, \ldots \tag{8.1}$$

and

$$\|u - \widetilde{u}_n\|_{L_2(\partial\Omega)} \leq C_8\alpha_3^n\|u\|_{H^\tau(\Omega)} \quad \textit{for} \;\; j = n, 2, \ldots \tag{8.2}$$

Thus $\widetilde{u}_n$ resulting from Algorithm 3 converges linearly to u in the L_2-norm in Ω and on $\partial\Omega$ if $\alpha_3 < 1$.

Proof. We first consider the solution in Ω. Using Lemma 6.3 and (4.13) again, we can see that

$$\begin{aligned}
\|u - \widetilde{u}_n\|_{L_2(\Omega)} &= \|e_n\|_{L_2(\Omega)} \\
&\leq Ch_{1,n}^{\tau-2}\|e_n\|_{H^\tau(\Omega)} \\
&\leq C\bar{h}_n^{\tau-2}\delta_{n+1}^{-\tau}\|\mathcal{E}_S e_n\|_{\Phi_{n+1}} \\
&\leq C\,\|\mathcal{E}_S e_n\|_{\Phi_{n+1}} \leq C\alpha_3^n\|u\|_{\Phi_1} \\
&\leq C\alpha_3^n\|u\|_{H^{\tau+1}(\Omega)},
\end{aligned}$$

since

$$\bar{h}_n^{\tau-2}\,\delta_{n+1}^{-\tau} = \nu^{-\tau}\,\bar{h}_n^{\tau-2}\,\bar{h}_{n+1}^{-\tau+2+d/2} \leq \nu^{-\tau}\left(\frac{\bar{h}_n}{\bar{h}_{n+1}}\right)^{\tau-2} \leq \nu^{-\tau}(c\mu)^{2-\tau}.$$

With (6.3), the proof for the second result follows in an identical fashion. In this case we need

$$h_{2,n}^{\tau-1/2}\delta_{n+1}^{-\tau} \leq \nu^{-\tau}\,\bar{h}_n^{\tau-1/2}\,\bar{h}_{n+1}^{-\tau+1/2} \leq C(c\mu)^{1/2-\tau}.$$

□

Corollary 8.3. *There exist constants $C_9 > 0$ and $C_{10} > 0$ such that for the solutions of the multiscale symmetric collocation algorithm we have the following error bounds*

$$\|u - \widetilde{u}_n\|_{L_\infty(\Omega)} \leq C_9\alpha_3^n\|u\|_{H^\tau(\Omega)} \quad \text{for} \quad n = 1, 2, \ldots \tag{8.3}$$

and

$$\|u - \widetilde{u}_n\|_{L_\infty(\partial\Omega)} \leq C_{10}\alpha_3^n\|u\|_{H^\tau(\Omega)} \quad \text{for} \quad n = 1, 2, \ldots \tag{8.4}$$

Thus $\widetilde{u}_n$ resulting from Algorithm 3 converges linearly to u in the L_∞-norm in Ω and on $\partial\Omega$ if $\alpha_3 < 1$.

Proof. The proofs are very similar to the previous corollary and we only highlight the differences in both cases. In Ω, we clearly have

$$\|u - \widetilde{u}_n\|_{L_\infty(\Omega)} \leq C\|\mathcal{L}u - \mathcal{L}\widetilde{u}_n\|_{L_\infty(\Omega)}$$

if we assume that the coefficients of $\mathcal{L}$ are in, say, C^2. Then from [18, Theorem 3.10] we know that

$$\|\mathcal{L}u - \mathcal{L}s\|_{L_\infty(\Omega)} \leq Ch_1^{\tau-2-d/2}\|u\|_{H^\tau(\Omega)}$$

and since

$$h_{1,n}^{\tau-2-d/2}\delta_{n+1}^{-\tau} = \nu^{-\tau}\left(\frac{\bar{h}_n}{\bar{h}_{n+1}}\right)^{\tau-2-d/2} \le C(c\mu)^{\tau-2-d/2},$$

the result follows. On $\partial\Omega$, we need to use [18, Theorem 3.10]

$$\|u-\widetilde{u}\|_{L_\infty(\partial\Omega)} \le Ch_2^{\tau-d/2}\|u-\widetilde{u}\|_{H^\tau(\Omega)}, \tag{8.5}$$

and that

$$h_{2,n}^{\tau-d/2}\,\delta_{n+1}^{-\tau} \le \nu^{-\tau}\,\bar{h}_n^{\tau-d/2}\,\bar{h}_{n+1}^{-\tau+d/2} \le C(c\mu)^{-\tau+d/2}.$$

□

8.1.1 Numerical experiments

In this section, we present the results from applying the symmetric collocation algorithms to the following Poisson problem with Dirichlet boundary conditions from [12].

$$\begin{aligned}
\nabla^2 u(x,y) &= -\frac{5}{4}\pi^2\sin(\pi x)\cos\left(\frac{\pi y}{2}\right), \quad (x,y)\in\Omega := [0,1]^2,\\
u(x,y) &= \sin(\pi x), \quad (x,y)\in\Gamma_1 := \{(x,y): 0\le x\le 1, y=0\},\\
u(x,y) &= 0, \quad (x,y)\in\Gamma_2 := \partial\Omega\setminus\Gamma_1.
\end{aligned}$$

The exact solution is given by

$$u(x,y) = \sin(\pi x)\cos\left(\frac{\pi y}{2}\right).$$

We note that these same experiments, with different scaling parameters δ_i and point sets, can be found in [12, Table 41.4] where convergence was observed essentially only for several levels. This indicates the importance of the theoretical results given in this chapter.

We again use the C^6 Wendland radial basis function given by (7.8) which is positive definite on $\mathbb{R}^2$ (cf. [51]). We used five levels for the approximation, with equally spaced point sets at each level. The number of points, N, and the mesh norms, h, are given in Table 8.1. We note that the mesh norms decrease by almost exactly one half at each level and hence we select $\mu = \frac{1}{2}$. There are also $4(\sqrt{N}-1)$ equally spaced boundary centres. For the scaling parameters, we note that $m = d = 2$ in this example and $\tau = 4.5$ (cf. [51]). Algorithm 3 specifies that

$$\delta_j = \nu\bar{h}_j^{1-(d+4)/(2\tau)}$$

with ν constant. With the given value of h_1 in Table 8.1, we select ν such that $\delta_1 = 2$. This gives $\nu = 3.58$ and we use this to generate the other δ values which are given along with

Level	1	2	3	4	5
N	25	81	289	1089	4225
$\bar{h}$	1.75e-1	8.755e-2	4.37e-2	2.19e-2	1.09e-2

Table 8.1. *The number of equally spaced points used at each level and the associated mesh norm for the numerical experiments*

the L_2 and L_∞ errors and condition numbers (κ) of the collocation matrices in Table 8.2. The L_2 error was estimated using Gaussian quadrature with a 300×300 tensor product grid of Gauss-Legendre points and the L_∞ error was estimated with the same tensor product grid.

Level	1	2	3	4	5
δ_j	2	1.59	1.26	1	0.79
$\|e_j\|_2$	3.32e-3	1.69e-4	1.50e-5	8.58e-7	3.94e-8
$\|e_j\|_\infty$	6.06e-3	8.52e-4	6.20e-5	5.80e-6	5.38e-7
κ_j	1.18e+6	2.27e+8	4.23e+10	6.63e+12	1.32e+15

Table 8.2. *The scaling factors, approximation errors and condition numbers of the collocation matrices for the multiscale symmetric collocation algorithm example*

8.2 Multiscale symmetric collocation approximation to the Stokes problem

We can now formally state our multiscale algorithm for the symmetric collocation solution of (6.19)-(6.21) which is stated as Algorithm 4. To simplify notation, we write $\mathbf{S}_i\mathbf{v} = \mathbf{S}_{X_i}\mathbf{v}$ and $\mathbf{\Psi}_i = \mathbf{\Psi}_{\delta_i}$ and denote the mesh norms for the interior and boundary collocation points at level i as $h_{1,i}$ and $h_{2,i}$ respectively.

We require a technical lemma regarding the error in the estimation of the velocity u.

Lemma 8.4. *Let $d = 3$. Assume that $\mathbf{u} \in \mathbf{H}^\tau(\Omega; \mathrm{div})$ with $\tau > 0$ and let $\widetilde{\boldsymbol{\mathcal{E}}}_{\mathrm{div}}$ be defined by* (6.22). *Then we have the following bound*

$$\int\limits_{\mathbb{R}^d} \frac{\left\| \widehat{\widetilde{\boldsymbol{\mathcal{E}}}_{\mathrm{div}}\mathbf{u}}(\boldsymbol{\omega}) \right\|_2^2}{\|\boldsymbol{\omega}\|_2^2} \mathrm{d}\boldsymbol{\omega} \leq C\|\mathbf{u}\|^2_{L_2(\Omega)}.$$

Proof. With the definitions of the $\widetilde{\boldsymbol{\mathcal{E}}}_{\mathrm{div}}$, $\mathcal{E}_S$ and $\mathcal{T}$ operators, we have

$$\int\limits_{\mathbb{R}^d} \frac{\left\| \widehat{\widetilde{\boldsymbol{\mathcal{E}}}_{\mathrm{div}}\mathbf{u}}(\boldsymbol{\omega}) \right\|_2^2}{\|\boldsymbol{\omega}\|_2^2} \mathrm{d}\boldsymbol{\omega} = \int\limits_{\mathbb{R}^d} \frac{\left\| \boldsymbol{\omega} \times \widehat{\mathcal{E}_S\mathcal{T}\mathbf{u}}(\boldsymbol{\omega}) \right\|_2^2}{\|\boldsymbol{\omega}\|_2^2} \mathrm{d}\boldsymbol{\omega}$$

Algorithm 4 Multiscale symmetric collocation approximation to the Stokes problem

Input n: number of levels

$X_i := \{X_{1,i}, X_{2,i}\}_{i=1}^n$: the interior and boundary collocation points for each level i, with mesh norms at each level given by $\{h_{1,i}, h_{2,i}\}_{i=1}^n$ satisfying $c\mu\bar{h}_i \leq \bar{h}_{i+1} \leq \mu\bar{h}_i$, where $\bar{h}_i := \max(h_{1,i}, h_{2,i})$ with fixed $\mu \in (0,1), c \in (0,1]$ and $\bar{h}_1$ sufficiently small

$\{\delta_i\}_{i=1}^n$: the scale parameters to use at each level, satisfying $\delta_i = \beta\bar{h}_i^{1-3/(\tau+1)}$, β is a fixed constant.

Set $\mathbf{M}_0\mathbf{v} = \mathbf{0}, \mathbf{f}_0 = \mathbf{f}, \mathbf{g}_0 = \mathbf{g}$.

for $i = 1$ to n **do**

With the scaled kernel $\mathbf{\Psi}_i$, solve the symmetric collocation linear system

$$\begin{aligned} \left(\mathcal{L}^S\mathbf{S}_i\mathbf{v}(\mathbf{x})\right)_j &= f_{i-1,j}(\mathbf{x}), \quad 1 \leq j \leq d, \ \mathbf{x} \in X_{1,i} \\ \left(\mathbf{S}_i\mathbf{v}(\mathbf{x})\right)_j &= g_{i-1,j}(\mathbf{x}), \quad 1 \leq j \leq d, \ \mathbf{x} \in X_{2,i}. \end{aligned}$$

Update the solution and residual according to

$$\begin{aligned} \mathbf{M}_i\mathbf{v} &= \mathbf{M}_{i-1}\mathbf{v} + \mathbf{S}_i\mathbf{v} \\ \mathbf{f}_i &= \mathbf{f}_{i-1} - \mathcal{L}^S\mathbf{S}_i\mathbf{v} \\ \mathbf{g}_i &= \mathbf{g}_{i-1} - \mathbf{S}_i\mathbf{v} \end{aligned}$$

end for

Output Approximate solution at level n, $\mathbf{M}_n\mathbf{v}$

The error at level n, $\mathbf{e}_n := \mathbf{v} - \mathbf{M}_n\mathbf{v}$.

$$\begin{aligned} &\leq C\int_{\mathbb{R}^d} \left\|\widehat{\mathcal{E}_S\mathcal{T}\mathbf{u}}(\boldsymbol{\omega})\right\|_2^2 \mathrm{d}\boldsymbol{\omega} \\ &= C\|\mathcal{E}_S\mathcal{T}\mathbf{u}\|_{L_2(\mathbb{R}^d)}^2 \\ &\leq C\|\mathcal{E}_S\mathcal{T}\mathbf{u}\|_{H^1(\mathbb{R}^d)}^2 \\ &\leq C\|\mathcal{T}\mathbf{u}\|_{H^1(\Omega)}^2 \\ &\leq C\|\mathbf{u}\|_{L_2(\Omega)}^2, \end{aligned}$$

where we have also used that the $\mathcal{E}_S$ and $\mathcal{T}$ operators are bounded (Lemma 2.1, [52]). □

The following theorem and corollary are our main results on the convergence of the multiscale symmetric collocation algorithm for solving the Stokes problem.

Theorem 8.5. *Assume that Ω and $\mathbf{f}, \mathbf{g}$ satisfy the smoothness assumptions of Theorem 6.6. Suppose the kernel $\mathbf{\Psi}$ is chosen such that $\mathcal{N}_{\mathbf{\Psi}}(\mathbb{R}^d) = \widetilde{\mathbf{H}}^{\tau}(\mathbb{R}^d; \mathrm{div}) \times H^{\tau-1}(\mathbb{R}^d)$ and define the scaled kernels by* (6.35) *with scale factor δ_j. Then for Algorithm 4 there exists a constant α_4 such that*

$$\|\boldsymbol{\mathcal{E}}\mathbf{e}_j\|_{\mathcal{N}_{\mathbf{\Psi}_{j+1}}(\mathbb{R}^d)} \leq \alpha_4 \|\boldsymbol{\mathcal{E}}\mathbf{e}_{j-1}\|_{\mathcal{N}_{\mathbf{\Psi}_j}(\mathbb{R}^d)}, \tag{8.6}$$

where α_4 is a constant independent of the point sets $X_1, X_2, \ldots$ and $\boldsymbol{\mathcal{E}}\mathbf{e}_j$ is the extension operator for $\mathbf{v}$ defined in (6.34) *applied to the error at level j defined in Algorithm 4. The constant α_4 satisfies $\alpha_4 < 1$ if in Algorithm 4 ν is sufficiently small and μ is sufficiently large.*

Proof. With the notation $\boldsymbol{\mathcal{E}}\mathbf{e_j} = (\mathbf{u} - \mathbf{M}_j\widetilde{\boldsymbol{\mathcal{E}}}_{\mathrm{div}}\mathbf{u}, p - M_j\mathcal{E}_{\mathrm{S}}p)^T = (\widetilde{\boldsymbol{\mathcal{E}}}_{\mathrm{div}}\mathbf{e}_{\mathbf{u},j}, \mathcal{E}_S e_{p,j})^T$, (6.36), (6.26) and (6.27), we have

$$\begin{aligned}
\|\boldsymbol{\mathcal{E}}\mathbf{e}_j\|^2_{\mathcal{N}_{\mathbf{\Psi}_{j+1}}(\mathbb{R}^d)} &\leq \bar{C}_1 \int\limits_{\mathbb{R}^d} \left[\frac{\left\|\widehat{\widetilde{\boldsymbol{\mathcal{E}}}_{\mathrm{div}}\mathbf{e}_{\mathbf{u},j}}(\boldsymbol{\omega})\right\|_2^2}{\|\boldsymbol{\omega}\|_2^2} \left(1 + \delta_{j+1}^2\|\boldsymbol{\omega}\|_2^2\right)^{\tau+1} \right. \\
&\quad + \left. \left|\widehat{\mathcal{E}_S e_{p,j}}(\boldsymbol{\omega})\right|^2 \left(1 + \delta_{j+1}^2\|\boldsymbol{\omega}\|_2^2\right)^{\tau-1} \right] \mathrm{d}\boldsymbol{\omega} \\
&=: I_1 + I_2,
\end{aligned}$$

with

$$\begin{aligned}
I_1 &:= \int\limits_{\|\boldsymbol{\omega}\|_2 \leq \frac{1}{\delta_{j+1}}} \left[\frac{\left\|\widehat{\widetilde{\boldsymbol{\mathcal{E}}}_{\mathrm{div}}\mathbf{e}_{\mathbf{u},j}}(\boldsymbol{\omega})\right\|_2^2}{\|\boldsymbol{\omega}\|_2^2} \left(1 + \delta_{j+1}^2\|\boldsymbol{\omega}\|_2^2\right)^{\tau+1} + \widehat{\mathcal{E}_S e_{p,j}}(\boldsymbol{\omega}) \left(1 + \delta_{j+1}^2\|\boldsymbol{\omega}\|_2^2\right)^{\tau-1} \right] \mathrm{d}\boldsymbol{\omega}, \\
I_2 &:= \int\limits_{\|\boldsymbol{\omega}\|_2 \geq \frac{1}{\delta_{j+1}}} \left[\frac{\left\|\widehat{\widetilde{\boldsymbol{\mathcal{E}}}_{\mathrm{div}}\mathbf{e}_{\mathbf{u},j}}(\boldsymbol{\omega})\right\|_2^2}{\|\boldsymbol{\omega}\|_2^2} \left(1 + \delta_{j+1}^2\|\boldsymbol{\omega}\|_2^2\right)^{\tau+1} + \widehat{\mathcal{E}_S e_{p,j}}(\boldsymbol{\omega}) \left(1 + \delta_{j+1}^2\|\boldsymbol{\omega}\|_2^2\right)^{\tau-1} \right] \mathrm{d}\boldsymbol{\omega}.
\end{aligned}$$

For I_1, we can use that $\delta_{j+1}\|\boldsymbol{\omega}\|_2 \leq 1$, Lemmas 6.4 and 8.4 and Theorem 6.6 to yield

$$\begin{aligned}
I_1 &\leq C\left(\|\boldsymbol{\mathcal{E}}_{\mathrm{div}}\mathbf{e}_{\mathbf{u},j}\|^2_{\mathbf{L}_2(\mathbb{R}^d)} + \|\mathcal{E}_S e_{p,j}\|^2_{L_2(\mathbb{R}^d)}\right) \\
&\leq C\left(\|\mathbf{e}_{\mathbf{u},j}\|^2_{\mathbf{L}_2(\Omega)} + \|e_{p,j}\|^2_{L_2(\Omega)}\right) \\
&\leq C\bar{h}_j^{2\tau-4}\|\boldsymbol{\mathcal{E}}\mathbf{e}_j\|^2_{\mathcal{N}_{\mathbf{\Psi}}(\mathbb{R}^d)} \\
&\leq C\frac{\bar{h}_j^{2\tau-4}}{\delta_j^{2\tau+2}}\|\boldsymbol{\mathcal{E}}\mathbf{e}_{j-1}\|^2_{\mathcal{N}_{\mathbf{\Psi}_j}(\mathbb{R}^d)} \\
&= C_{11}\beta^{-2\tau-2}\|\boldsymbol{\mathcal{E}}\mathbf{e}_{j-1}\|^2_{\mathcal{N}_{\mathbf{\Psi}_j}(\mathbb{R}^d)},
\end{aligned}$$

where in the second last step we have used that since the interpolant at X_j to $\mathbf{e}_{j-1}$ is the same as the interpolant to $\boldsymbol{\mathcal{E}}\mathbf{e}_{j-1}$ (both functions take the same values on $X_j \subseteq \Omega$), we have

$$\begin{aligned}
\|\mathbf{e}_j\|_{H^\tau(\Omega)} &= \|\mathbf{e}_{j-1} - \mathbf{S}_j\mathbf{e}_{j-1}\|_{\mathbf{H}^\tau(\Omega)} \\
&= \|\boldsymbol{\mathcal{E}}\mathbf{e}_{j-1} - \mathbf{S}_j\boldsymbol{\mathcal{E}}\mathbf{e}_{j-1}\|_{\mathbf{H}^\tau(\Omega)} \\
&\le \|\boldsymbol{\mathcal{E}}\mathbf{e}_{j-1} - \mathbf{S}_j\boldsymbol{\mathcal{E}}\mathbf{e}_{j-1}\|_{\mathbf{H}^\tau(\mathbb{R}^d)} \\
&\le C\delta_j^{-\tau-1}\|\boldsymbol{\mathcal{E}}\mathbf{e}_{j-1} - \mathbf{S}_j\boldsymbol{\mathcal{E}}\mathbf{e}_{j-1}\|_{\mathcal{N}_{\mathbf{\Psi}_j}(\mathbb{R}^d)} \\
&\le C\delta_j^{-\tau-1}\|\boldsymbol{\mathcal{E}}\mathbf{e}_{j-1}\|_{\mathcal{N}_{\mathbf{\Psi}_j}(\mathbb{R}^d)}.
\end{aligned}$$

For I_2, since $\delta_{j+1}^2\|\boldsymbol{\omega}\|_2^2 \ge 1$, we have

$$\left(1+\delta_{j+1}^2\|\boldsymbol{\omega}\|_2^2\right)^\tau \le 2^\tau\delta_{j+1}^{2\tau}\|\boldsymbol{\omega}\|)2^{2\tau} \le \left(2\delta_{j+1}^2\|\boldsymbol{\omega}\|_2^2\right)^\tau \le 2^\tau\mu^{2\tau}\left(1+\delta_j^2\|\boldsymbol{\omega}\|_2^2\right)^\tau,$$

and hence if $\mu, \delta \le 1$, we have

$$\begin{aligned}
I_2 &\le C\mu^{2\tau-2}\|\boldsymbol{\mathcal{E}}\mathbf{e}_j\|^2_{\mathcal{N}_{\mathbf{\Psi}_j}(\mathbb{R}^d)} \\
&\le C_{12}\mu^{2\tau-2}\|\boldsymbol{\mathcal{E}}\mathbf{e}_{j-1}\|^2_{\mathcal{N}_{\mathbf{\Psi}_j}(\mathbb{R}^d)}.
\end{aligned}$$

The result follows with

$$\alpha_4 := \left(C_{11}\beta^{-2\tau-2} + C_{12}\mu^{2\tau-2}\right)^{1/2}.$$

□

Corollary 8.6. *There exist positive constants C_{13} and C_{14} such that*

$$\|\mathbf{v} - \mathbf{M}_n\mathbf{v}\|_{\mathbf{L}_2(\Omega)} \le C_{13}\alpha_4^n\left(\|\mathbf{u}\|_{\mathbf{H}^\tau(\Omega)} + \|p\|_{H^{\tau-1}(\Omega)}\right) \quad \textit{for} \;\; n = 1, 2, \ldots$$

and

$$\|\mathbf{u} - \mathbf{M}_n\mathbf{u}\|_{\mathbf{L}_2(\partial\Omega)} \le C_{14}\alpha_4^n\left(\|\mathbf{u}\|_{\mathbf{H}^\tau(\Omega)} + \|p\|_{H^{\tau-1}(\Omega)}\right) \quad \textit{for} \;\; n = 1, 2, \ldots$$

Thus the multiscale approximation $\mathbf{M}_n\mathbf{v}$ resulting from Algorithm 4 converges linearly to $\mathbf{v}$ in the L_2-norm in Ω and on $\partial\Omega$ if $\alpha_4 < 1$.

Proof. With Lemma 6.4, Theorems 6.6 and 8.5 and recalling that Algorithm 4 specifies that $\delta_n = \beta\bar{h}_n^{1-3/(\tau+1)}$, we have

$$\begin{aligned}
\|\mathbf{v} - \mathbf{M}_n\mathbf{v}\|_{\mathbf{L}_2(\Omega)} &\le \|\mathbf{e}_n\|_{\mathbf{L}_2(\Omega)} \\
&\le C\bar{h}_n^{\tau-2}\|\boldsymbol{\mathcal{E}}\mathbf{e}_n\|_{\mathcal{N}_{\mathbf{\Psi}}(\mathbb{R}^d)} \\
&\le C\|\boldsymbol{\mathcal{E}}\mathbf{e}_n\|_{\mathcal{N}_{\mathbf{\Psi}_{n+1}}(\mathbb{R}^d)} \\
&\le C\alpha_4^n\|\boldsymbol{\mathcal{E}}\mathbf{v}\|_{\mathcal{N}_{\mathbf{\Psi}_1}(\mathbb{R}^d)}
\end{aligned}$$

$$
\begin{aligned}
&\leq C\alpha_4^n \|\mathcal{E}\mathbf{v}\|_{\mathcal{N}_{\Psi}(\mathbb{R}^d)} \\
&\leq C\alpha_4^n \left(\|\mathbf{u}\|_{\mathbf{H}^{\tau}(\Omega)} + \|p\|_{H^{\tau-1}(\Omega)}\right),
\end{aligned}
$$

which proves the first result. For the second result, with (6.40) we can see that

$$
\begin{aligned}
\|\mathbf{u} - \mathbf{M}_n\mathbf{u}\|_{\mathbf{L}_2(\partial\Omega)} &\leq \|\mathbf{u} - \mathbf{M}_n\mathbf{u}\|_{\mathbf{H}^{3/2}(\partial\Omega)} \\
&\leq Ch_{2,n}^{\tau-2}\|\mathbf{u} - \mathbf{M}_n\mathbf{u}\|_{\mathbf{H}^{\tau}(\Omega)} \\
&\leq C\bar{h}_n^{\tau-2}\|\mathcal{E}\mathbf{e}_n\|_{\mathcal{N}_{\Psi}(\mathbb{R}^d)},
\end{aligned}
$$

and the remainder of the proof is the same as for the first result. □

8.2.1 Condition numbers

In this section, we present upper and lower bounds for the eigenvalues of the multiscale symmetric collocation algorithm for the Stokes problem. At each step of the multiscale algorithm, we need to solve a linear system resulting from the collocation conditions (6.31) and (6.32) on a set $X = \{\mathbf{x}_1, \dots, \mathbf{x}_M\}$:

$$\mathbf{A}_\delta \mathbf{b} = (\mathbf{f}\ \ \mathbf{g})^T.$$

The next theorem gives a lower bound on the minimum eigenvalue of $\mathbf{A}_\delta$.

Theorem 8.7. *Suppose the kernel Ψ is defined by* (6.28) *and define the scaled kernel Ψ_δ by* (6.35) *with a positive scaling factor δ. Then the smallest eigenvalue of the collocation matrix defined by* (6.31) *and* (6.32) *can be bounded by*

$$\lambda_{\min}(\mathbf{A}_\delta) \geq C\left(\frac{q_X}{\delta}\right)^{2\tau+2} q_X^{-d-2},$$

where the constant C is independent of the point set X.

Proof. We follow the proof of [18, Theorem 4.1]. We will adopt the functional notation

$$
\xi_{i,j}(\mathbf{v}) := \begin{cases} \left(\mathcal{L}^S\mathbf{v}\right)_i(\mathbf{x}_j) & \text{for} \quad 1 \leq j \leq N, \quad 1 \leq i \leq d, \\ \mathbf{v}_i(\mathbf{x}_j) & \text{for} \quad N+1 \leq j \leq M, \quad 1 \leq i \leq d. \end{cases}
$$

We will use the superscript $\mathbf{y}$ to denote that the functional acts with respect to its second argument. Then with $\beta \in \mathbb{R}^{dM}$, we need to show that

$$\sum_{i,i'=1}^{d}\sum_{j,k=1}^{M} \beta_{i,j}\beta_{i',k}\xi_{i,j}\xi_{i',k}^{\mathbf{y}}\Psi_\delta(\mathbf{x}-\mathbf{y}) \geq C\left(\frac{q_X}{\delta}\right)^{2\tau+2} q_X^{-d-2}\|\beta\|_2^2. \tag{8.7}$$

With the inverse Fourier transform, the left hand side of (8.7) becomes

$$\sum_{i,i'=1}^{d}\sum_{j,k=1}^{M}\beta_{i,j}\beta_{i',k}\xi_{i,j}\xi_{i',k}^{\mathbf{y}}\mathbf{\Psi}_{\delta}(\mathbf{x}-\mathbf{y})$$
$$= (2\pi)^{-d/2}\int_{\mathbb{R}^d}\sum_{i,i'=1}^{d}\sum_{j,k=1}^{M}\beta_{i,j}\beta_{i',k}\xi_{i,j}\xi_{i',k}^{\mathbf{y}}\widehat{\mathbf{\Psi}}_{\delta}(\boldsymbol{\omega})e^{I(\mathbf{x}-\mathbf{y})\cdot\boldsymbol{\omega}},\mathrm{d}\boldsymbol{\omega}$$

where $I^2 = -1$. Now we define a second scaled kernel $\mathbf{\Psi}_a$ by (6.35) with $0 < a \leq 1$ and $a \leq \delta$. Recalling that $\phi_{\tau-1}$ satisfies (6.27) gives

$$\begin{aligned}
\widehat{\phi_{\tau-1,\delta}}(\boldsymbol{\omega}) &= \widehat{\phi_{\tau-1}}(\delta\boldsymbol{\omega}) \geq c_{1,\tau-1}\left(1+\|\delta\boldsymbol{\omega}\|_2^2\right)^{-\tau+1} \\
&= c_{1,\tau-1}\left(\frac{a}{\delta}\right)^{2\tau-2}\left(\left(\frac{a}{\delta}\right)^2+\|a\boldsymbol{\omega}\|_2^2\right)^{-\tau+1} \\
&\geq c_{1,\tau-1}\left(\frac{a}{\delta}\right)^{2\tau-2}\left(1+\|a\boldsymbol{\omega}\|_2^2\right)^{-\tau+1} \\
&\geq \frac{c_{1,\tau-1}}{c_{2,\tau-1}}\left(\frac{a}{\delta}\right)^{2\tau-2}\widehat{\phi_{\tau-1,a}}(\boldsymbol{\omega}).
\end{aligned}$$

Since $\phi_{\tau+1}$ satisfies (6.26) and with (6.29), we proceed similarly to get

$$\begin{aligned}
\widehat{\mathbf{\Phi}_{\tau+1,\delta}}(\boldsymbol{\omega}) &= \left(\|\boldsymbol{\omega}\|_2^2\mathbf{I}-\boldsymbol{\omega}\boldsymbol{\omega}^T\right)\widehat{\phi_{\tau+1}}(\delta\|\boldsymbol{\omega}\|_2) \\
&\geq c_{1,\tau+1}\left(\frac{a}{\delta}\right)^{2\tau+2}\left(\|\boldsymbol{\omega}\|_2^2\mathbf{I}-\boldsymbol{\omega}\boldsymbol{\omega}^T\right)\left(\left(\frac{a}{\delta}\right)^2+\|a\boldsymbol{\omega}\|_2^2\right)^{-\tau-1} \\
&\geq c_{1,\tau+1}\left(\frac{a}{\delta}\right)^{2\tau+2}\left(\|\boldsymbol{\omega}\|_2^2\mathbf{I}-\boldsymbol{\omega}\boldsymbol{\omega}^T\right)\left(1+\|a\boldsymbol{\omega}\|_2^2\right)^{-\tau-1} \\
&\geq \frac{c_{1,\tau+1}}{c_{2,\tau+1}}\left(\frac{a}{\delta}\right)^{2\tau+2}\left(\|\boldsymbol{\omega}\|_2^2\mathbf{I}-\boldsymbol{\omega}\boldsymbol{\omega}^T\right)\widehat{\phi_{\tau+1}}(a\|\boldsymbol{\omega}\|_2) \\
&= \frac{c_{1,\tau+1}}{c_{2,\tau+1}}\left(\frac{a}{\delta}\right)^{2\tau+2}\widehat{\mathbf{\Phi}_{\tau+1,a}}(\boldsymbol{\omega}).
\end{aligned}$$

Since $a/\delta < 1$, we have the following bound on $\widehat{\mathbf{\Psi}_{\delta}}$

$$\widehat{\mathbf{\Psi}_{\delta}}(\boldsymbol{\omega}) \geq c\left(\frac{a}{\delta}\right)^{2\tau+2}\widehat{\mathbf{\Psi}_{a}}(\boldsymbol{\omega}),$$

and hence

$$\sum_{i,i'=1}^{d}\sum_{j,k=1}^{M}\beta_{i,j}\beta_{i',k}\xi_{i,j}\xi_{i',k}^{\mathbf{y}}\mathbf{\Psi}_{\delta}(\mathbf{x}-\mathbf{y}) \geq c\left(\frac{a}{\delta}\right)^{2\tau+2}\sum_{i,i'=1}^{d}\sum_{j,k=1}^{M}\beta_{i,j}\beta_{i',k}\xi_{i,j}\xi_{i',k}^{\mathbf{y}}\mathbf{\Psi}_{a}(\mathbf{x}-\mathbf{y}).$$

If we select $a = q_X \leq 1$ such that we need only consider entries of the quadratic form corresponding to equal centres, with the definition of the scaled kernel, this reduces to

$$\sum_{i,i'=1}^{d}\sum_{j,k=1}^{M}\beta_{i,j}\beta_{i',k}\xi_{i,j}\xi_{i',k}^{\mathbf{y}}\mathbf{\Psi}_{\delta}(\mathbf{x}-\mathbf{y})$$
$$\geq c\left(\frac{q_X}{\delta}\right)^{2\tau+2}q_X^{-d}\sum_{i=1}^{d}\left\{\sum_{j=1}^{N}\beta_{i,j}^2\left(-\sum_{j=\{1:d\}\setminus i}q_X^{-6}\partial_{jj}\Delta^2\phi_{\tau+1}(0)-q_X^{-2}\partial_{ii}\phi_{\tau-1}(0)\right)+\right.$$
$$\left.\sum_{j=N+1}^{M}\beta_{i,j}^2\left(-\sum_{j=\{1:d\}\setminus i}q_X^{-2}\partial_{jj}\phi_{\tau+1}(0)\right)\right\},$$

since for interior centres we have

$$\xi_{i,j}\zeta^{\mathbf{y}}_{i',k}\mathbf{\Psi}(\mathbf{x}-\mathbf{y})|_{j=k} = \begin{cases} -\nu^2\sum_{j=1:d\setminus i}\partial_{jj}\Delta^2\phi_{\tau+1}(0)-\partial_{ii}\phi_{\tau-1}(0) & \text{for} \quad i=i', \\ -\nu^2\partial_{ii'}\Delta^2\phi_{\tau+1}(0)-\partial_{ii'}\phi_{\tau-1}(0)=0 & \text{for} \quad i\neq i', \end{cases} \tag{8.8}$$

with Lemmas 3.3 and 3.4. Similarly for the boundary centres

$$\xi_{i,j}\zeta^{\mathbf{y}}_{i',k}\mathbf{\Psi}(\mathbf{x}-\mathbf{y})|_{j=k} = \begin{cases} -\sum_{j=1:d\setminus i}\partial_{jj}\phi_{\tau+1}(0) & \text{for} \quad i=i', \\ -\partial_{ii'}\phi_{\tau+1}(0)=0 & \text{for} \quad i\neq i'. \end{cases} \tag{8.9}$$

Then the result follows as

$$\sum_{i=1}^{d}\sum_{j,k=1}^{M}\beta_{i,j}\beta_{i,k}\xi_{i,j}\zeta^{\mathbf{y}}_{i,k}\mathbf{\Psi}_\delta(\mathbf{x}-\mathbf{y}) \geq c\,\tilde{c}\left(\frac{q_X}{\delta}\right)^{2\tau} q_X^{-d-2}\|\beta\|_2^2,$$

with Lemmas 3.5 and 3.6 which give

$$\begin{aligned} \tilde{c} &:= \min_{1\leq i\leq d}\left(-\sum_{j=\{1:d\}\setminus i} q_X^{-4}\partial_{jj}\Delta^2\phi_{\tau+1}(0)-\partial_{ii}\phi_{\tau-1}(0), -\sum_{j=\{1:d\}\setminus i}\partial_{jj}\phi_{\tau+1}(0)\right) \\ &\geq \min_{1\leq i\leq d}\left(-\sum_{j=\{1:d\}\setminus i}\partial_{jj}\Delta^2\phi_{\tau+1}(0)-\partial_{ii}\phi_{\tau-1}(0), -\sum_{j=\{1:d\}\setminus i}\partial_{jj}\phi_{\tau+1}(0)\right) \\ &= \min\left(-\sum_{j=2}^{d}\partial_{jj}\Delta^2\phi_{\tau+1}(0)-\partial_{11}\phi_{\tau-1}(0), -\sum_{j=2}^{d}\partial_{jj}\phi_{\tau+1}(0)\right), \end{aligned}$$

since $\phi_{\tau+1}$ is a radial function and $\partial_{ii}\phi_{\tau+1}(0)$ is independent of i from Lemma 3.5. □

Our next result bounds the maximum eigenvalue $\lambda_{\max}(\mathbf{A}_\delta)$.

Theorem 8.8. *Suppose the kernel $\mathbf{\Psi}_\delta$ is defined as in Theorem 8.7. Then if we assume that*

$$M \leq C\bar{h}^{-d}, \tag{8.10}$$

where M denotes the number of (interior and boundary) centres, then the largest eigenvalue of the collocation matrix constructed with $\mathbf{\Psi}_\delta$ defined by (6.31) *and* (6.32) *can be bounded by*

$$\lambda_{\max}(\mathbf{A}_\delta) \leq C\,\delta^{-d-2}\,\bar{h}^{-d},$$

if $\delta \geq 1$ and by

$$\lambda_{\max}(\mathbf{A}_\delta) \leq C\,\delta^{-d-6}\,\bar{h}^{-d},$$

if $\delta < 1$, where the constants C are independent of the point set X.

Proof. Using the notation from Theorem 8.7, together with Gershgorin's theorem, we have

$$|\lambda_{\max}(\mathbf{A}_\delta)-\xi_{i,j}\zeta^{\mathbf{y}}_{i,j}\mathbf{\Psi}_\delta(\mathbf{x},\mathbf{x})| \leq \sum_{i'=1}^{d}\sum_{\substack{k=1\\ i'\neq i,k\neq j}}^{M}|\xi_{i,j}\zeta^{\mathbf{y}}_{i,k}\mathbf{\Psi}_\delta(\mathbf{x},\mathbf{y})|, \quad 1\leq i\leq d$$

which since $\mathbf{\Psi}$ is positive definite, using (8.10), Lemmas 3.5 and 3.6, the definition of the scaled kernels and (8.8) and (8.9), if $\delta \geq 1$

$$
\begin{aligned}
\lambda_{\max}(\mathbf{A}_\delta) &\leq dM\|\xi_{i',\cdot}\xi^{\mathbf{y}}_{i,\cdot}\mathbf{\Psi}_\delta(\cdot,\cdot)\|_{L_\infty(\Omega\times\Omega)} \\
&\leq C\,d\,\bar{h}^{-d}\max\left(-\sum_{j=2}^{d}\partial_{jj}\Delta^2\phi_{\tau+1,\delta}(0)-\partial_{11}\phi_{\tau-1,\delta}(0),-\sum_{j=2}^{d}\partial_{jj}\phi_{\tau+1,\delta}(0)\right) \\
&\leq C\,d\,\bar{h}^{-d}\delta^{-d-2}\max\left(-\sum_{j=2}^{d}\partial_{jj}\Delta^2\phi_{\tau+1}(0)-\partial_{11}\phi_{\tau-1}(0),-\sum_{j=2}^{d}\partial_{jj}\phi_{\tau+1}(0)\right),
\end{aligned}
$$

where in the last step we have used that

$$\partial_{jj}\Delta^2\phi_{\tau+1,\delta}(0)=\delta^{-d}\partial_{jj}\Delta^2\delta^{-6}\phi_{\tau+1}(0)\leq\delta^{-d-2}\partial_{jj}\Delta^2\phi_{\tau+1}(0),$$

since $\delta \geq 1$. If $\delta < 1$, we have

$$
\begin{aligned}
\lambda_{\max}(\mathbf{A}_\delta) &\leq dM\|\xi_{i',\cdot}\xi^{\mathbf{y}}_{i,\cdot}\mathbf{\Psi}_\delta(\cdot,\cdot)\|_{L_\infty(\Omega\times\Omega)} \\
&\leq C\,d\,\bar{h}^{-d}\delta^{-d-6}\max\left(-\sum_{j=2}^{d}\partial_{jj}\Delta^2\phi_{\tau+1}(0)-\partial_{11}\phi_{\tau-1}(0),-\sum_{j=2}^{d}\partial_{jj}\phi_{\tau+1}(0)\right),
\end{aligned}
$$

where in the last step we have used, for example, that

$$\partial_{11}\phi_{\tau+1,\delta}(0)=\delta^{-d}\partial_{11}\delta^{-2}\phi_{\tau+1}(0)\leq\delta^{-d-6}\partial_{11}\phi_{\tau+1}(0),$$

which completes the proof. □

We note that (8.10) will hold if, for example, the dataset is quasi-uniform, which means that h_j/q_j is bounded above by a constant.

Now with (7.6) and Theorems 8.7 and 8.8, we obtain the following theorem where we write $q_j := q_{X_j}$.

Theorem 8.9. *Suppose the kernel $\mathbf{\Psi}_\delta$ is defined as in Theorem 8.7. Then the condition number of the multiscale symmetric collocation matrix in Algorithm 4 is level-dependent and is bounded by*

$$\kappa_j \leq C\left(\frac{\bar{h}_j}{q_j}\right)^{2\tau-d}\bar{h}_j^{-\frac{3}{\tau+1}(2\tau-d)-d},$$

if $\delta \geq 1$ and by

$$\kappa_j \leq C\left(\frac{\bar{h}_j}{q_j}\right)^{2\tau-d}\bar{h}_j^{-\frac{3}{\tau+1}(2\tau-d-4)-d-4},$$

if $\delta < 1$. In the case of quasi-uniform datasets and $h_j \leq 1$, these reduce to

$$\kappa_j \leq C\,\bar{h}_j^{-2\tau}.$$

Proof. The first two results follows with $\delta_j = \beta\bar{h}_j^{1-3/(\tau+1)}$ and (7.6) and Theorems 8.7 and 8.8. If the datasets are quasi-uniform, which means that h_j/q_j is bounded above by a constant, the final result follows by simplifying the first two expressions. □

8.2.2 Numerical experiments

In this section, we present the results from applying the multiscale algorithm described in Algorithm 4 with $\Omega = [0,1]^2$ and $\nu = 1$ to the Stokes problem with exact solution given by

$$\mathbf{u}(x_1, x_2) = \begin{pmatrix} 2\cos(5x_1)\cos(2x_2) \\ 5\sin(5x_1)\sin(x_2) \end{pmatrix},$$

$$p(x_1, x_2) = \sin(3x_1)\sin(3x_2) + C.$$

This gives

$$\mathbf{f}(x_1, x_2) = \begin{pmatrix} 58\cos(5x_1)\cos(2x_2) + 3\cos(3x_1)\sin(3x_2) \\ 145\sin(5x_1)\sin(2x_2) + 3\sin(3x_1)\cos(3x_2) \end{pmatrix}$$

and $\mathbf{g}$ equal to the restriction of $\mathbf{u}(\mathbf{x})$ to $\partial\Omega$.

We use the C^8 Wendland radial basis function given by

$$\phi_{6,4}(\|\mathbf{x}\|) = (1 - \|\mathbf{x}\|)_+^{10}(429\|\mathbf{x}\|^4 + 450\|\mathbf{x}\|^3 + 210\|\mathbf{x}\|^2 + 50\|\mathbf{x}\| + 5),$$

which is positive definite on $\mathbb{R}^2$ and generates the Sobolev space $H^{5.5}(\mathbb{R}^2)$ [51]. We use the same kernel for both $\phi_{\tau+1}$ and $\phi_{\tau-1}$. Consequently, in this case $\tau = 4.5$. Since $d = 2$, our approximate solution takes the form

$$\begin{aligned}\mathbf{S}_X\mathbf{v}(\mathbf{x}) = \sum_{j=1}^{N} \alpha_{1,j} \begin{pmatrix} \nu\partial_{22}\Delta\phi_{\tau+1}(\|\mathbf{x}-\mathbf{x}_j\|_2) \\ -\nu\partial_{12}\Delta\phi_{\tau+1}(\|\mathbf{x}-\mathbf{x}_j\|_2) \\ -\partial_1\phi_{\tau-1}(\|\mathbf{x}-\mathbf{x}_j\|_2) \end{pmatrix} + \sum_{j=N+1}^{M} \alpha_{1,j} \begin{pmatrix} -\partial_{22}\phi_{\tau+1}(\|\mathbf{x}-\mathbf{x}_j\|_2) \\ \partial_{12}\phi_{\tau+1}(\|\mathbf{x}-\mathbf{x}_j\|_2) \\ 0 \end{pmatrix} \\ + \sum_{j=1}^{N} \alpha_{2,j} \begin{pmatrix} -\nu\partial_{12}\Delta\phi_{\tau+1}(\|\mathbf{x}-\mathbf{x}_j\|_2) \\ \nu\partial_{11}\Delta\phi_{\tau+1}(\|\mathbf{x}-\mathbf{x}_j\|_2) \\ -\partial_2\phi_{\tau-1}(\|\mathbf{x}-\mathbf{x}_j\|_2) \end{pmatrix} + \sum_{j=N+1}^{M} \alpha_{2,j} \begin{pmatrix} \partial_{12}\phi_{\tau+1}(\|\mathbf{x}-\mathbf{x}_j\|_2) \\ -\partial_{11}\phi_{\tau+1}(\|\mathbf{x}-\mathbf{x}_j\|_2) \\ 0 \end{pmatrix}.\end{aligned}$$

We used five levels for the approximation, with N equally spaced points for the interior point sets and $4(\sqrt{N} - 1)$ equally spaced boundary centres. The number of interior points, N_j, the number of boundary points, $M_j - N_j$, and the maximum mesh norms at each level, $\bar{h}_j$, are given in Table 8.3. We note that the (maximum) mesh norms decrease by one half at each level and hence we select $\mu = \frac{1}{2}$. For the scaling parameters, since $\tau = 4.5$, Algorithm 4 specifies that

$$\delta_j = \beta\bar{h}_j^{2.5/5.5}$$

with β constant. With the given value of $\bar{h}_1$ in Table 8.3, we select β such that $\delta_1 = 10$. This gives $\beta = 18.779$ and we use this to generate the other δ values which are given

Level	1	2	3	4	5
N	25	81	289	1089	4225
$M-N$	16	32	64	128	256
$\bar{h}$	$1/4$	$1/8$	$1/16$	$1/32$	$1/64$

Table 8.3. *The number of interior and boundary points used at each level and the maximum mesh norm at each level for the multiscale symmetric collocation Stokes problem example*

along with the L_2 and L_∞ errors and condition numbers (κ) collocation matrix in Table 8.4. The L_2 error was estimated using Gaussian quadrature with a 300×300 tensor product grid of Gauss-Legendre points and the L_∞ error was estimated with the same tensor product grid. We used MATLAB for the calculations and worked with double precision.

Level	1	2	3	4	5
δ_j	10	7.29	5.33	3.89	2.84
$\|\mathbf{e}_{\mathbf{u},j}\|_{\mathbf{L}_2(\Omega)}$	1.59e-02	6.50e-04	3.27e-05	1.65e-06	1.03e-07
$\|\mathbf{e}_{\mathbf{u},j}\|_{\mathbf{L}_\infty(\Omega)}$	2.74e-02	2.23e-03	1.46e-04	8.27e-06	4.58e-07
$\|\nabla e_{p,j}\|_{L_2(\Omega)}$	1.11e+00	1.22e-01	1.24e-02	2.56e-03	5.61e-04
$\|\nabla e_{p,j}\|_{L_\infty(\Omega)}$	4.21e+00	3.34e-01	1.05e-01	3.65e-02	1.21e-02
κ_j	1.27e+09	7.77e+11	2.57e+14	6.88e+16	1.67e+19

Table 8.4. *The scaling factors, approximation errors and condition numbers of the collocation matrices for the multiscale symmetric collocation Stokes problem example*

Finally we note that from Theorem 8.9, the expected numerical order of the condition number is $2\tau = 9$ for this example. In Table 8.5, we present the observed numerical order of the condition number, which is computed as

$$-\frac{\log \frac{\kappa_{j+1}}{\kappa_j}}{\log \frac{h_{j+1}}{h_j}}.$$

Level	1	2	3	4	5
Order		9.26	8.37	8.06	7.92

Table 8.5. *The observed order for the condition numbers for the multiscale symmetric collocation Stokes problem example*

Bibliography

[1] M. Abramowitz and I. A. Stegun. *Handbook of Mathematical Functions with Formulas, Graphs and Mathematical Tables*, volume 65 of *National Bureau of Standards Applied Mathematics Series*. Dover Publications, 1972.

[2] R. A. Adams. *Sobolev Spaces*. Academic Press, Boston, 1975.

[3] G. E. Andrews, R. Askey, and R. Roy. *Special Functions*, volume 71 of *Encylopedia of Mathematics and its Applications*. Cambridge University Press, Cambridge, 2000.

[4] R. K. Beatson, W. A. Light, and S. Billings. Fast solution of the radial basis function interpolation equations: Domain decomposition methods. *SIAM J. Sci. Comput.*, 22:1717–1740, 2000.

[5] J. Blowey, A. Craig, and T. Shardlow. *Frontiers in Numerical Analysis*. Universitext. Springer, 2003.

[6] M. Bozzini, L. Lenarduzzi, M. Rossini, and R. Schaback. Interpolation by basis functions of different scales and shapes. *Calc.*, 41:77–87, 2004.

[7] S. C. Brenner and L. R. Scott. *The Mathematical Theory of Finite Element Methods*. Texts in Applied Mathematics. Springer, 3 edition, 2008.

[8] A. Chernih and S. Hubbert. Closed form representations and properties of the generalised Wendland functions, preprint. 2013.

[9] F. Deutsch. The method of alternating orthogonal projections. In S. P. Singh, editor, *Approximation Theory, Spline Functions and Applications*, pages 105–121. Kluwer Academic Publishers, 1990.

[10] R. A. Devore and R. C. Sharpley. Besov spaces on domains in $\mathbb{R}^d$. *Trans. Amer. Math. Soc.*, 335:843–864, 1993.

[11] DLMF. *Digital Library of Mathematical Functions*. National Institute of Standards and Technology, 2011.

[12] G. E. Fasshauer. *Meshfree Approximation Methods with MATLAB*, volume 6 of *Interdisciplinary Mathematical Sciences*. World Scientific Publishing Co., Singapore, 2007.

[13] J. L. Fields and M. E.-H. Ismail. On the positivity of some ${}_1F_2$'s. *SIAM J. Math. Anal.*, 6:551–559, 1975.

[14] M. S. Floater and A. Iske. Multistep scattered data interpolation using compactly supported radial basis functions. *J. Comput. Appl. Math.*, 73:65–78, 1996.

[15] M. Fornefett, K. Rohr, and H.S. Stiehl. Radial basis functions with compact support for elastic registration of medical images. *Image Vis. Comput.*, 19:87–96, 2001.

[16] R. Franke. A critical comparison of some methods for interpolation of scattered data. Technical Report NPS-53-79-003, Naval Postgraduate School, March 1979.

[17] E. Fuselier. Improved stability estimates and a characterization of the native space for matrix-valued rbfs. *Adv. Comput. Math*, 29:269–290, 2008.

[18] P. Giesl and H. Wendland. Meshless collocation: Error estimates with application to dynamical systems. *SIAM J. Numer. Anal.*, 45:1723–1741, 2007.

[19] D. Gilbarg and N.S. Trudinger. *Elliptic Partial Differential Eequations of Second Order*, volume 224 of *Grundlehren Math. Wiss.* Springer, Heidelberg, 1977.

[20] T. Gneiting. Compactly supported correlation functions. *J. Multivar. Anal.*, 83:493–508, 2002.

[21] I. S. Gradshteyn and I. M. Ryzhik. *Table of Integrals, Series and Products*. Elsevier, 7 edition, 2007.

[22] M. Griebel and M.A. Schweitzer. A particle-partition of unity method. part v: boundary conditions. In S. Hildebrandt and H. Karcher, editors, *Geometric Analysis and Nonlinear Partial Differential Equations*, pages 519–542. Springer, Berlin, 2002.

[23] S. Hubbert. Closed form representations for a class of compactly supported radial basis functions. *Adv. Comput. Math.*, 36:115–136, 2012.

[24] K. S. Kang and D. Y. Kwak. Convergence estimates for multigrid algorithms with Kaczmarz smoothing. In R. Glowinski, J. Périaux, Z.-C. Shi, and O. Widlund, editors, *8th International Conference on Domain Decomposition Methods*. John Wiley and Sons, 1997.

[25] Q. T. Le Gia, I. H. Sloan, and H. Wendland. Multiscale analysis in Sobolev spaces on the sphere. *SIAM J. Numer. Anal.*, 48:2065–2090, 2010.

[26] D. E. Longsine and S. F. McCormick. Simultaneous Rayleigh-quotient minimization methods for $ax = \lambda bx$. *Lin. Alg. Appl*, 34:195–234, 1980.

[27] V. Maz'ya. *Sobolev Spaces: with Applications to Elliptic Partial Differential Equations*, volume 342 of *Grundlehren der mathematischen Wissenschaften*. Springer, 2 edition, 2011.

[28] S. F. McCormick. *Multilevel Projection Methods for Partial Differential Equations*, volume 62 of *CBMS-NSF Regional Conference Series in Applied Mathematics*. SIAM, Philadelphia, 1992.

[29] D. S. Moak. Completely monotonic functions of the form $s^{-b}\left(s^2+1\right)^{-a}$. *Rocky Mt. J. Math.*, 17:719–725, 1987.

[30] G. Moreaux. Compactly supported radial covariance functions. *J. Geod.*, 82:431–443, 2008.

[31] F. J. Narcowich and J. D. Ward. Generalized Hermite interpolation via matrix-valued conditionally positive definite functions. *Math. Comput.*, 63:661–687, 1994.

[32] F. J. Narcowich, J. D. Ward, and H. Wendland. Sobolev bounds on functions with scattered zeros, with applications to radial basis function surface fitting. *Math. Comput.*, 74:743–763, 2005.

[33] F. J. Narcowich, J. D. Ward, and H. Wendland. Sobolev error estimates and a Bernstein inequality for scattered data interpolation via radial basis functions. *Constr. Approx.*, 24:175–186, 2006.

[34] J. Nitsche. Über ein Variationsprinzip zur Lösung von Dirichlet-Problemen bei Verwendung von Teilräumen, die keinen Randbedingungen unterworfen sind. *Abh. Math. Univ. Hamburg*, 36:9–15, 1970–1971.

[35] A. P. Prudnikov, Yu. A. Brychkov, and O. I. Marichev. *Integrals and Series: More Special Functions, Vol. 3*. Gordon and Breach Science Publishers, New York, 1986.

[36] A. P. Prudnikov, Yu. A. Brychkov, and O. I. Marichev. *Integrals and Series: Special Functions, Vol. 2*. Gordon and Breach Science Publishers, New York, 1986.

[37] R. Schaback. On the efficiency of interpolation by radial basis functions. In C. Rabut A. Le Méhauté and L. L. Schumaker, editors, *Surface Fitting and Multiresolution Methods*, pages 309–318. Vanderbilt University Press, 1996.

[38] R. Schaback. The missing Wendland functions. *Adv. Comput. Math.*, 34:67–81, 2011.

[39] K. T. Smith, D. C. Solmon, and S. L. Wagner. Practical and mathematical aspects of the problem of reconstructing objects from radiographs. *Bull. Am. Math. Soc.*, 83:1227–1270, 1977.

[40] E. M. Stein. *Singular Integrals and Differentiability Properties of Functions*. Princeton University Press, Princeton, New Jersey, 1970.

[41] E.M. Stein and G. Weiss. *Introduction to Fourier Analysis on Euclidean Spaces*, volume 32 of *Princeton Mathematical Series*. Princeton University Press, Princeton, New Jersey, 1971.

[42] G. Strang. Piecewise polynomials and the finite element method. *Bull. Am. Math. Soc.*, 79:1128–1137, 1973.

[43] R. Temam. *Navier-Stokes Equations, Theory and Numerical Analysis*. AMS Chelsea Publishing, North-Holland, Amsterdam, 1977.

[44] J. P. Ward. L^p error estimates for approximation by Sobolev splines and Wendland functions on $\mathbb{R}^d$. Preprint 2012, 2012.

[45] G. N. Watson. *A Treatise on the Theory of Bessel Functions*. Cambridge University Press, Cambridge, 1966.

[46] J. G. Wendel. Note on the gamma function. *Am. Math. Mon.*, 55:563–564, 1948.

[47] H. Wendland. Piecewise polynomial, positive definite and compactly supported radial functions of minimal degree. *Adv. Comput. Math.*, 4:389–396, 1995.

[48] H. Wendland. Error estimates for interpolation by compactly supported radial basis functions of minimal degree. *J. Approx. Theory*, 93:258–272, 1998.

[49] H. Wendland. Meshless Galerkin methods using radial basis functions. *Math. Comput.*, 68(228):1521–131, 1998.

[50] H. Wendland. Numerical solution of variational problems by radial basis functions. In Charles K. Chui and Larry L. Schumaker, editors, *Approximation Theory IX, Volume 2: Computational Aspects*, pages 361–368. Vanderbilt University Press, 1998.

[51] H. Wendland. *Scattered Data Approximation*, volume 17 of *Cambridge Monographs on Applied and Computational Mathematics*. Cambridge University Press, Cambridge, 2005.

[52] H. Wendland. Divergence-free kernel methods for approximating the Stokes problem. *SIAM J. Numer. Anal.*, 47:3158–3179, 2009.

[53] H. Wendland. Multiscale analysis in Sobolev spaces on bounded domains. *Numer. Math.*, 116:493–517, 2010.